

INFORMATION TO USERS

This manuscript has been reproduced from the microfilm master. UMI films the text directly from the original or copy submitted. Thus, some thesis and dissertation copies are in typewriter face, while others may be from any type of computer printer.

The quality of this reproduction is dependent upon the quality of the copy submitted. Broken or indistinct print, colored or poor quality illustrations and photographs, print bleedthrough, substandard margins, and improper alignment can adversely affect reproduction.

In the unlikely event that the author did not send UMI a complete manuscript and there are missing pages, these will be noted. Also, if unauthorized copyright material had to be removed, a note will indicate the deletion.

Oversize materials (e.g., maps, drawings, charts) are reproduced by sectioning the original, beginning at the upper left-hand corner and continuing from left to right in equal sections with small overlaps.

Photographs included in the original manuscript have been reproduced xerographically in this copy. Higher quality 6" x 9" black and white photographic prints are available for any photographs or illustrations appearing in this copy for an additional charge. Contact UMI directly to order.

**Bell & Howell Information and Learning
300 North Zeeb Road, Ann Arbor, MI 48106-1346 USA
800-521-0600**

UMI[®]

Oxygen transfer reactions catalyzed by rhenium(VII) and rhenium(V) complexes

by

Ruili Huang

A dissertation submitted to the graduate faculty
in partial fulfillment of the requirements for the degree of
DOCTOR OF PHILOSOPHY

Major: Inorganic Chemistry
Major Professor: James H. Espenson

Iowa State University
Ames, Iowa
2000

UMI Number: 9990454



UMI Microform 9990454

Copyright 2001 by Bell & Howell Information and Learning Company.

**All rights reserved. This microform edition is protected against
unauthorized copying under Title 17, United States Code.**

**Bell & Howell Information and Learning Company
300 North Zeeb Road
P.O. Box 1346
Ann Arbor, MI 48106-1346**

Graduate College
Iowa State University

This is to certify that the Doctoral dissertation of


Ruili Huang

has met the dissertation requirements of Iowa State University

Signature was redacted for privacy.

 **Major Professor**

Signature was redacted for privacy.

 **For the Major Program**

Signature was redacted for privacy.


 **For the Graduate College**

TABLE OF CONTENTS

	<u>Page</u>
GENERAL INTRODUCTION	1
Introduction	1
Re(V)-Catalyzed oxo-transfer reactions and molecular oxygen activation	2
Sulfoxidations of thioketones and thioketone S-oxides (sulfines)	3
SO-Bridged diplatinum(I) halides from sulfoxidation and SO insertion	4
Dissertation Organization	5
References	6
 CHAPTER I. SYNTHESIS, CHARACTERIZATION, AND MOLECULAR STRUCTURE OF AN OXORHENIUM(V) COMPOUND, $\text{Re}_2(\text{O})_2(\text{MTP})_3$ (MTPH_2 = 2- MERCAPTOMETHYLTHIOPHENOL) AND ITS ACTIVATION OF MOLECULAR OXYGEN	 8
Introduction	8
Results and Discussion	9
Summary	12
References	12
Supporting Information	17
 CHAPTER II. A MECHANISTIC STUDY OF OXYGEN TRANSFER REACTION CATALYZED BY AN OXORHENIUM(V) COMPOUND	 24
Abstract	24
Introduction	24
Results	28
Discussion	37
References	40
Supporting Information	45
 CHAPTER III. MOLECULAR OXYGEN REACTIONS CATALYZED BY AN OXORHENIUM(V) COMPOUND	 51
Abstract	51

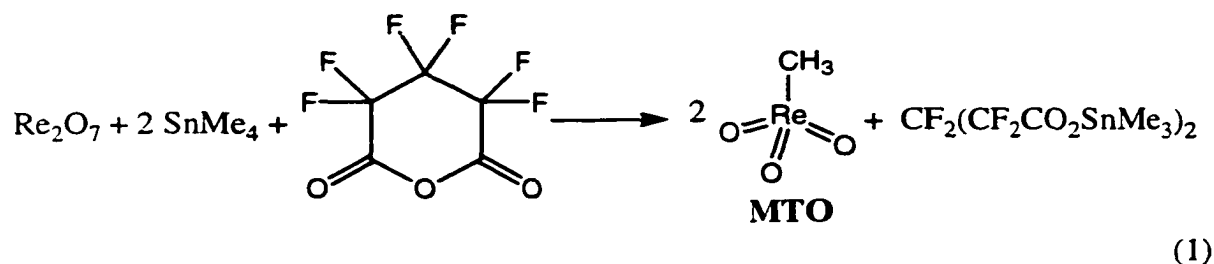
Introduction	51
Results and Interpretation	52
Discussion	59
Conclusion	62
References	62
CHAPTER IV. KINETICS AND MECHANISM OF THE METHYLTRIOXORHENIUM-CATALYZED SULFOXIDATION OF THIOKETONES AND SULFINES	65
Abstract	65
Introduction	65
Results	68
Discussion	74
References	78
Supporting Information	84
CHAPTER V. A CONVENIENT PREPARATION OF SULFINES ($R_2C=S=O$) FROM THIOKETONES	86
Introduction	86
Results and Discussion	86
References	89
CHAPTER VI. TWO ROUTES TO BIS(μ-DIPHENYLPHOSPHINO)METHANE DIPLATINUM HALIDES BRIDGED BY SULFUR MONOXIDE	93
Abstract	93
Introduction	93
Results and Discussion	94
Summary	97
References	97
Supporting Information	102
GENERAL CONCLUSIONS	122
ACKNOWLEDGMENTS	124

GENERAL INTRODUCTION

Introduction

Organometallic chemistry, a discipline that combines aspects of both inorganic and organic chemistry, has had an enormous impact on research and development in the past 50 years. An important application following the explosive growth in organometallic chemistry, homogeneous catalysis, offers higher selectivity, milder reaction conditions and high atom economy.¹ The chemistry and reactivities of transition metal-oxo complexes have attracted extensive attention in the past decade due to their application in catalysis.² Oxygen atom transfer reactions catalyzed by high valent transition metal-oxo complexes hold great interest for being key steps in many chemical and biological transformations.³⁻⁶ In the work described in this thesis, the utility of the high valent organorhenium oxide, methyltrioxorhenium (MTO), and the new binuclear oxothiolatorhenium(V) complex (**D**₁, Re₂O₂(mtp)₃, mtpH₂ = 2-mercaptomethylthiophenol) in catalytic oxygen atom transfer and molecular oxygen activation reactions were explored.

The colorless compound MTO was first prepared by Beattie and Jones in 1979 as needlelike crystals.⁷ The catalytic properties of MTO were not discovered until the early 90's.⁸ In 1991, an improved route (eq 1) for MTO synthesis was devised by Herrmann and coworkers who recognized the ability of MTO to activate hydrogen peroxide.⁹ The spectroscopic properties of MTO are summarized in Table 1. Its ease of synthesis and purification, air stability, solubility in water and most organic solvents and its effectiveness have made MTO an attractive homogeneous catalyst.

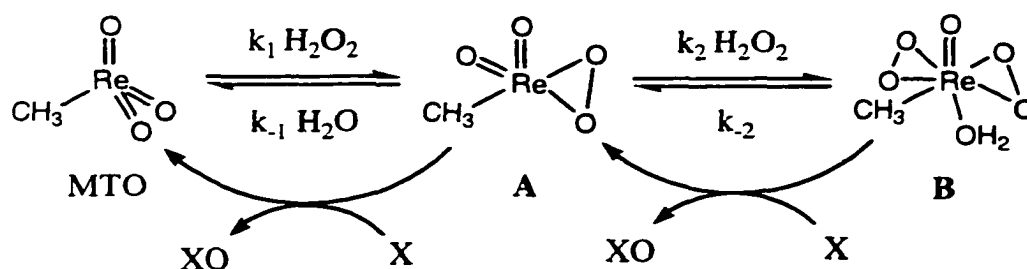


MTO catalyzes selective oxidation reactions with hydrogen peroxide as the oxygen source.¹⁰⁻¹³ Kinetics and mechanism of these reactions have been studied in detail. Peroxide activation is realized by the formation of two η^2 -peroxorhenium complexes, **A**

[MeRe(O)₂(η^2 -O₂)] and **B** [MeRe(O)(η^2 -O₂)₂(H₂O)]. Both of these complexes are capable of transferring oxygen atoms to various nucleophilic acceptors (X) in a catalytic cycle shown in **Scheme 1**. MTO also catalyzes various atom transfer reactions from a donor to an acceptor.¹⁴ In this second group of reactions, lower oxidation state rhenium intermediates, most importantly those of Re(V), have been postulated from kinetics evidence and sometimes detected.^{15,16}

Table 1. Spectroscopic features of MTO.

spectroscopy	signals
IR in CH ₂ Cl ₂	1000 (w), 967 (vs) cm ⁻¹
¹ H NMR in CDCl ₃	δ 2.63 (s) ppm
¹³ C NMR in CDCl ₃	δ 19.03 ppm
UV-Vis in H ₂ O	239 nm (ϵ 1900 L mol ⁻¹ cm ⁻¹)
	270 nm (ϵ 1300 L mol ⁻¹ cm ⁻¹)



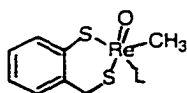
Scheme 1 Catalytic cycle for oxidations with MTO and H₂O₂.

Re(V)-Catalyzed Oxo-Transfer Reactions and Molecular Oxygen Activation

New classes of oxygen-atom transfer catalysts were discovered in our lab based on novel Re(V) compounds, e.g., MeReO(dithiolate)L (L = pyridine, phosphine, halide, etc.), where the dithiolate ligands are derived from H₂mtp (2-mercaptomethyl-thiophenol)^{17,18} and H₂edt (ethane-1,2-dithiol).¹⁹ Their parent dinuclear compounds, [MeReO(mtp or edt)]₂, made from the reaction between MTO and either dithiol, are key catalyst precursors, although none of these compounds activates molecular oxygen. Moreover, the Me-Re group often present in earlier catalysts was hardly essential to the success of catalytic reactions, as it

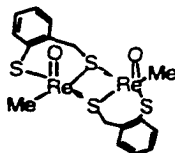
invariably emerged unchanged. In this work, the synthesis and characterization of a new thiolatorhenium(V) compound, $\text{Re}_2\text{O}_2(\text{mtp})_3$, **D₁**, from H_2mtp and dirhenium heptoxide, **Chart 1**, is reported. In addition to having a novel molecular structure, **D₁** proves not only a catalyst for O-atom transfer reactions like the others, but also the only stable Re(V) complex catalyzes oxidations with molecular oxygen.²⁰⁻²²

Chart 1

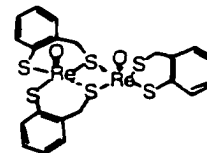


MeReO(mtp)L

(L = Py, PR_3 , X^- , etc.)



[MeReO(mtp)]₂



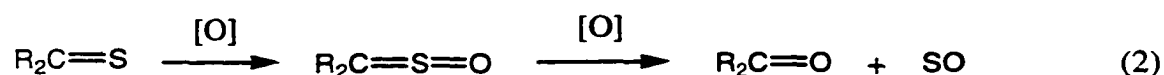
D₁: Re₂O₂(mtp)₃

D₁ was found to be a versatile catalyst for the oxidations of phosphines, arsines, stilbenes, sulfides, and dienes by pyridine N-oxides. Some of these reactions cannot be catalyzed by MeReO(mtp)L , e.g., the oxidation of sulfides and dienes; and by molecular oxygen. The corresponding oxidation products were obtained in high yields. Reactivity of **D₁** towards ligand coordination, detailed kinetics and mechanism for the **D₁**-catalyzed oxidation of *tris*(*para*-substituted phenyl)phosphines and methylphenylphosphines, as well as reactivity comparisons of phosphines and the other substrates toward oxidation were investigated by ^1H and ^{31}P NMR spectroscopy in benzene at 25 °C. These results and further investigations of compound **D₁** are summarized in chapters I, II, and III.

Sulfoxidations of Thioketones and Thioketone S-Oxides (Sulfines)

Thioketone S-oxides (sulfines) are attractive heterocumulenes exhibiting specific behavior towards various organic transformations involving thioepoxidation, cycloaddition or sulfur atom transfer reactions.²³⁻²⁵ Several routes have been developed for the synthesis of sulfines, however, most of these methods suffer from over-oxidation to ketones resulting in low yields of the desired products. Furthermore, most of these methods for synthesis cannot be conducted under ambient conditions, so either low temperature or inert atmosphere is required.

In the present study, hydrogen peroxide was found capable of oxidizing substituted aromatic thioketones and thiocamphor to their sulfines and ketones in the presence of catalytic amount of MTO (eq 2). The reactions were very rapid and were conducted at room temperature in aqueous acetonitrile solution. All thioketones were converted 100% to sulfines. The uncatalyzed reaction proceeds more than 10^3 times slower, thus no effort was made to exclude atmosphere oxygen. Kinetics and mechanism for both steps of oxidations were studied to see whether the peroxide was activated electrophilically or nucleophilically. ^1H NMR and UV-Vis methods were employed in the kinetics studies. Trapping experiments with 1,3-dienes were performed to identify the sulfur monoxide released from the oxidation of sulfines. Thiophene-1-oxides were found as the trapping products.

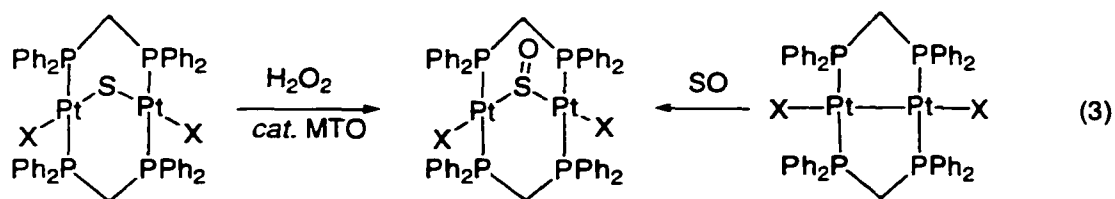


The oxidation rates for sulfines turned out to be less than 10^{-3} as rapid as those of their corresponding thioketones. When one equivalent of hydrogen peroxide vs thioketone was used the reaction stopped at the sulfine as the final product. The catalytic oxidation of thioketones with MTO by hydrogen peroxide is by far the most superior method for sulfine synthesis. With this method, sulfines were synthesized and isolated in >90% yields. Two of the previously unknown sulfines, 4, 4'-difluoro- and 3, 3'-bis(trifluoromethyl)-phenylthioketone S-oxides, were also prepared in high yields. The results of these investigations are summarized in chapters IV and V.

SO-Bridged Diplatinum Halides From Sulfoxidation and SO Insertion

The use of simple chemical methods to generate and examine the chemistry of reactive diatomic molecule, such as sulfur monoxide (SO), has attracted considerable amount of interest. However, relatively few studies have been carried out.^{26,27} Existing methods for generating and trapping SO have been proved unsatisfactory.²⁸ To explore further this chemistry, a more convenient source of SO was needed and alternative trapping reagents should be considered. The use of transition metal complexes also received much attention.²⁹ Small atom or molecules were known to insert into the Pt-Pt bond of $\text{Pt}_2(\text{dppm})_2\text{X}_2$, yielding

A-frame molecules $\text{Pt}_2(\text{dppm})_2\text{X}_2\mu\text{-Y}$ ($\text{Y} = \text{S}, \text{SO}_2, \text{CO}, \text{CH}_3\text{NC}, \text{etc.}$).³⁰ A few SO-bridged complexes were made by oxidation of the corresponding S-bridged complexes.³¹⁻³³



In this work, Two independent pathways leading to the formation of the first examples of SO-bridged diplatinum(I) complexes, $\text{Pt}_2(\text{dppm})_2(\mu\text{-SO})\text{X}_2$, $\text{X} = \text{Cl}, \text{I}$ (eq 3) are reported. The first method is the oxidation of $\text{Pt}_2(\text{dppm})_2(\mu\text{-S})\text{X}_2$ by hydrogen peroxide catalyzed by MTO. The reactions were performed in chloroform at room temperature. One equivalent of hydrogen peroxide was used to prevent over-oxidation. Both products were isolated in high yields and characterized by ^1H and ^{31}P NMR spectroscopy. The chloride derivative was also characterized by X-ray crystallography. When more than one equivalent peroxide was used, the SO-bridged complexes were further oxidized to the SO_2 -bridged compounds. The other method is to trap the SO released from the oxidation of sulfines by the Pt-Pt bonded complexes, $\text{Pt}_2(\text{dppm})_2\text{X}_2$. The sulfone bridged complexes, $\text{Pt}_2(\text{dppm})_2(\mu\text{-SO}_2)\text{X}_2$, were also prepared by SO_2 insertion. The first method, MTO catalyzed oxidation, is by far superior than any previously existing methods for making SO-bridged transition metal complexes. The reaction was carried out at ambient conditions and high yields of products were achieved. The results of these investigations are summarized in chapter VI.

Dissertation Organization

The dissertation consists of six chapters. Chapter I has been submitted as a communication to *Chemical Communications*. Chapter II and Chapter III correspond to two manuscripts accepted for publication in *Inorganic Chemistry* and *Journal of Molecular Catalysis* accordingly. Chapters IV and V correspond to two manuscripts published in *Journal of Organic Chemistry*. And Chapter VI has been published in *Organometallics*. Each chapter is self-contained with its own equations, figures, tables and references. Following the last manuscript is general conclusions. Except for X-ray structural analysis, all the work in this dissertation was performed by the author of this thesis.

References

- (1) Herrmann, W. A.; Cornils, B. *Applied Homogeneous Catalysis with Organometallic Compounds*; VCH: New York, 1996; Vol. 1-2.
- (2) Casey, C.P. *Science* **1993**, 259, 1552.
- (3) Holm, R. H. *Chem. Rev.* **1987**, 87, 1401.
- (4) Sheldon, R. A.; Kochi, J. K. *Metal-Catalyzed Oxidations of Organic Compounds*; Academic Press: New York, 1981.
- (5) Mayer, J. M. in *Advances in Transition Metal Coordination Chemistry*; Che, C.-M., Ed.; JAI Press: New York, 1996; Vol. 1, 105.
- (6) *Metalloporphyrins Catalyzed Oxidations*; Montanari, F.; Casella, L., Eds.; Kluwer Academic Publishers: Dordrecht, 1994.
- (7) Beattie, I. R.; Jones, P. J. *Inorg. Chem.* **1979**, 18, 2318.
- (8) Herrmann, W. A.; Fischer, R. W.; Marz, D. W. *Angew. Chem. Int. Ed. Engl.* **1991**, 30, 1638.
- (9) Herrmann, W. A.; Kuhn, F. E.; Fischer, R. W.; Thiel, R. W.; Ramao, C. C. *Inorg. Chem.* **1992**, 31, 4431.
- (10) Espenson, J. H.; Abu-Omar, M. M. *Adv. Chem. Ser.* **1997**, 253, 99.
- (11) Herrmann, W. A.; Kühn, F. E. *Acc. Chem. Res.* **1997**, 30, 169.
- (12) Gable, K. P. *Adv. Organomet. Chem.* **1997**, 41, 127.
- (13) Owens, G. S.; Arias, J.; Abu-Omar, M. M. *Catal. Today* **2000**, 55, 317.
- (14) Espenson, J. H. *Chem. Commun.* **1999**, 479.
- (15) Abu-Omar, M. M.; Appelmann, E. H.; Espenson, J. H. *Inorg. Chem.* **1996**, 35, 7751.
- (16) Abu-Omar, M. M.; Espenson, J. H. *Inorg. Chem.* **1996**, 34, 6239.
- (17) Jacob, J.; Guzei, I. A.; Espenson, J. H. *Inorg. Chem.* **1999**, 38, 1040.
- (18) Jacob, J.; Guzei, I. A.; Espenson, J. H. *Inorg. Chem.* **1999**, 38, 3266.
- (19) Shan, X.; Espenson, J. H., unpublished results.
- (20) Eager, M. D.; Espenson, J. H. *Inorg. Chem.* **1999**, 38, 2533.
- (21) Böhm, G.; Wieghardt, K.; Nuber, B.; Weiss, J. *Angew. Chem., Int. Ed. Engl.* **1990**, 29, 787.

- (22) Herrmann, W. A.; Roesky, P. W.; Wang, M.; Scherer, W. *Organometallics* **1994**, *13*, 4531.
- (23) Zwanenburg, B. *Recl. Trav. Chim. Pays-Bas* **1982**, *101*, 1.
- (24) Adam, W.; Deeg, O.; Weinkotz, S. *J. Org. Chem.* **1997**, *62*, 7084.
- (25) Braverman, S.; Grinstein, D.; Gottlieb, H. *J. Chem. Soc., Perkin Trans. 1*, **1998**, 103.
- (26) Abu-Yousef, I. A.; Harpp, D. N. *Sulfur Rep.* **1997**, *20*, 1.
- (27) Abu-Yousef, I. A.; Harpp, D. N. *Tetrahedron Lett.* **1995**, *36*, 201.
- (28) Harpp, D. N. *Phosphorus, Sulfur, Silicon Relat. Elem.* **1997**, *120/121*, 41.
- (29) Schenk, W. A. *Angew. Chem. Int. Ed. Engl.* **1987**, *26*, 98.
- (30) Muralidharan, S.; Espenson, J. H.; Ross, S. A. *Inorg. Chem.* **1986**, *25*, 2557.
- (31) Gong, J. K.; Fanwich, P. E.; Kubiak, C. P. *J. Chem. Soc. Chem. Commun.* **1990**, 1190.
- (32) Chihara, T.; Tase, T.; Ogawa, H.; Wakatsuki, Y. *Chem. Commun.* **1999**, 279.
- (33) Lorenz, I. -P.; Messelhäuser, J.; Hiller, W.; Huag, K. *Angew. Chem. Int. Ed. Engl.* **1985**, *24*, 228.

CHAPTER I. SYNTHESIS, CHARACTERIZATION, AND MOLECULAR STRUCTURE OF AN OXORHENIUM(V) COMPOUND, $\text{Re}_2(\text{O})_2(\text{MTP})_3$ ($\text{MTPH}_2 = 2\text{-MERCAPTOMETHYLTHIOPHENOL}$) AND ITS ACTIVATION OF MOLECULAR OXYGEN

A communication submitted to Chemical Communications

Ruili Huang, Ilia A. Guzei and James H. Espenson*

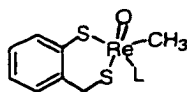
Introduction

Oxorhenium complexes are potent catalysts for oxo-transfer reactions, but to date not for O_2 activation. Most notably, MeReO_3 catalyzes oxygen atom transfer from hydrogen peroxide to a nucleophilic acceptor:¹⁻³



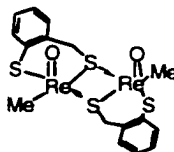
Oxygen-atom transfer can also be catalyzed by the Re(V) compounds $\text{MeReO}(\text{mtp})\text{L}$, where mtpH_2 is 2-mercaptomethylthiophenol and L is pyridine, phosphine, halide, etc.,⁴⁻⁶ **Chart 1**.

Chart 1 Structural formulas of oxorhenium(V) compounds

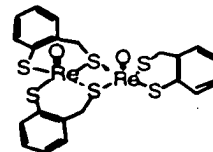


$\text{MeReO}(\text{mtp})\text{L}$

($\text{L} = \text{Py}, \text{PR}_3, \text{X}^-, \text{etc.}$)

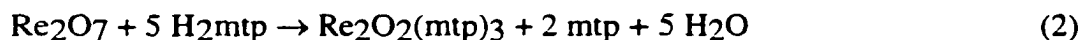


$[\text{MeReO}(\text{mtp})]_2$



D1: $\text{Re}_2\text{O}_2(\text{mtp})_3$

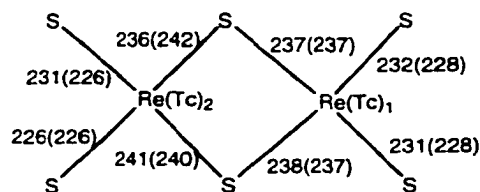
The usual Me-Re group seems hardly essential to the success of catalytic reactions, as it invariably emerges unchanged. We have now isolated $\text{Re}_2\text{O}_2(\text{mtp})_3$, **D1**. In addition to having a novel molecular structure, it proves not only to catalyze O-atom catalyst like the others, but also oxidations with molecular oxygen. **D1** was prepared from 2-mercaptomethylthiophenol^{7,8} and dirhenium heptoxide:⁹



Results and Discussion

D1 was characterized by elemental analysis¹⁰ and spectroscopically, including its mass spectrum,¹¹ UV-Vis spectrum,¹² and ¹H and ¹³C NMR spectra.¹³ The ¹H NMR spectrum of **D1** in the region of the CH₂ groups showed six doublets of equal intensity. Clearly the three methylene groups are inequivalent, each being split by the proton on the same carbon, showing that the three mtp ligands of **D1** are inequivalent. The crystallographic results¹⁴ are fully consistent with the spectroscopic conclusions. The ORTEP diagram from the crystal structure solution is given in **Figure 1**.

Each rhenium atom lies in a distorted square-pyramid with the two S₄Re=O units sharing the S(1)–S(3) edge and the two axial Re=O groups on the same side. In the Re(1) pyramid the four sulfur atoms S(1), S(2), S(3), S(4) are planar within 3 pm with the Re(1)=O(1) vector at 178.5(1)° to the basal plane. The Re(1) atom is situated 74.2(1) pm above the basal plane. The corresponding parameters for the Re(2) pyramid comprise 15 pm, 179.8(1)° and 73.9(1) pm, respectively. The two Re=O bond distances are practically the same (168 pm), and fall well into the region for terminal rhenium–oxo bonds. The bond distances in the diamond core, given in **Table S-1**, show that the Re–S bond lengths are nearly the same, averaging 238 pm for bonds to a bridged sulfur and 230 pm otherwise, as shown (to ± 1 pm) in this diagram (values in parentheses are for the technetium complex):



The rhenium atoms are inequivalent; one has a coordinated mtp group unshared with the second rhenium, along with sulfur atoms bridging from each of two mtp ligands. The other rhenium atom has two chelating mtp ligands, one sulfur atom of each also being coordinated to the other atom. The dihedral angle between the basal planes defined by atoms S(1), S(2), S(3), S(4) and S(1), S(2), S(5), S(6) is 112.86(3)°. The technetium edt complex (TcO)₂(edt)₃,

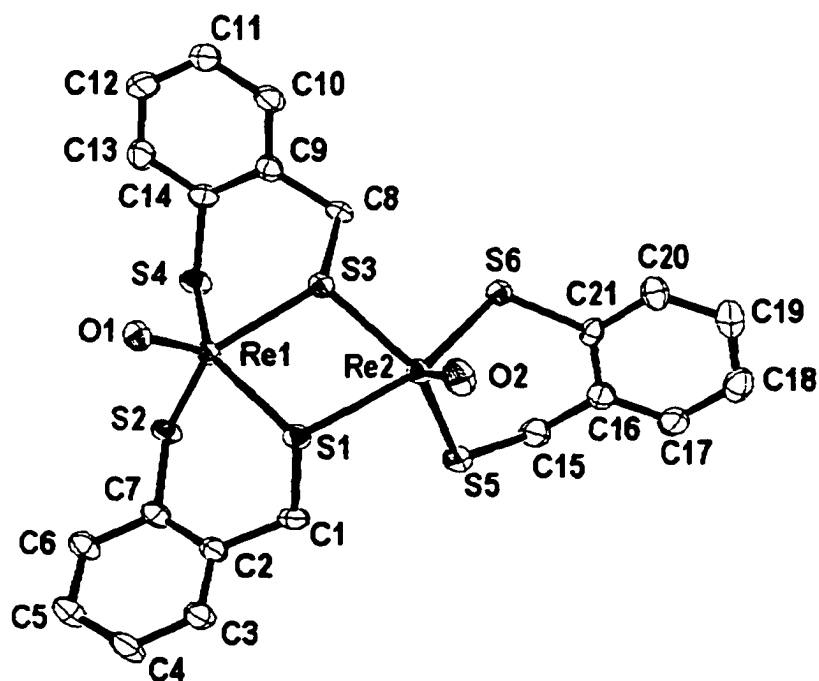


Figure 1. Perspective view of the dinuclear rhenium (V) compound **D1** with thermal ellipsoids at the 40% probability level. Selected bond lengths (pm) and angles (°): Re(1)–O(1) 167.6(3); Re(1)–S(1) 237.65(12); Re(1)–S(2) 230.97(12); Re(1)–S(3) 237.43(11); Re(1)–S(4) 231.82(12); Re(2)–O(2) 168.3(3); Re(2)–S(1) 241.39(12); Re(2)–S(3) 236.40(11); Re(2)–S(5) 225.53(13); Re(2)–S(6) 231.27(12); S(2)–Re(1)–S(4) 81.23(4); O(1)–Re(1)–S(3) 108.70(11); O(1)–Re(1)–S(1) 109.95(11); S(1)–Re(1)–S(3) 74.91(4); S(5)–Re(2)–S(6) 91.62(4); O(2)–Re(2)–S(3) 112.26(12); O(2)–Re(2)–S(1) 104.22(11); S(1)–Re(2)–S(3) 74.41(4); Re(1)–S(1)–Re(2) 102.16(4); Re(1)–S(3)–Re(2) 103.74(4).

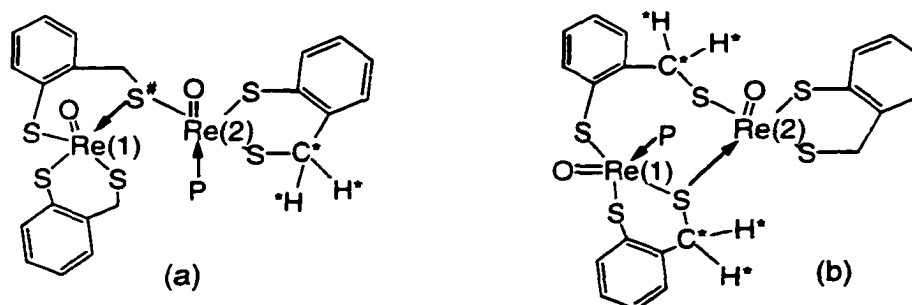
made from [n-Bu₄N] [TcOCl₄] and H₂edt was found to have a structure more symmetrical than that of **D1**.¹⁵ The technetium complex has two square-pyramidal Tc atoms and three edt ligands, one of which is a terminal edt ligand coordinated to one Tc and two bridging edt ligands to the other. Unlike **D1**, which has absolutely no symmetrical element in the structure, (TcO)₂(edt)₃ has a symmetry plane along the Tc–Tc axis. The M–S bond lengths in the two compounds are quite comparable, as shown in the above diagram. The bridging M–S–M angles are ~103° in the rhenium compound and ~100° in the technetium compound. The dihedral angle of the two square-pyramid basal planes in the technetium compound is 106°, compared to 113° in the rhenium compound.

D1 is the first example of a rhenium complex with this type of structure. There are other examples of thiolato complexes with a core composed of two edge-sharing square-pyramids, each pyramid having a transition metal in the center, four sulfur atoms in the basal plane, two of which are bridging sulfurs connecting the two pyramids (see the Diagram above). These complexes are usually bridged by two elemental sulfur atoms, or less commonly, sulfides. The axial atoms/groups can be oxygens, sulfurs, oxygen–sulfur mixed, and sometimes cyclopentadienyl groups. The two axial groups can be either on the same (cis), or opposite (trans) side of the pyramid basal planes. There is only one example of a rhenium (V) complex, with two trans axial sulfur atoms.¹⁶ The most common central transition metal is molybdenum, with ligands composed of both sulfur and nitrogen, due to their biological importance.¹⁷ Other transition metals include, tungsten,¹⁸ titanium,¹⁹ vanadium²⁰ and zirconium.²¹

D1 reacts rapidly (<0.5 s) with phosphines forming the adducts R₃P-**D1** with R₃P coordinated to the rhenium center. Spectroscopic data showed that only one phosphine is coordinated, probably due to steric hindrance of the phosphines. The ¹H, ¹³C, COSY and ¹H-¹³C spectra²² for **D1** and Ph₃P-**D1** confirmed that Ph₃P-**D1** was formed through nucleophilic attack of the phosphine on Re(2) not Re(1), **Chart 2**. The ¹H chemical shifts of the methylene protons in each dithiolate ligand are more alike after phosphine coordination owing to free rotation around the #S–Re(2) bond; the ¹³C spectrum shows only one

methylene carbon (*C) shifted significantly down-field after coordination.). The ^{31}P NMR resonances of **D1**-PR₃ are shifted upfield of the resonance for the free phosphine.²³

Chart 2. Structural formulas probable (a) and less likely (b) of **D1**-PR₃



Molecular Oxygen Activation by **D1**

The oxidation of (*p*-YC₆H₄)₃P and Me_nPh_{3-n}P by molecular oxygen is unimportant without a catalyst during the times required to complete the catalytic oxidation. In air, less than 5% Ar₃P=O was found after 24 h, and for Tol₃P none occurred in 8 h. With **D1** as a catalyst (1-5% of phosphine), successful oxidations were carried out in benzene at room temperature and under air; the conversions were monitored by ^1H and ^{31}P NMR. The time periods for different phosphines to reach 100% conversion are given in **Table 1**. The major product (74–95% yield) is phosphine oxide, the balance being largely (80–90% of the remainder) phosphine sulfide accompanied by unidentified phosphorous compounds from side reactions between phosphine and the dithiolate ligands of **D1**. Phosphine sulfide formation was greatly reduced or eliminated by using less catalyst.

Summary

The new dimeric Re(V) thiolato complex **D1** was synthesized in high yield and characterized. **D1** proves to be a facile oxidase, converting phosphines to phosphine oxides.

References

- (1) Herrmann, W. A.; K  hn, F. E. *Acc. Chem. Res.* **1997**, *30*, 169.
- (2) Gable, K. P. *Adv. Organomet. Chem.* **1997**, *41*, 127.
- (3) Espenson, J. H. *Chem. Commun.* **1999**, 479.
- (4) Jacob, J.; Guzei, I. A.; Espenson, J. H. *Inorg. Chem.* **1999**, *38*, 1040.

- (5) Jacob, J.; Guzei, I. A.; Espenson, J. H. *Inorg. Chem.* **1999**, *38*, 3266.
- (6) Shan, X.; Espenson, J. H., unpublished results.
- (7) Klingsberg, E.; Schreiber, A. M. *J. Am. Chem. Soc.* **1962**, *84*, 2941.
- (8) Hortmann, A. G.; Aron, A. J.; Bhattacharya, A. K. *J. Org. Chem.* **1978**, *43*, 3374.
- (9) 2-Mercaptomethyl-thiophenol (3.0 g, 19 mmol) was added to a solution of Re_2O_7 (1.5 g, 3.1 mmol) in 20 mL THF. The dark brown solution was left to stand at room temperature for 2.5 h. Then 70 mL hexane was added, and the reaction mixture was kept at $-11\text{ }^\circ\text{C}$ for 2 days. After filtering and extensive washing with hexane, the product **D₁** was isolated in 85% yield as a dark solid. Yellow needle-shaped crystals suitable for x-ray diffraction were obtained by slow evaporation of a benzene solution of **D₁** at room temperature for one week.
- (10) For $\text{Re}_2\text{O}_2(\text{mtp})_3 0.5 \text{ C}_6\text{H}_6$: C 31.70 found (31.81 calcd), H 2.45 (2.34), S 21.03 (21.23). The benzene given here was also found in the crystallographic determination.
- (11) MS (ESI): 868 (**D₁H⁺**).
- (12) UV-Vis in benzene, $\lambda_{\text{max}}(\epsilon)/\text{nm}$: 390 (5 200), 420 (3 800).
- (13) ^1H NMR/ CDCl_3 : δ/ppm : 7.50–7.35 (m, 8H, arom), 7.30–7.15 (m, 4H, arom), 5.67 (d, 1H, CH_2 , $J = 11.2$), 5.21 (d, 1H, CH_2 , $J = 11.2$), 5.06 (d, 1H, CH_2 , $J = 12.4$), 4.30 (d, 1H, CH_2 , $J = 11.6$), 3.75 (d, 1H, CH_2 , $J = 12.4$), 3.62 (d, 1H, CH_2 , $J = 11.2$); ^{13}C NMR/ CDCl_3 : δ/ppm : 140.92, 140.36, 139.71, 139.02, 135.70, 135.47, 131.07, 130.94, 130.90, 130.58, 130.56, 130.38, 129.22, 128.97, 128.85, 128.70, 128.54, 128.42, 42.29, 40.92, 38.90.
- (14) X-ray crystal data for compound **D₁** ($\text{C}_{21}\text{H}_{18}\text{O}_2\text{Re}_2\text{S}_6 0.5 \text{ C}_6\text{H}_6$): monoclinic, C2/c , $a = 35.2466(18) \text{ \AA}$, $b = 7.5740(4) \text{ \AA}$, $c = 20.8584(11) \text{ \AA}$, $\alpha = 90^\circ$, $\beta = 106.9931(10)^\circ$, $\gamma = 90^\circ$, $V = 5325.2(5) \text{ \AA}^3$, $Z = 8$, $T = 173(2) \text{ K}$, $D_{\text{calcd}} = 2.261$

Mg/m³, R(F) = 2.50% for 5433 independent observed ($I \geq 2(I)$) reflections ($4 \leq 2 \leq 53^\circ$). All non-hydrogen atoms were refined with anisotropic displacement coefficients. All hydrogen atoms were included in the structure factor calculation at idealized positions and were allowed to ride on the neighboring atoms with relative isotropic displacement coefficients. There is also half a molecule of solvate benzene per molecule of complex in the asymmetric unit. All software and sources of the scattering factors are contained in the SHELXTL (version 5.1) program library (G. Sheldrick, Bruker Analytical X-Ray Systems, Madison, WI). Absorption corrections were carried out by programs SADABS (Blessing, R. H. *Acta Cryst.* 1995, A51, 33–38).

- (15) Davison, A.; DePamphilis, B. V.; Faggiani, R.; Jones, A. G.; Lock, C. J. L.; Orvig, C. *Can. J. Chem.* **1985**, 63, 319.
- (16) Goodman, J. T.; Rauchfuss, T. B. *Inorg. Chem.* **1998**, 37, 5040.
- (17) (a) Muller, A.; Reinsch-Vogell, U.; Krickemeyer, E.; Bogge, H. *Angew. Chem. Int. Ed. Engl.* **1982**, 21, 796 (b) Miller, W. K.; Haltiwanger, R. C.; VanDerveer, M. C.; Dubois, M. R. *Inorg. Chem.* **1983**, 22, 2973; (c) Pan, W.-H.; Harmer, M. A.; Halbert, T. R.; Stiefel, E. I. *J. Am. Chem. Soc.* **1984**, 106, 459; (d) Lee, C. C.; Halbert, T. R.; Pan, W.-H.; Harmer, M. A.; Wei, L.; Leonowicz, M. E.; Dim, C.O.B.; Miller, K. F.; Bruce, A. E.; McKenna, S.; Corbin, J. L.; Wherland, S.; Stiefel, E. I. *Inorg. Chim. Acta* **1996**, 243, 147; (e) Howlader, N. C.; Haight Jr. G. P.; Hambley, T. W.; Snow, M. R.; Lawrance, G. A. *Inorg. Chem.* **1984**, 23, 1811; (f) Alyea, E. C.; Ferguson, G.; Parvez, M.; Somogyvari, A. *Polyhedron* **1985**, 4, 783; (g) Coucouvanis, D.; Koo, Sang-Man *Inorg. Chem.* **1989**, 28, 2; (h) Xin, X.; Jin, G.; Wang, B.; Pope, M. T. *Inorg. Chem.* **1990**, 29, 553; (i) Chou, J.-H.; Hanko, J. A.; Kanatzidis, M. G. *Inorg. Chem.* **1997**, 36, 4; (j) Barber, D. E.; Bryan, R. F.; Sabat, M.; Bose, K. S.; Averill, B. A. *Inorg. Chem.* **1996**, 35, 4635; (k) Coucouvanis, D.; Toupadakis, A.; Lane, J. D.; Koo, S. M.; Kim, C. G.; Hadjikyriacou, A. *J. Am. Chem. Soc.* **1991**, 113, 5271.
- (18) (a) Secheresse, F.; Lefebvre, J.; Daran, J. C.; Jeannin, Y. *Inorg. Chem.* **1982**, 21, 1311; (b) Rajan, O. A.; McKenna, M.; Noordik, J.; Haltiwanger, R. C.; DuBois,

- M. R. *Organometallics*, **1984**, 3, 831; (c) Pan, W.-H.; Chandler, T.; Enemark, J. H.; Stiefer, E. I. *Inorg. Chem.* **1984**, 23, 4265; (d) Mackay, M. F.; Oliver, P. J.; Young, C. G. *Aust. J. Chem.* **1989**, 42, 837; (e) Chakrabarty, P. K.; Ghosh, I.; Bhattacharyya, R.; Mukherjee, A. K.; Mukherjee, M.; Helliwell, M. *Polyhedron* **1996**, 15, 1443.
- (19) (a) Firth, A. V.; Witt, E.; Stephan, D. W. *Organometallics*, **1998**, 17, 3716; (b) Nadasdi, T. T.; Stephan, D. W. *Inorg. Chem.* **1993**, 32, 5933.
- (20) Zhu, H.; Liu, Q.; Huang, X.; Wen, T.; Chen, C.; Wu, D. I. C., 37, 2678 *Inorg. Chem.* **1998**, 37, 2678.
- (21) Heyn, R. H.; Stephan, D. W. *Inorg. Chem.* **1995**, 34, 2804.
- (22) ^1H NMR/ CDCl_3 : δ/ppm : 7.82 (m, 6H, arom., ligand), 7.57 (m, 9H, arom., ligand), 7.70 (d, 1H, arom., $J = 8.8$), 7.55-7.03 (m, 10H, arom.), 6.78 (d, 1H, arom., $J = 7.6$), 4.96 (d, 1H, CH_2 , $J = 11.6$), *4.94 (d, 1H, CH_2 , $J = 12.8$), *4.62 (d, 1H, CH_2 , $J = 12.4$), 4.54 (d, 1H, CH_2 , $J = 12.0$), 3.50 (d, 1H, CH_2 , $J = 11.6$), 3.01 (d, 1H, CH_2 , $J = 11.6$). (* See Chart 2a.)
- (23) ^{13}C NMR/ CDCl_3 : δ/ppm : 141.76 (arom.), 141.43 (arom.), 141.31 (arom.), 137.80 (d, arom., ligand, $^1J_{\text{P-C}} = 312$), 137.37 (d, arom., ligand, $^2J_{\text{P-C}} = 42$), 134.73 (d, arom., ligand, $^3J_{\text{P-C}} = 35.6$), 132.65 (arom.), 132.52 (arom.), 132.48 (arom.), 132.40 (arom.), 131.84 (d, arom., ligand, $^4J_{\text{P-C}} = 10$), 130.92 (arom.), 130.67 (arom.), 130.50 (arom.), 130.43 (arom.), 130.34 (arom.), 129.66 (arom.), 129.26 (arom.), 129.12 (arom.), 127.48 (arom.), 127.24 (arom.), 126.91 (arom.), *51.07 (CH_2), 41.71 (CH_2), 41.16 (CH_2). (* See Chart 2a.)
- (24) The ^{31}P NMR resonances, δ/ppm for $\text{D}_1\text{-P}(\text{C}_5\text{H}_5\text{Y})_3$ for coordinated (and free) ligands are: Y = CH_3O $\delta = -9.31$ (-6.99); CH_3 , -6.98 (-5.98); H, -4.50 (-6.64); Cl, -8.70 (-7.95); CF_3 , -5.63 (-9.10); MePh_2P , -26.29 (-19.21); Me_2PhP , -45.54 (-34.92).

Table 1. Conversion, reaction times, and yields of phosphine oxides for (p-YC₆H₄)₃P and PMe_nPh_{3-n}^a

Y	time for 100% conversion (h)	yield (%)
CH ₃ O	10	85
CH ₃	20	95
H	40	90
Cl	25	95
CF ₃	15	90
PMePh ₂	2.5	85
PMe ₂ Ph	1.5	74

^a Using 50 mM PR₃ in benzene under air. Diffusion of air into the solution completes the reaction.

Supporting Information

Table S–1. Crystal data and structure refinement for **D1**

Empirical formula	C₂₄H₂₁O₂Re₂S₆	
Formula weight	906.17	
Temperature	173(2) K	
Wavelength	0.71073 Å	
Crystal system	Monoclinic	
Space group	C2/c	
Unit cell dimensions	a = 35.2466(18) Å	α = 90°.
	b = 7.5740(4) Å	β = 106.9931(10)°
	c = 20.8584(11) Å	γ = 90°.
Volume	5325.2(5) Å³	
Z	8	
Density (calculated)	2.261 Mg/m³	
Absorption coefficient	9.577 mm⁻¹	
F(000)	3416	
Crystal size	0.50 × 0.20 × 0.10 mm³	
Theta range for data collection	2.04 to 26.37°.	
Index ranges	-44 ≤ h ≤ 42, 0 ≤ k ≤ 9, 0 ≤ l ≤ 26	
Reflections collected	23432	
Independent reflections	5433 [R(int) = 0.0410]	
Completeness to theta = 26.37°	99.6 %	
Absorption correction	Empirical with SADABS	
Max. and min. transmission	0.4477 and 0.0866	
Refinement method	Full-matrix least-squares on F²	
Data / restraints / parameters	5433 / 3 / 307	
Goodness-of-fit on F ²	1.023	
Final R indices [I > 2σ(I)]	R1 = 0.0250, wR2 = 0.0533	

Table S-1. (continued)

R indices (all data)	R1 = 0.0343, wR2 = 0.0554
Largest diff. peak and hole	1.252 and -0.866 e.Å ⁻³

Table S-2. Atomic coordinates (Å × 10⁴) and equivalent isotropic displacement parameters (Å² × 10³) for **D1**. U(eq) is defined as one-third of the trace of the orthogonalized U^{ij} tensor.

	x	y	z	U(eq)
Re(1)	1066(1)	1463(1)	4987(1)	20(1)
Re(2)	2036(1)	3565(1)	5858(1)	20(1)
S(1)	1330(1)	4054(1)	5597(1)	23(1)
S(2)	651(1)	1002(2)	5648(1)	27(1)
S(3)	1740(1)	1555(1)	4989(1)	22(1)
S(4)	1104(1)	-1590(2)	5055(1)	29(1)
S(5)	2038(1)	3825(2)	6936(1)	29(1)
S(6)	2571(1)	1654(2)	6148(1)	26(1)
O(1)	778(1)	2007(4)	4221(2)	31(1)
O(2)	2206(1)	5386(4)	5570(2)	33(1)
C(1)	1135(1)	4383(6)	6315(2)	28(1)
C(2)	689(1)	4519(6)	6084(2)	27(1)
C(3)	509(2)	6094(6)	6165(3)	33(1)
C(4)	95(2)	6220(7)	5986(3)	39(1)
C(5)	-134(2)	4776(6)	5732(3)	33(1)
C(6)	42(1)	3195(6)	5636(3)	29(1)
C(7)	455(1)	3080(6)	5808(2)	25(1)
C(8)	1965(1)	-665(6)	5014(2)	24(1)
C(9)	1718(1)	-1737(6)	4450(2)	24(1)
C(10)	1863(1)	-2249(6)	3930(3)	29(1)

Table S-2. (continued)

C(11)	1636(2)	-3252(6)	3404(3)	34(1)
C(12)	1262(2)	-3762(7)	3397(3)	41(1)
C(13)	1104(2)	-3222(6)	3900(3)	36(1)
C(14)	1332(1)	-2232(6)	4433(2)	26(1)
C(15)	2467(1)	2763(7)	7526(3)	34(1)
C(16)	2860(1)	3102(6)	7431(3)	28(1)
C(17)	3165(2)	3875(6)	7932(3)	36(1)
C(18)	3539(2)	4108(7)	7856(3)	41(1)
C(19)	3616(2)	3569(6)	7278(3)	37(1)
C(20)	3313(1)	2829(7)	6772(3)	32(1)
C(21)	2937(1)	2613(6)	6839(2)	22(1)
C(22)	175(2)	7366(18)	2470(3)	117(3)
C(23)	358(4)	8980(20)	2438(5)	196(8)
C(24)	173(3)	10569(18)	2470(3)	142(5)

Table S-3. Bond lengths [Å] and angles [°] for **D1**.

Re(1)-O(1)	1.676(3)		
Re(1)-S(2)	2.3097(12)	C(5)-C(6)	1.390(6)
Re(1)-S(4)	2.3182(12)	C(6)-C(7)	1.395(6)
Re(1)-S(3)	2.3743(11)	C(8)-C(9)	1.483(6)
Re(1)-S(1)	2.3765(12)	C(9)-C(10)	1.382(6)
Re(2)-O(2)	1.683(3)	C(9)-C(14)	1.403(6)
Re(2)-S(5)	2.2553(13)	C(10)-C(11)	1.381(7)
Re(2)-S(6)	2.3127(12)	C(11)-C(12)	1.372(7)
Re(2)-S(3)	2.3640(11)	C(12)-C(13)	1.383(7)
Re(2)-S(1)	2.4139(12)	C(13)-C(14)	1.385(7)
S(1)-C(1)	1.840(5)	C(15)-C(16)	1.476(7)
S(2)-C(7)	1.790(5)	C(16)-C(21)	1.391(6)

Table S-3. (continued)

S(3)-C(8)	1.854(4)	C(16)-C(17)	1.393(7)
S(4)-C(14)	1.783(5)	C(17)-C(18)	1.383(7)
S(5)-C(15)	1.834(5)	C(18)-C(19)	1.374(8)
S(6)-C(21)	1.783(5)	C(19)-C(20)	1.384(7)
C(1)-C(2)	1.505(6)	C(20)-C(21)	1.382(6)
C(2)-C(3)	1.384(6)	C(22)-C(22)#1	1.274(16)
C(2)-C(7)	1.387(6)	C(22)-C(23)	1.390(14)
C(3)-C(4)	1.400(7)	C(23)-C(24)	1.382(15)
C(4)-C(5)	1.372(7)	C(24)-C(24)#1	1.258(19)
O(1)-Re(1)-S(2)	107.12(12)	C(2)-C(3)-C(4)	120.3(5)
O(1)-Re(1)-S(4)	108.18(12)	C(5)-C(4)-C(3)	120.0(5)
S(2)-Re(1)-S(4)	81.23(4)	C(4)-C(5)-C(6)	120.2(5)
O(1)-Re(1)-S(3)	108.70(11)	C(5)-C(6)-C(7)	119.6(5)
S(2)-Re(1)-S(3)	144.13(4)	C(2)-C(7)-C(6)	120.5(4)
S(4)-Re(1)-S(3)	89.41(4)	C(2)-C(7)-S(2)	123.5(4)
O(1)-Re(1)-S(1)	109.95(11)	C(6)-C(7)-S(2)	116.0(4)
S(2)-Re(1)-S(1)	91.29(4)	C(9)-C(8)-S(3)	109.1(3)
S(4)-Re(1)-S(1)	141.67(5)	C(10)-C(9)-C(14)	118.8(4)
S(3)-Re(1)-S(1)	74.91(4)	C(10)-C(9)-C(8)	120.7(4)
O(2)-Re(2)-S(5)	112.72(12)	C(14)-C(9)-C(8)	120.5(4)
O(2)-Re(2)-S(6)	104.96(11)	C(11)-C(10)-C(9)	121.2(4)
S(5)-Re(2)-S(6)	91.62(4)	C(12)-C(11)-C(10)	119.6(5)
O(2)-Re(2)-S(3)	112.26(12)	C(11)-C(12)-C(13)	120.5(5)
S(5)-Re(2)-S(3)	133.82(4)	C(12)-C(13)-C(14)	120.1(5)
S(6)-Re(2)-S(3)	86.63(4)	C(13)-C(14)-C(9)	119.7(4)
O(2)-Re(2)-S(1)	104.22(11)	C(13)-C(14)-S(4)	117.0(4)
S(5)-Re(2)-S(1)	85.04(4)	C(9)-C(14)-S(4)	123.3(4)
S(6)-Re(2)-S(1)	149.55(4)	C(16)-C(15)-S(5)	117.1(4)

Table S-3 (continued)

S(3)-Re(2)-S(1)	74.41(4)	C(21)-C(16)-C(17)	118.0(5)
C(1)-S(1)-Re(1)	111.48(16)	C(21)-C(16)-C(15)	120.5(4)
C(1)-S(1)-Re(2)	116.40(16)	C(17)-C(16)-C(15)	121.5(5)
Re(1)-S(1)-Re(2)	102.16(4)	C(18)-C(17)-C(16)	121.5(5)
C(7)-S(2)-Re(1)	108.97(15)	C(19)-C(18)-C(17)	120.1(5)
C(8)-S(3)-Re(2)	118.25(15)	C(18)-C(19)-C(20)	118.9(5)
C(8)-S(3)-Re(1)	113.17(15)	C(21)-C(20)-C(19)	121.4(5)
Re(2)-S(3)-Re(1)	103.74(4)	C(20)-C(21)-C(16)	120.1(4)
C(14)-S(4)-Re(1)	104.90(16)	C(20)-C(21)-S(6)	117.1(4)
C(15)-S(5)-Re(2)	113.15(17)	C(16)-C(21)-S(6)	122.9(4)
C(21)-S(6)-Re(2)	107.36(15)	C(22)#1-C(22)-C(23)	118.6(8)
C(2)-C(1)-S(1)	110.7(3)	C(24)-C(23)-C(22)	122.1(13)
C(3)-C(2)-C(7)	119.3(4)	C(24)#1-C(24)-C(23)	119.2(8)
C(3)-C(2)-C(1)	119.5(4)		
C(7)-C(2)-C(1)	121.2(4)		

Symmetry transformations used to generate equivalent atoms: #1 -x,y,-z+1/2

Table S-4. Anisotropic displacement parameters ($\text{\AA}^2 \times 10^3$) for **D1**. The anisotropic displacement factor exponent takes the form: $-2p^2 [h^2 a^{*2} U^{11} + \dots + 2 h k a^* b^* U^{12}]$.

	U ¹¹	U ²²	U ³³	U ²³	U ¹³	U ¹²
Re(1)	16(1)	18(1)	26(1)	0(1)	5(1)	1(1)
Re(2)	17(1)	17(1)	25(1)	1(1)	5(1)	-1(1)
S(1)	20(1)	18(1)	30(1)	-1(1)	7(1)	1(1)
S(2)	24(1)	20(1)	40(1)	0(1)	16(1)	0(1)
S(3)	18(1)	22(1)	25(1)	-2(1)	5(1)	1(1)
S(4)	33(1)	20(1)	41(1)	-2(1)	20(1)	-1(1)
S(5)	23(1)	35(1)	28(1)	-5(1)	5(1)	3(1)

Table S-4 (continued)

S(6)	21(1)	26(1)	28(1)	-6(1)	2(1)	4(1)
O(1)	24(2)	33(2)	32(2)	0(2)	2(2)	5(2)
O(2)	26(2)	25(2)	49(2)	9(2)	10(2)	-4(2)
C(1)	27(3)	26(2)	33(3)	-8(2)	13(2)	1(2)
C(2)	22(3)	26(3)	36(3)	-4(2)	11(2)	2(2)
C(3)	28(3)	25(3)	50(4)	-7(2)	18(3)	-3(2)
C(4)	26(3)	35(3)	57(4)	3(3)	15(3)	13(2)
C(5)	22(3)	34(3)	47(3)	6(3)	15(2)	6(2)
C(6)	21(3)	30(3)	40(3)	3(2)	14(2)	-1(2)
C(7)	23(3)	23(2)	30(3)	7(2)	10(2)	5(2)
C(8)	19(2)	24(2)	27(3)	-4(2)	7(2)	6(2)
C(9)	22(3)	20(2)	28(3)	1(2)	4(2)	5(2)
C(10)	23(3)	27(3)	39(3)	-4(2)	14(2)	-2(2)
C(11)	33(3)	35(3)	37(3)	-7(2)	14(3)	0(2)
C(12)	35(3)	40(3)	48(4)	-22(3)	14(3)	-6(2)
C(13)	24(3)	33(3)	50(4)	-13(3)	8(3)	-6(2)
C(14)	30(3)	20(2)	30(3)	0(2)	12(2)	4(2)
C(15)	31(3)	41(3)	27(3)	-1(3)	5(2)	5(2)
C(16)	25(3)	21(2)	34(3)	0(2)	3(2)	5(2)
C(17)	32(3)	35(3)	37(3)	-8(2)	2(3)	7(2)
C(18)	33(3)	31(3)	48(4)	-5(3)	-7(3)	3(2)
C(19)	25(3)	35(3)	46(4)	7(3)	0(3)	-5(2)
C(20)	25(3)	37(3)	30(3)	7(2)	2(2)	1(2)
C(21)	22(3)	19(2)	21(3)	2(2)	-2(2)	0(2)
C(22)	64(6)	185(11)	94(7)	-16(8)	11(6)	9(7)
C(23)	91(10)	163(14)	320(20)	45(14)	31(11)	-29(9)
C(24)	83(8)	171(10)	142(10)	69(10)	-16(9)	-17(7)

Table S-5. Hydrogen coordinates ($\times 10^4$) and isotropic displacement parameters ($\text{\AA}^2 \times 10^3$) for **D1**.

	x	y	z	U(eq)
H(1A)	1215	3381	6630	33
H(1B)	1248	5477	6556	33
H(3)	668	7094	6344	40
H(4)	-27	7306	6040	47
H(5)	-415	4856	5620	40
H(6)	-117	2200	5455	35
H(8A)	2237	-556	4975	28
H(8B)	1980	-1249	5445	28
H(10)	2123	-1905	3934	34
H(11)	1739	-3588	3048	41
H(12)	1109	-4491	3045	49
H(13)	840	-3531	3880	43
H(15A)	2477	3145	7985	40
H(15B)	2422	1472	7502	40
H(17)	3116	4251	8335	43
H(18)	3743	4642	8205	49
H(19)	3874	3702	7227	45
H(20)	3364	2461	6369	38
H(22)	308	6288	2447	140
H(23)	618	8984	2394	235
H(24)	304	11651	2448	171

CHAPTER II. A MECHANISTIC STUDY OF OXYGEN TRANSFER REACTION CATALYZED BY AN OXORHENIUM(V) COMPOUND

A manuscript submitted to *Inorganic Chemistry*[†]

Ruili Huang and James H. Espenson*

Abstract

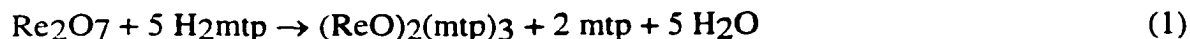
The new binuclear oxothiolatorhenium(V) compound, $\text{Re}_2\text{O}_2(\text{mtp})_3$ (**D1**, $\text{mtpH}_2 = 2$ -mercaptomethylthiophenol) was found to be an efficient catalyst for oxygen-transfer reactions. Electron donor ligands such as phosphines coordinate to one of the rhenium centers in **D1** strongly, breaking up one of the Re–S bridges. Dialkylsulfides coordinate weakly. Alkylarylsulfides, diarylsulfides, triphenylarsine and triphenylstibine, dienes and alkenes do not coordinate to **D1**. **D1** catalyzes the oxidation of phosphines, arsines, stilbenes, sulfides and dienes by pyridine N-oxides, and the oxidation of phosphines by dimethylsulfoxide. The kinetics and mechanism for the oxidation of triarylphosphines by pyridine N-oxides were investigated. The relative reactivities of all substrates were studied by competitive reactions. The order was found to be: phosphine > arsine > stilbene > sulfide > diene. The reaction is proposed to go through a Re(VII) intermediate with pyridine N-oxide as one of the ligands. The N–O bond was activated through coordination to rhenium and the oxygen atom was abstracted by a phosphine, forming a phosphine oxide.

Introduction

Oxygen atom transfer reactions are catalyzed by high-valent transition metal-oxo complexes, such as $\text{Re}^{\text{VII}}/\text{Re}^{\text{V}}$,¹⁻¹² $\text{Mo}^{\text{VI}}/\text{Mo}^{\text{IV}}$,^{13,14} and $\text{W}^{\text{VI}}/\text{W}^{\text{IV}}$.¹⁵⁻¹⁹ Molybdenum and tungsten systems have received the most attention because of their roles in biological systems. In such pairs, the oxidation states differ by two units in keeping with their role as oxotransferases; the metals exist in their highest oxidation states to stabilize the metal-oxo π

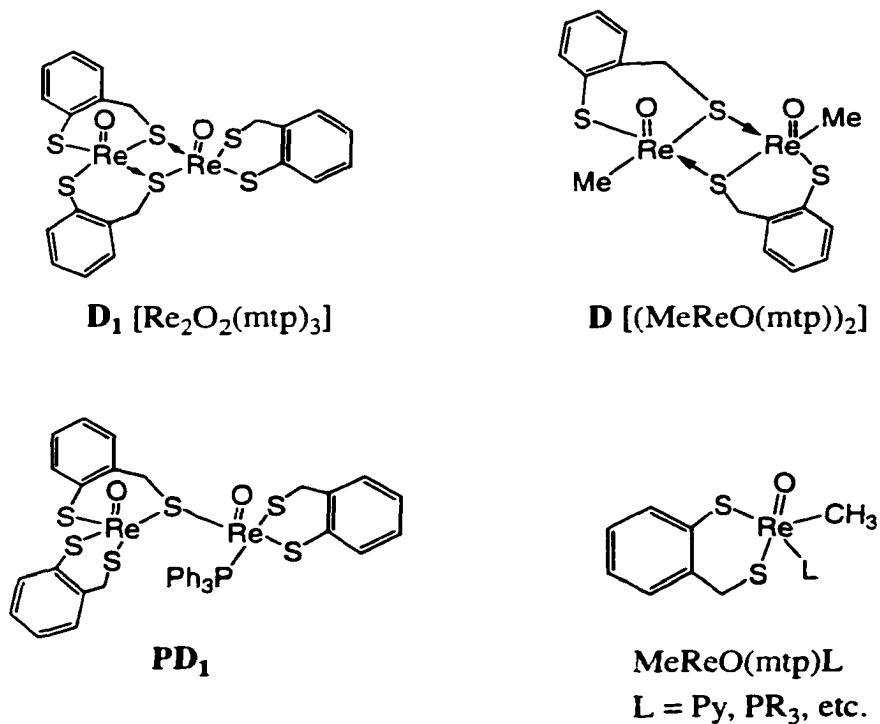
[†] Reproduced in part with permission from *Inorganic Chemistry*, submitted for publication. Unpublished work copyright 2000 American Chemical Society.

interaction. The most widely-studied rhenium compound is MeReO_3 (known as MTO), but in that case (only) a peroxo complex intervenes. A new oxorhenium(V) compound lacking the methyl group found in compounds prepared from MTO was recently described.²⁰ $(\text{ReO})_2(\text{mtp})_3$ was prepared from Re_2O_7 and mtpH_2 , which is 2-(mercaptomethyl)thiophenol, according to this equation:²⁰

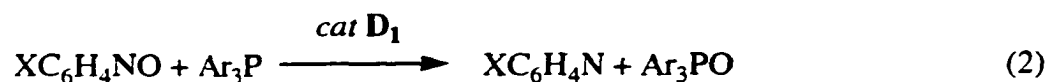


where the organic product mtp is the cyclic disulfide from the oxidation of mtpH_2 . The structure of the dirhenium compound, which we designate **D₁**, has been determined by X-ray crystallography.²⁰ Its structural formula, presented in **Chart 1**, bears certain similarities to the formulas of recently reported organometallic compounds with the mtp ligand, such as $[\text{MeReO}(\text{mtp})]_2$ and $\text{MeReO}(\text{mtp})\text{PPh}_3$.^{21,22} The structural formulas of these compounds

Chart 1. Structural formulas of key compounds in this study



are also given in **Chart 1**. Such comparisons led us to believe that **D1** might be a useful catalyst for oxygen-atom transfer reactions. This notion has been verified in a number of test cases, involving the **D1**-catalyzed oxidation of substrates such as phosphines, arsines, stilbenes, dialkyl sulfides and 1,3-dienes. The latter two substrates are notable, in that [MeReO(mtp)]₂ and MeReO(mtp)PPh₃ are unable to serve as catalysts for such oxidations. We have undertaken a study of oxygen atom transfer reactions catalyzed by **D1**, with the greatest emphasis being placed on O-atom transfer from pyridine N-oxides (XC₅H₄NO, X = MeO, Me, CN) to phosphines.



Experimental Section

The catalyst **D1** was prepared according to eq. 1. The details of this preparation and the structural and analytical characterization of the catalyst have been reported previously.²⁰ The other compounds were obtained commercially.

The intensity of the UV-Visible absorption spectrum of **D1** is so high (see **Figure 1**) that it masks the absorbance changes accompanying the conversion of the substrates to products in eq. 2. Thus spectrophotometry could not be used to record the reaction progress. All reactions were followed by ¹H or ³¹P NMR spectroscopy using a Bruker DRX-400 spectrometer. Benzene-d₆ was used as the solvent for kinetics measurements, most of which were carried out at 25.0 °C, except for reactions at -35 °C, where toluene-d₈ was employed. The ¹H chemical shifts were measured relative to the residual proton content of C₆D₅H at δ 7.15, and C₆D₅CD₂H at δ 2.09. Chemical shifts for ³¹P were referenced to 85% H₃PO₄. The intensities of the proton resonances were measured relative to a known concentration of tert-butyl alcohol, used as an internal standard, allowing the conversion of intensities into concentrations. These determinations were all carried out under Ar, because **D1** also catalyzes the oxidation of phosphines by O₂,²⁰ which we find to be remarkable in that its close relative, [MeReO(mtp)]₂ neither activates O₂ nor is oxidized by it.

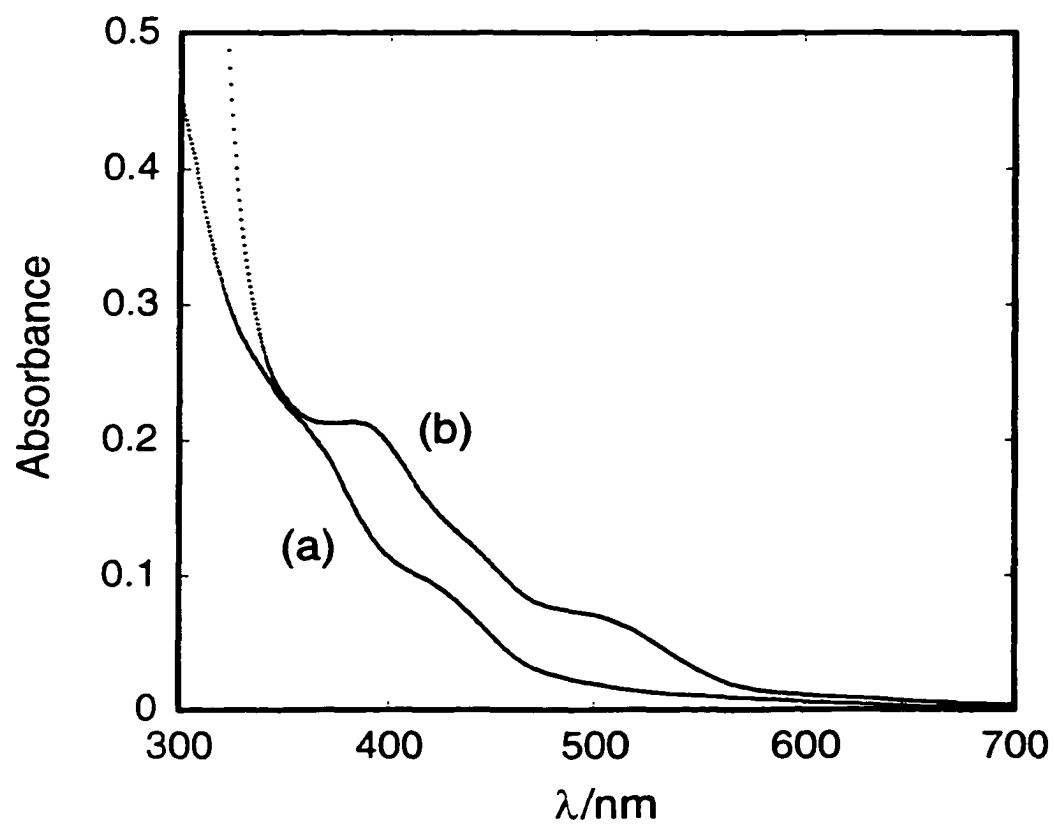


Figure 1. UV-Visible spectrum of the intensely-absorbing compound $\text{Re}_2\text{O}_2(\text{mtp})_3$ (**D₁**) (a) and its complex with triphenylphosphine (b).

Kinetic Data. Typical of catalytic reactions, the kinetics data do not fit a simple mathematical form owing to Michaelis-Menten behavior. Consequently, the method of initial rates was used.²³ The integrated NMR intensities were converted to concentrations and concentration-time data was then converted to a typically fifth-order polynomial function by means of the program KaleidaGraph. The initial rate v_i , in units $\text{mol L}^{-1} \text{s}^{-1}$ is then seen from this expression to be given by the coefficient m_1 :

$$C_t = C_0 - m_1 t - m_2 t^2 - m_3 t^3 \dots \quad (3)$$

Results

Rhenium–ligand intermediates, (a) phosphines and disulfides. Mixing **D1** and an equimolar amount of any of the phosphines led rapidly to the quantitative formation of a 1:1 adduct whose formula we represent as **PD1**, as indicated by ^1H and ^{31}P NMR data. A second phosphine ligand does not coordinate. On the other hand, AsPh_3 and SbPh_3 do not coordinate to **D1**, possibly for Lewis basicities. Dimethyl sulfide coordinates to **D1** weakly according to the ^1H NMR spectra which are broadened upon adding Me_2S . No reaction was observed between **D1** and MeSPh or Ph_2S , which are weaker Lewis bases and, more importantly we believe, larger.

The UV spectra of **D1** and **PD1** are substantially different, **Figure 1**. Although this is a rapid transformation, it is not instantaneous. A typical stopped-flow experiment for the reaction between **D1** and PPh_3 is displayed in **Figure 2**.

The equilibrium position in this reaction lies far to the right:



NMR spectroscopy was used to characterize the phosphine adducts. Data for eight phosphines were obtained, including $\text{P}(p\text{-YC}_6\text{H}_4)_3$, PPh_2Me , and PPhMe_2 . **Table 1** summarizes the spectroscopic data used to confirm the formation of the 1:1 adduct (2Re:1P). In these reactions one of the sulfido-rhenium bridges is broken, and the dimeric structure is sustained by the one remaining.

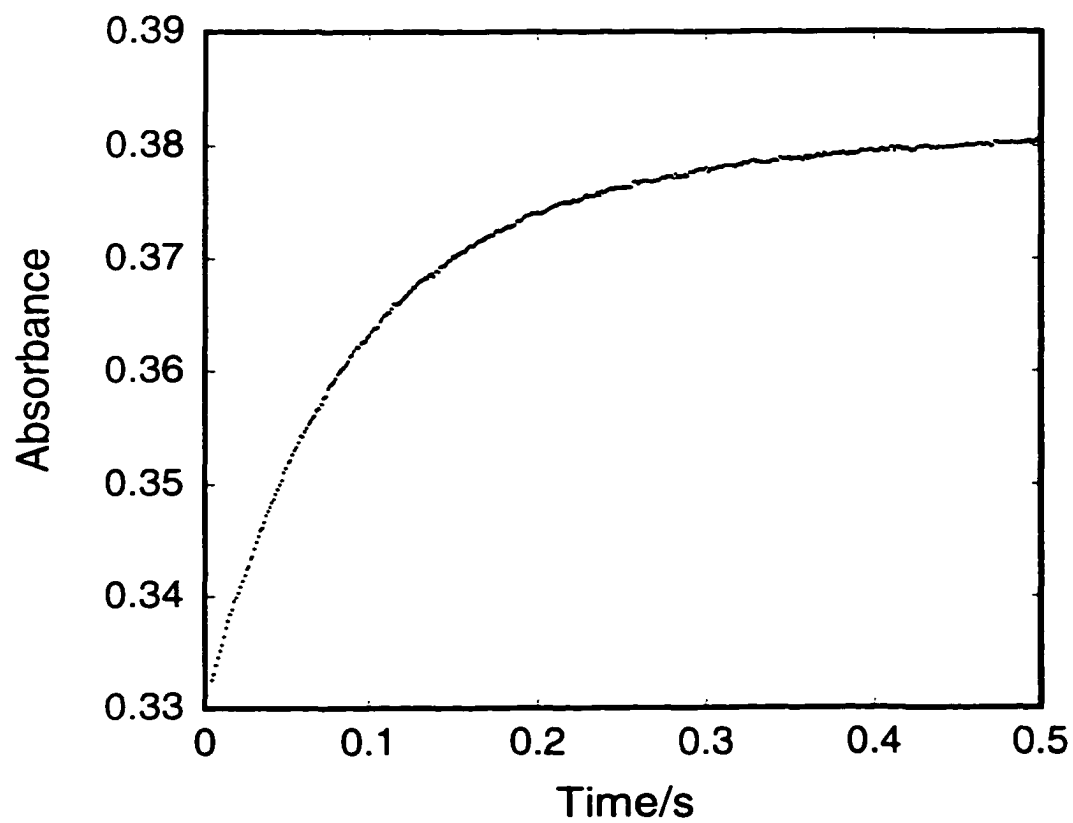


Figure 2. A stopped-flow experiment for the reaction between **D₁** (25 $\mu\text{mol L}^{-1}$) and PPh_3 (250 $\mu\text{mol L}^{-1}$) as monitored at 500 nm.

Rhenium–ligand intermediates, (b) pyridines, halides, amines. The addition of a pyridine to **D1** in solution does not lead to the corresponding **PyD1**, however. Instead, irreversible monomerization occurs, forming a new anion, $[\text{ReO}(\text{mtp})_2]^-$. The counter cation is an unidentified species containing Re, O, and mtp. The reaction in C_6D_6 and CD_3CN was complete by the time the first ^1H NMR spectrum could be recorded, ca. 1 min. A reaction was carried out using 3.5 mM **PD1** and 15 mM 4-MeC₅H₄N in C_6D_6 at 25 °C. **PD1** decomposed entirely in 12 h, yielding 5.2 mM $[\text{ReO}(\text{mtp})_2]^-$, 3.5 mM free PPh₃ and 3.6 mM of Py coordinated to an oxorhenium complex. It lacks any NMR signature other than that of Py. Mass balance provides the formula Py_2ReO_x . The initial step appears to be Py coordination to **PD1**, which was explored by NMR at 240 K. With equimolar concentrations of Py and **PD1**, ^1H and ^{31}P signals were seen for **PD1Py**.²⁴ With more py, the **PD1Py** signals first increased and then decreased as signals for free PPh₃, $[\text{ReO}(\text{mtp})_2]^-$ and Py_2ReO_x were building up. Excess PyO was then added, which caused **PD1Py** to disappear immediately and some Ph₃PO to be formed. As the solution warmed to room temperature, quantitative formation of Ph₃PO was realized.

The anion can also be formed from the known²⁵ compound $[\text{ReO}(\text{SPh})_4]^-$ by exchanging the PhS[−] ligands with mtpH₂, an exchange driven by the relative Lewis basicities of the RS[−] ligands and particularly by the chelate effect. This anion was characterized on the basis of mass spectrometry and ^1H and ^{13}C NMR spectroscopies.²⁶ The same monomerization reaction between **D1** and other small ligands also occurs with amines and halides, added as $[\text{Bu}_4\text{N}]^+\text{X}^-$.

Rhenium–ligand intermediates, (c) pyridine N-oxides and dimethylsulfoxide. The oxidation of **D1** by these oxygen-donor reagents causes the dithiolate ligands to be lost; mostly they are oxidized to mtp (the cyclic disulfide). The rhenium is oxidized to rhenium oxides; the latter material was not simply Re₂O₇, but appears to contain some residual coordinated mtp as well. Dimethylsulfide or pyridine formation accompanies these

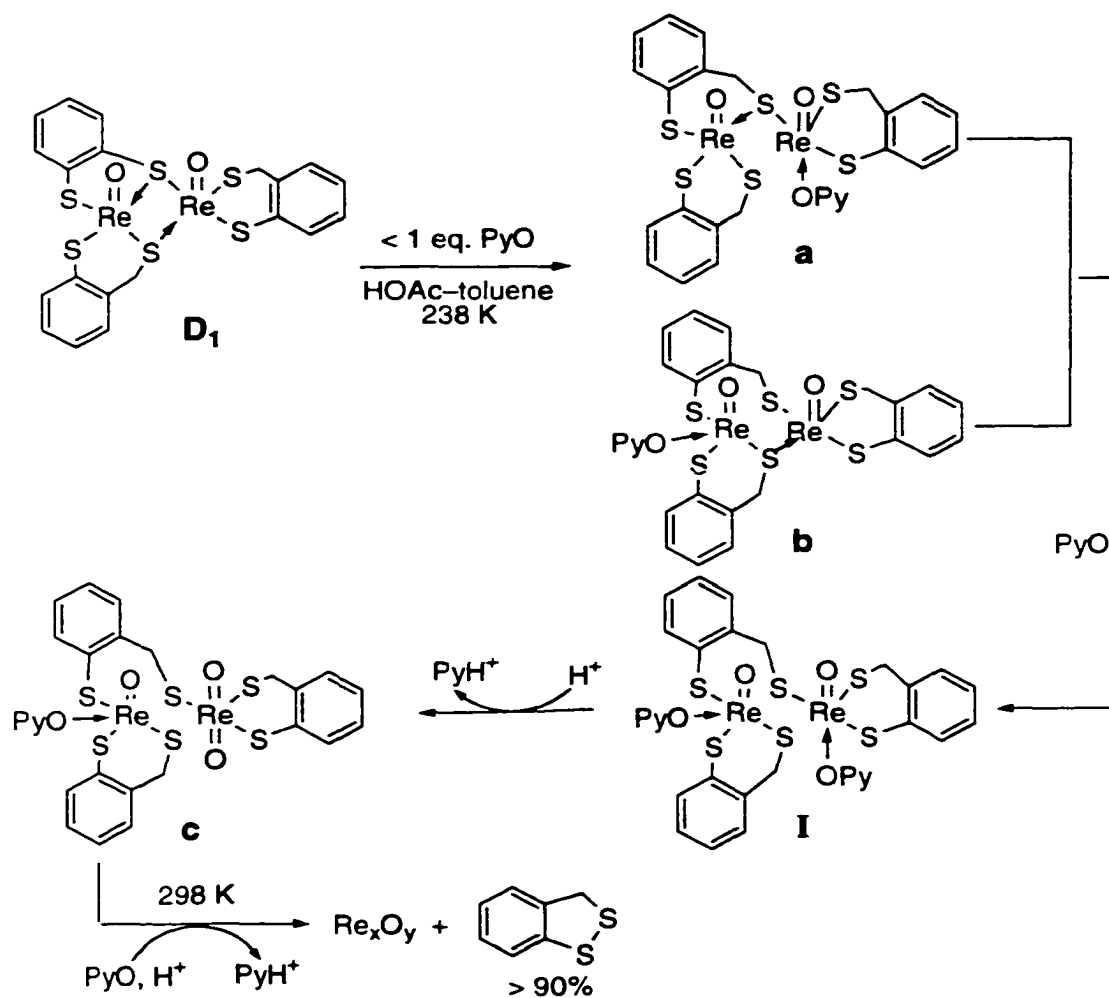
transformations. In C_6D_6 , pyridine N-oxides react much more rapidly than DMSO, as monitored by 1H NMR spectroscopy.

Even though pyridine coordinates to **D1** very rapidly, the coordination of pyridine N-oxide is ultimately favored. In an experiment with *p*-MeC₅H₄N and *p*-MeC₅H₄NO at the same concentration, **D1** was oxidized to mtp and rhenium oxides by the pyridine N-oxide rather than being monomerized by the pyridine. When one adds Py first and PyO immediately thereafter, some $ReO(mtp)_2^-$ was formed, but most of the **D1** was oxidized.

The reaction between **D1** and PyO was also carried out in the presence an oxygen-accepting reagent. These included phosphines, sulfides, and 1,3-dienes. In such cases, the O atom transferred to rhenium from PyO or DMSO (O-transfer to phosphine only) was then transferred to the given reagent, which restored **D1**. In these cases, therefore, **D1** acts as a catalyst for oxygen transfer. Discovering the reaction scheme for this catalytic cycle and the mechanism by which it takes place is the principal objective of this research. For that reason, it was important to characterize the interaction between **D1** and PyO. It occurs too rapidly for study by room temperature 1H NMR spectroscopy, so low-temperature experiments were carried out, as described in the next section. One consequence of this is that **D1** itself is not present at a detectable level during the catalytic oxidation reactions; the "resting state" of the catalyst in phosphine-containing solution is the more stable form, **PD1**.

Interaction of D1 and PyO studied by low-temperature NMR. A solution of **D1** was prepared in toluene-*d*₈ with excess acetic acid, so as to protonate any pyridine generated from the reaction and prevent it from coordinating to rhenium. The temperature was adjusted to $-35\text{ }^\circ C$, and PyO was added in small portions, with PyO:**D1** ratios of $R = 0.2, 0.6, 1.5, 2.0$ and 4.5 . Each solution was monitored at that temperature by 1H and COSY NMR spectroscopies. With $R < 1$, two **D1**-PyO adducts **a** and **b** were formed. The relative intensities of the signals in the NMR spectra²⁷ were used to show that each contained a 1:1 ratio of **D1** and PyO. The relative proportions of **a** and **b** were 1.2:1. Free PyO or Py were not detected, and the balance of **D1** remained as such. When more PyO was added, two new species were observed. One is a metastable species designated **I**, which has two PyO

coordinated to a single **D1**. The other species, formed from **I** and designated **c**, has a single PyO coordinated to a partially-oxidized **D1**. The aromatic proton signals of the three PyO ligands were clearly resolved for **a**, **b** and **c**, whereas **I** existed only admixed with the other species, thus obscuring the methylene ^1H signals; data for **I** were obtained.²⁸ As more PyO was added, the signals from **I** decreased, and free Py and more of species **c** grew in. Further addition of PyO did not, however, convert **c** into other products. When the temperature was allowed to increase to 25 °C, all of the **D1** derivatives were oxidized to oxorhenium species and the mtp ligands were oxidized to the disulfide within 10 min. The reactions involved are



Scheme 1. Reactions between **D1** and PyNO.

summarized in **Scheme 1**. The structural formulas of **a** and **b** may be reversed; they were assigned simply on an assumption of relative Lewis basicities.

O-atom transfer: competitive oxidation experiments. Before a presentation of the results of a direct study of the reaction kinetics, it is useful to consider experiments designed to measure the relative rates of formation of two phosphine oxides when a pair of phosphines was used in a single reaction. In these experiments the concentrations were 0.05–0.10 mM **D1**, 30–60 mM mM PyO, and 2–30 mM of each phosphine, which we represent as P^a and P^b . The concentration of each phosphine oxide, $P^a=O$ and $P^b=O$ was determined by the integration of the 1H or ^{31}P NMR signals at various times during the reaction. To analyze these data, let us assume (on the basis of the results of kinetics data to be presented in a subsequent section, that the step in which $P=O$ is formed proceeds at a rate given by

$$\frac{d[P^i=O]}{dt} = {}^ik[P^i][Int] \quad (5)$$

in which "Int" represents an intermediate common to each. Two such equations, for P^a and P^b , were divided, giving:

$$\frac{d[P^aO]/dt}{d[P^bO]/dt} = \left(\frac{{}^ak}{{}^bk} \right) \frac{[P^a]}{[P^b]} \quad (6)$$

Integration of eq 6 between the limits $t = 0$ and t gives this expression:

$$\ln ([P^a]_0 - [P^aO]_t) = \frac{{}^ak}{{}^bk} \ln ([P^b]_0 - [P^bO]_t) + C \quad (7)$$

This method allows the evaluation of the reactivity ratio for any pair of phosphines. The concentration of each phosphine oxide was determined over time from the integrations of the NMR signals. Each logarithmic term was evaluated, and one plotted against the other. An example for the case $P^a = P(C_6H_4-p-OMe)_3$ and $P^b = P(C_6H_4-p-Me)_3$ is shown in **Figure 3**. The data define a straight line within the precision of the results, consistent with

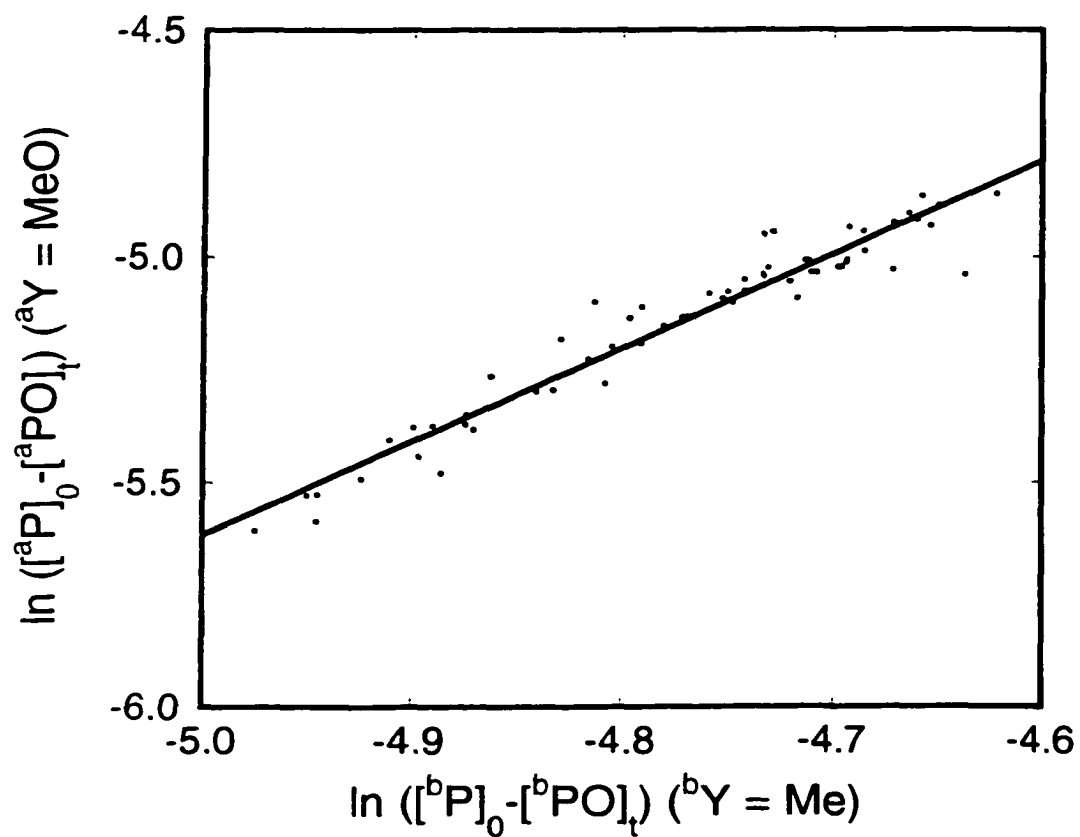


Figure 3. Kinetic data for the concurrent and competitive oxidation reactions for $\text{P}(\text{C}_6\text{H}_4\text{-}p\text{-OMe})_3$ and $\text{P}(\text{C}_6\text{H}_4\text{-}p\text{-Me})_3$ by 4-MeC₅H₄NO at 25 °C. The rate constant ratio is given by the slope of this double logarithmic plot, according to eq 7.

eq. 7. The slope of the line gives the rate constant ratio, in this case with a value of 2.1 in favor of the methoxy- over the methyl-substituted triaryl phosphine. To test that this method gives results that are independent of the PyO used, similar experiments were carried out with 4-NCC₅H₄NO using the same pair of triaryl phosphines. As it happens, the rate constant ratio was again 2.1, proving the point.

Various combinations of P^a and P^b were then used in a pairwise manner, with concentrations and partners chosen so that a balance between the two reactions would be maintained. For P(C₆H₄-*p*-Y)₃, the combinations studied were ^aY/^bY = MeO/Me, MeO/H, Cl/H, Cl/CF₃, and CF₃/H. The reactivities of AsPh₃ and SbPh₃ were also determined by the same method, except that a 10–20-fold excess over PPh₃ was needed, since these reagents are considerably less reactive than the phosphine. The rate constant ratios so determined were normalized relative to that for PPh₃ (*k*_{rel} = 1.000). The values of *k*_Y/*k*_H, and of log(*k*_Y/*k*_H), are presented in **Table 2**. Data for two comparison systems are also presented. They are the oxidation of PAr₃ by a peroxorhenium compound, MeReO(O₂)₂(OH₂),²⁹ and by the ruthenium porphyrin compound, *trans*-Ru(TMP)(O)₂.³⁰

O-atom transfer: reaction kinetics for triarylphosphines. The kinetics of the reactions of PyO with various phosphines were determined, and some competition experiments were also carried out for AsPh₃, SbPh₃, Me₂S, MeSTol, 2-methyl-1,3-pentadiene and cyclohexene. The reactions were carried out in the presence of a catalytic amount of **D1** (<1%); it was confirmed that **PD1** is the only form of rhenium that could be detected during the catalytic oxidations. Control experiments showed that no reaction occurred without the catalyst. Both the disappearance of the substrate and the buildup of the product were monitored by ¹H NMR spectroscopy.

For purposes of kinetics two phosphines were used, P(4-YC₆H₄)₃, Y = MeO and H; the pyridine N-oxide was 4-MeC₅H₄NO. Data were obtained in benzene at 25 °C under argon. Unlike the competition experiments, phosphines were used separately and not in pairs. Four ¹H NMR signals were monitored with time: PAr₃, PyO, Ar₃PO and Py. The products were formed in a 1:1 ratio, confirming the stoichiometry shown in eq. 2. In all experiments,

[PyO] was greater than [PAr₃], and both were \gg [PD₁], usually set at 1×10^{-4} M. Kinetics data were analyzed by the initial rate method. The initial rate was evaluated as a function of [PD₁] with 7.4 mM PPh₃, 90.0 mM PyO, and 100 mM HOAc, over the range 42–100 μ M. This showed that v_i is directly proportional to the catalyst concentration.

The initial rate data are given in **Table 3**. For P(4-MeOC₆H₅)₃, the data (**Table 3**, part a) clearly show that the initial rate is independent of the phosphine concentration and directly proportional to the PyO concentration. (See **Figure S–1** in the **Supporting Information**). Thus the rate law is

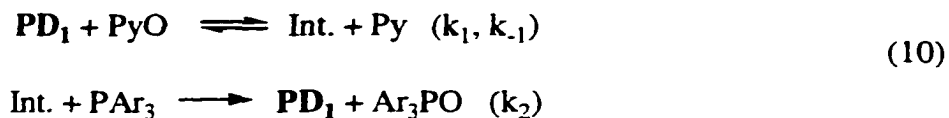
$$v_i = k_1[\text{PD}_1] \cdot [\text{PyO}] \quad (8)$$

where $k_1 = 0.24 \text{ L mol}^{-1} \text{ s}^{-1}$ in benzene at 25 °C. This suggests that the rate is controlled by a reaction between PD₁ and PyO and that PAr₃ enters the reaction cycle at a later and more rapid step. The step with PAr₃ involved directly was studied in the previously-described competition experiments using pairs of phosphines. As far as the kinetics go, it is both the concentration of PAr₃ and its rate constant that together determine whether the rate limit given in eq. 8 can be sustained.

To test this point, we moved from P(4-MeOC₆H₅)₃, the most reactive of the phosphines, to PPh₃, the least reactive (refer to **Table 2**). Included in this set (**Table 3**, part b) were several experiments in which acetic acid was added to protonate the released pyridine, eliminating any possible effect from it. Another series was then run with 17–36 mM pyridine added, a level higher than would be produced in the reaction. An inhibiting effect of pyridine was evident at the highest concentrations. The initial rates for these experiments take the form

$$v_i = \frac{k_1[\text{PD}_1] [\text{PyO}]_0 [\text{PPh}_3]_0}{\frac{k_{-1}}{k_2} [\text{Py}]_0 + [\text{PPh}_3]_0} \quad (9)$$

The rate law suggests a scheme of (at least) two reactions. In sketchy form, it is



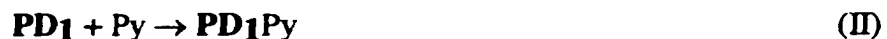
With HOAc present, the first denominator term will be absent; the same is true when the first term is much less than [PPh₃], which is usually so even without added HOAc. Analysis of these data (see **Figures S-2 and S-3** in the Supporting Information) afford these values: $k_1 = 0.20 \pm 0.04 \text{ L mol}^{-1} \text{ s}^{-1}$ and $k_{-1}/k_2 = 0.59$. This value of k_1 differs slightly from $0.24 \text{ L mol}^{-1} \text{ s}^{-1}$ because a different phosphine is present in **PD**₁; also, the presence of acetic acid may cause a minor medium effect.

O-atom transfer: other substrates. Sulfides (Me₂S and MeSTol) can be used in place of phosphines in the reaction with 4-MeC₅H₄NO, catalyzed by **D**₁ (<1%). Sulfide oxidation is comparable in rate to the self-oxidation of the mtp ligands of **D**₁, which stopped the reaction before sulfoxide formation was complete. When PTol₃ and MeSTol were used together, with PTol₃ just 0.2% of MeSTol, no sulfoxide was detected until all the Tol₃PO had been formed. With less than 0.2% of PTol₃, a mixture of the phosphine oxide and sulfoxide was detected. From that we estimate from the ratio of products that PTol₃ is ca. 5×10^2 times more reactive than MeSTol (this refers to the relative values of k_2 in eq. 10).

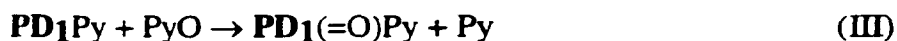
An attempt was made to oxidize 2-methyl-1,3-pentadiene with the **D**₁-PyO combination, but only disulfide from oxidation of the mtp ligand was detected. Another oxidant, di-*tert*-butyl peroxide was successful with **D**₁ as a catalyst. With 250 mM peroxide, 25 mM diene, and 2.0 mM **D**₁, about 30% of the epoxide was formed in 6 h. Cyclohexene was not oxidized under the same conditions.

Discussion

Direct evidence was obtained for these two reactions, as cited previously. Both reactions are very rapid and both occur to completion

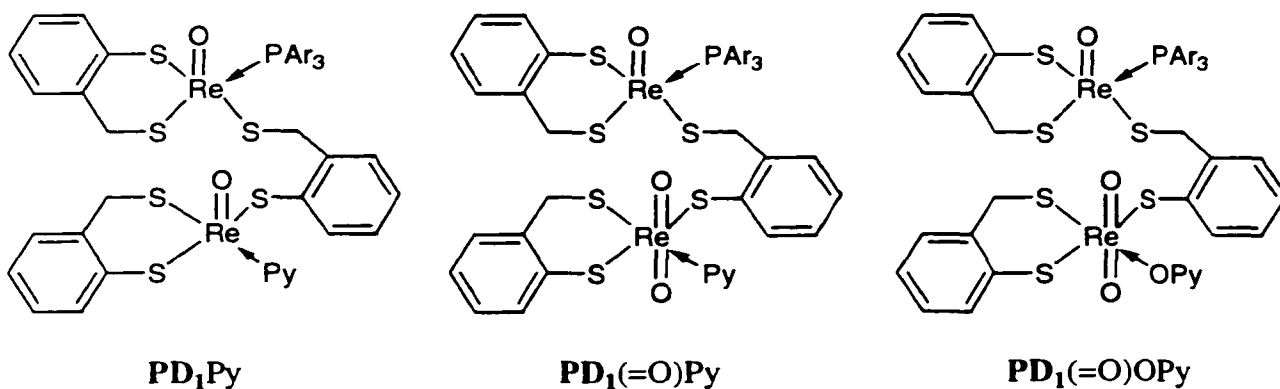


The structure of **PD₁Py** was not determined; our suggestion is given in **Chart 2** (see also **Chart 1**). This species can interact with PyO, removing an oxygen atom, thereby oxidizing one of the Re atoms to Re(VII). This generates the important intermediate **PD₁(=O)Py**, which the data identifies as the important recycling form of the catalyst. The chemical equation is

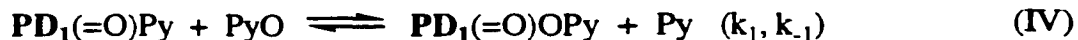


This reaction is driven not only by the previously-cited preference for PyO over Py as a ligand, but particularly by the decrease in Gibbs energy when Re(V) is oxidized to Re(VII) by PyO. The dissociation energies lie in the order Re–O > Py–O. A double-labeling experiment was carried out with YPyO to which XPy was added at the beginning of the reaction. No XPyO was detected at any point, showing that reaction III is irreversible. Clearly, once Py has been released, it cannot be reincorporated into any PyO.

Chart 2. Suggested structures for the reaction intermediates



The first of two competing rate-controlling steps is also a reaction of PyO important in the kinetics. It is a reversible reaction with Py as a product:

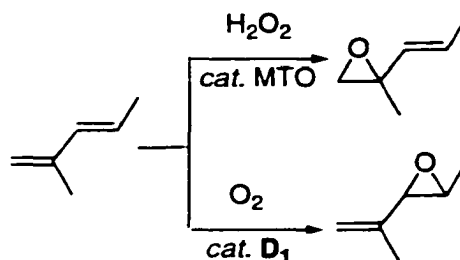


This step represents a PyO-for-Py ligand replacement reaction. It is crucial, giving rise to the species that actually leads to O-atom transfer:

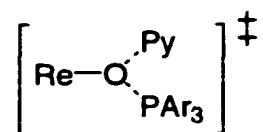


In this step it seems highly probable that the oxygen atom being transferred is not that of $\text{Re}=\text{O}$, but of $\text{Re}-\text{O}-\text{Py}$. On the basis of the presumed bond energies, which are not known here but can be roughly estimated from species closely related, $B(\text{Re}=\text{O}) \gg B(\text{Py}-\text{O})$, the $\text{Py}-\text{O}$ bond may be weakened further by PyO coordination. Reaction V is not limited to the most reactive phosphine reagents, but occurs as well for $\text{X} = \text{AsPh}_3$, SbPh_3 , Me_2S and *trans*-3-methyl-1,3-pentadiene. The latter two reagents, and perhaps all four, would be unable to abstract an oxygen atom from $\text{Re}=\text{O}$. It is not possible, however, to design a labeling experiment, since ultimately all oxygen atoms derive from PyO .

A different epoxide is formed from the diene with this rhenium catalyst as compared to the result when oxidation occurs with H_2O_2 and MTO is the catalyst.³¹



Rate comparisons can be made concerning the group of PAr_3 compounds studied here with two other cases from the literature. One is the $\text{H}_2\text{O}_2/\text{MTO}$ case, where oxidation occurs from a peroxo rhenium group. The other is a reaction in which a $\text{Ru}=\text{O}$ group of a metalloporphyrin, *trans*- $\text{Ru}(\text{TMP})(\text{O})_2$, is attacked directly by PAr_3 , AsPh_3 , or SbPh_3 . These LFER correlations have been attempted (see **Table 2** and **Figures S-5** and **S-6** in the Supporting Information). Neither correlation, however, is particularly persuasive.



Reaction V is accelerated by ring substituents in the series $P(C_6H_5Y)_3$. In terms of electronic influence, the effect is irregular. The rate order (**Table 2**) follows this rather unusual ordering of Y: $MeO > Me \gg Cl > CF_3 \sim H$. These are the only data, however, and an overinterpretation is hardly justified. In the presumed transition state for V, one can easily envisage opposing effects of electron density that could give rise to this trend.

References

- (1) Owens, G. S.; Arias, J.; Abu-Omar, M. M. *Catal. Today* **2000**, *55*, 317-363.
- (2) Yudin, A. K.; Sharpless, K. B. *J. Am. Chem. Soc.* **1997**, *119*, 11536.
- (3) Weiner, D. P.; Wiemann, T.; Wolfe, M. M.; Wentworth, P., Jr; Janda, K. D. *J. Am. Chem. Soc.* **1997**, *119*, .
- (4) Herrmann, W. A.; Roesky, P. W.; Wang, M.; Scherer, W. *Organometallics* **1994**, *13*, 4531-4535.
- (5) Gable, K. P.; Brown, E. C. *Organometallics* **2000**, *19*, 944.
- (6) Rybak, W. K.; Zagicek, A. *J. Coord. Chem.* **1992**, *26*, 79.
- (7) Dirghangi, B. K.; Menon, M.; Banerjee, S.; Chakravotry, A. *Inorg. Chem.* **1997**, *36*, 1095.
- (8) Arterburn, J. B.; Nelson, S. L. *J. Org. Chem.* **1996**, *61*, 2260.
- (9) Over, D. E.; Critchlow, S. C.; Mayer, J. M. *Inorg. Chem.* **1992**, *31*, 4643.
- (10) Kim, Y.; Gallucci, J.; Wojcicki, A. *J. Am. Chem. Soc.* **1991**, *112*, 8600.
- (11) Bryan, J. C.; Stenkamp, R. E.; Tulip, T. H.; Mayer, J. M. *Inorg. Chem.* **1987**, *26*, 2283.
- (12) Conry, R. R.; Mayer, J. M. *Inorg. Chem.* **1990**, *29*, 4862-4867.
- (13) Hille, R. *Chem. Rev.* **1996**, *96*, 2757-2816.
- (14) Johnson, M. K.; Rees, D. C.; Adams, M. M. W. *Chem. Rev.* **1996**, *96*, 2817.
- (15) Adams, M. W. W. *Soc. Appl. Microbiol. Symp. Ser.* **1999**, *28*, 108S-117S.
- (16) Juszczak, A.; Aono, S.; Adams, M. W. W. *J. Biol. Chem.* **1991**, *266*, 13834-41.
- (17) Schmitz, R. A.; Albracht, S. P. J.; Thauer, R. K. *Eur. J. Biochem.* **1992**, *209*, 1013-18.
- (18) Taya, M.; Hinoki, H.; Kobayashi, T. *Agric. Biol. Chem.* **1985**, *49*, 2513-15.

- (19) Winter, J.; Lerp, C.; Zabel, H. P.; Wildenauer, F. X.; Koenig, H.; Schindler, F. *Syst. Appl. Microbiol.* **1984**, *5*, 457-66.
- (20) Huang, R.; Espenson, J. H. *Angew. Chem., Int. Ed. Engl.* submitted for publication.
- (21) Lente, G.; Espenson, J. H. *Inorg. Chem.* **2000**, *39*, 0.
- (22) Wang, Y.; Espenson, J. H. submitted for publication.
- (23) Hall, K. J.; Quickenden, T. I.; Watts, D. W. *J. Chem. Educ.* **1976**, *53*, 493.
- (24) **PD₁Py₂**, ¹H: 9.07 (d, 2H, Py1, arom), 8.95 (d, 2H, Py2, arom), 6.40 (d, 2H, Py1, arom), 6.29 (d, 2H, Py2, arom), 6.50-7.80 (m, 27H, arom), 5.22 (d, 1H), 5.10 (d, 1H), 4.74 (d, 1H), 4.66 (d, 1H), 4.45 (d, 1H), 3.06 (d, 1H), 1.69 (s, 3H, Py1), 1.63 (s, 3H, Py2); ³¹P, -5.84 ppm.
- (25) Dilworth, J. R.; Neaves, B. D.; Hutchinson, J. P.; Zubieta, J. A. *Inorg. Chim. Acta* **1982**, *65*, L223-L224.
- (26) Spectroscopic data in CD₃CN for [ReO(mtp)₂]⁻ are as follows: ¹H NMR: δ 7.35 (d, 2H, arom, J = 7.6), 7.27 (d, 2H, arom, J = 7.6 Hz), 7.16 (t, 2H, arom, J = 7.2 Hz), 7.08 (t, 2H, arom, J = 7.2 Hz), 4.74 (d, 2H, CH₂, J = 11.6 Hz), 3.25 (d, 2H, CH₂, J = 12.0 Hz) ppm; ¹³C NMR: δ 133.18 (arom), 133.08 (arom), 130.65 (arom), 130.53 (arom), 40.00 (CH₂) ppm; MS (ESI): 510 (anion).
- (27) ¹H NMR spectra in toluene-**d**₈ at -35 °C for *p*-MePyO-**D**₁ adducts **a**, **b**, and **c**. δ/ppm, **a**: 9.06 (d, 2H, arom), 8.0-6.5 (m, 12H, arom), 6.42 (d, 2H, arom), 5.06 (d, 1H), 4.65 (d, 1H), 4.42 (d, 1H), 4.27 (d, 1H), 3.29 (d, 1H), 3.01 (d, 1H), 1.77 (s, 3H); **b**: 8.93 (d, 2H, arom), 8.0-6.5 (m, 12H, arom), 6.30 (d, 2H, arom), 5.18 (d, 1H), 4.74 (d, 1H), 4.72 (d, 1H), 4.51 (d, 1H), 4.34 (d, 1H), 4.18 (d, 1H), 1.75 (s, 3H); **c**: 8.80 (d, 2H, arom), 8.0-6.5 (m, 12H, arom), 6.62 (d, 2H, arom), 5.10 (d, 1H), 4.80 (d, 1H), 4.61 (d, 1H), 4.38 (d, 1H), 3.94 (d, 1H), 3.69 (d, 1H), 1.92 (s, 3H).

- (28) ^1H NMR spectra in toluene- d_8 at $-35\text{ }^\circ\text{C}$ for $p\text{-MePyO-D}_1$ adduct **I** (aromatic protons of coordinated $p\text{-MePyO}$), free $p\text{-MePyO}$, and $p\text{-MePyH}^+$. δ/ppm , **I**: 8.63 (d, 2H, arom), 6.25 (d, 2H, arom), 8.85 (d, 2H, arom), 6.38 (d, 2H, arom); $p\text{-MePyO}$: 8.36 (d, 2H, arom), 6.39 (d, 2H, arom), 2.35 (s, 3H); $p\text{-MePyH}^+$: 8.26 (d, 2H, arom), 6.06 (d, 2H, arom), 1.44 (s, 3H).
- (29) Abu-Omar, M. M.; Espenson, J. H. *J. Am. Chem. Soc.* **1995**, *117*, 272.
- (30) Cheng, S. Y. S.; James, B. R. *J. Mol. Catal.* **1997**, *117*, 272-280.
- (31) Tan, H.; Espenson, J. H. *Inorg. Chem.* **1998**, *37*, 467-472.

Table 1. NMR Chemical Shifts for the Adducts $\text{Re}_2\text{O}_2(\text{mtp})_3\cdot\text{PAr}_3$ (**PD1**)

phosphine	^{31}P (δ/ppm)	
	PD1	Free Phosphine
$\text{P}(4\text{-MeOC}_6\text{H}_4)_3$	-6.99	-9.31
$\text{P}(4\text{-MeC}_6\text{H}_4)_3$	-5.98	-6.98
$\text{P}(\text{C}_6\text{H}_5)_3$ *	-6.64	-4.50
$\text{P}(4\text{-ClC}_6\text{H}_4)_3$	-7.95	-8.70
$\text{P}(4\text{-CF}_3\text{C}_6\text{H}_4)_3$	-9.10	-5.63
PPh_2Me	-19.21	-26.29
PPhMe_2	-34.92	-45.54

*Selected ^1H and ^{13}C NMR chemical shifts for $\text{Ph}_3\text{PD1}$ are as follows, with the values in bold showing the group coordinated to Re: ^1H δ 7.82 (m, 6H, arom, ligand), 7.57 (m, 9H, arom, ligand), 7.70 (d, 1H, arom, $J = 8.8$ Hz), 7.03-7.55 (m, 10H, arom), 6.78 (d, 1H, arom, $J = 7.6$ Hz), 4.96 (d, 1H, CH_2 , $J = 11.6$ Hz), **4.94 (d, 1H, CH_2 , $J = 12.8$ Hz)**, **4.62 (d, 1H, CH_2 , $J = 12.4$ Hz)**, 4.54 (d, 1H, CH_2 , $J = 12.0$ Hz), 3.50 (d, 1H, CH_2 , $J = 11.6$ Hz), 3.01 (d, 1H, CH_2 , $J = 11.6$ Hz) ppm and ^{13}C δ 141.76 (arom), 141.43 (arom), 141.31 (arom), 137.80 (d, arom, ligand, $^1\text{J}_{\text{P-C}} = 312$), 137.37 (d, arom, ligand, $^2\text{J}_{\text{P-C}} = 42$ Hz), 134.73 (d, arom, ligand, $^3\text{J}_{\text{P-C}} = 35.6$ Hz), 132.65 (arom), 132.52 (arom), 132.48 (arom), 132.40 (arom), 131.84 (d, arom, ligand, $^4\text{J}_{\text{P-C}} = 10$ Hz), 130.92 (arom), 130.67 (arom), 130.50 (arom), 130.43 (arom), 130.34 (arom), 129.66 (arom), 129.26 (arom), 129.12 (arom), 127.48 (arom), 127.24 (arom), 126.91 (arom), **51.07 (CH_2)**, 41.71 (CH_2), 41.16 (CH_2) ppm.

Table 2. Relative rate constants for oxidation of PAr_3 , AsPh_3 , and SbPh_3 by 4-methylpyridine N-oxide, catalyzed by **D1**, and for comparison reactions

reagent	$3\sigma_Y$	k_Y/k_H ^a	log (k_Y/k_H)		
			PD₁	MeReO(O ₂) ₂ ^b	(TMP)Ru(O) ₂ ^c
$\text{P}(\text{C}_6\text{H}_5\text{-4-OMe})_3$	-0.81	8.57	0.933		0.314
$\text{P}(\text{C}_6\text{H}_5\text{-4-Me})_3$	-0.51	5.46	0.737	0.105	0.030
PPh_3	0	(1.00)	0	0	0
$\text{P}(\text{C}_6\text{H}_5\text{-4-F})_3$	0.186				0.296
$\text{P}(\text{C}_6\text{H}_5\text{-4-Cl})_3$	0.69	1.45	0.161	-0.182	0.372
$\text{P}(\text{C}_6\text{H}_5\text{-4-CF}_3)_3$	1.62	0.95	-0.022	-0.330	0.248
AsPh_3		0.23	-0.638	-0.235	-1.69
SbPh_3		0.32	-0.495	-0.140	1.66

^a Determined according to eq 7; ^b Data from ref. 29; ^c Data from ref. 30.

Table 3. Kinetic data (initial reaction rates) for the oxidation of PAr₃ by 4-MeC₅H₄NO, catalyzed by **D1** under argon. ^a

[PAr ₃] ₀ /mM	[PyO] ₀ /mM	[Py] ₀ /mM	[HOAc]/mM	$v_i/10^{-7} \text{ mol L}^{-1} \text{ s}^{-1}$
(a) P(4-MeOC ₆ H ₄) ₃				
1.58	64.0			15.4
3.80	64.0			15.0
3.80	35.5			8.3
(b) PPh ₃				
2.56	34.6		100	5.37
6.92	34.5		100	5.74
5.23	41.7		100	6.73
8.00	90.0		100	15.1
6.44	35.0	36.0		1.91
6.44	58.3	36.0		2.94
12.4	58.3	36.0		5.27
12.4	55.8	17.3		10.5
12.0	54.0			11.3

^a Conditions: under argon at 25 °C in C₆D₆; [**PD1**] = 1×10^{-4} M.

Supporting Information

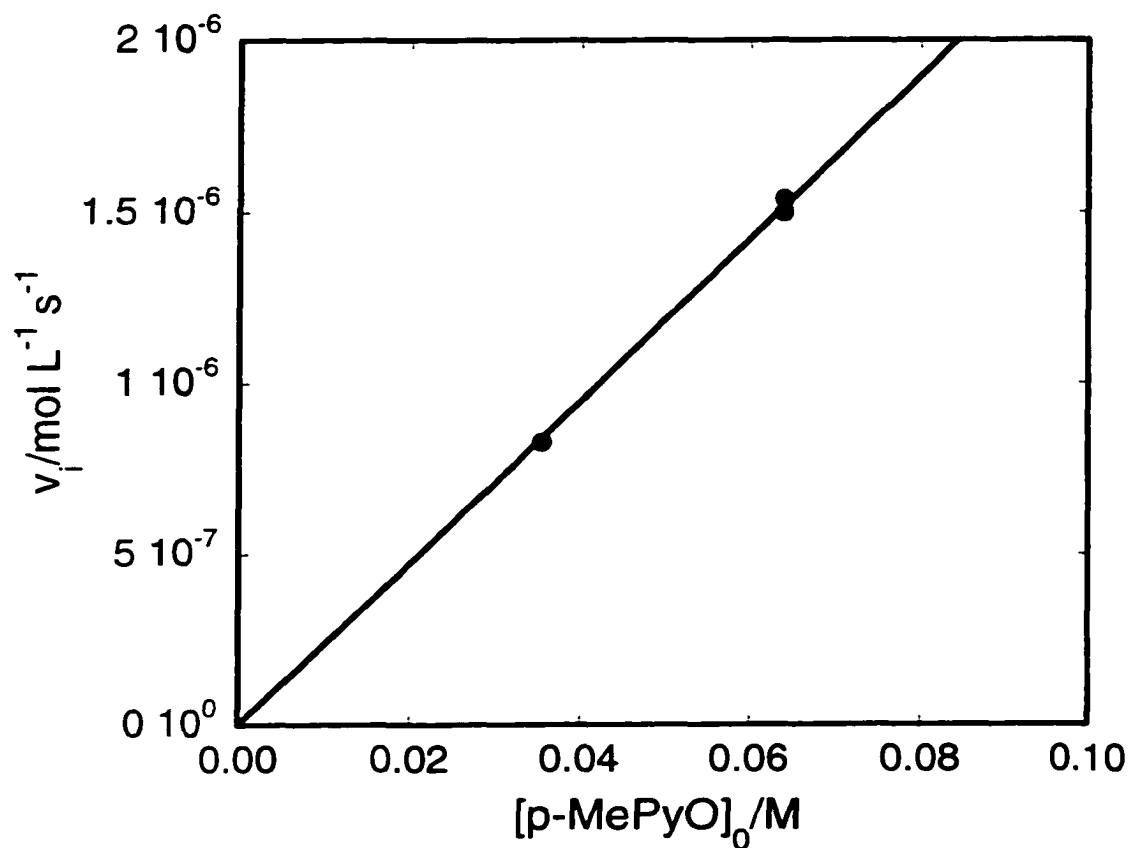


Figure S–1. Values of the initial rates for the oxidation of tris(*para*-methoxyphenyl)phosphine by *para*-methylpyridine N-oxide catalyzed by **D1** are a linear function of $[\text{PyO}]_0$.

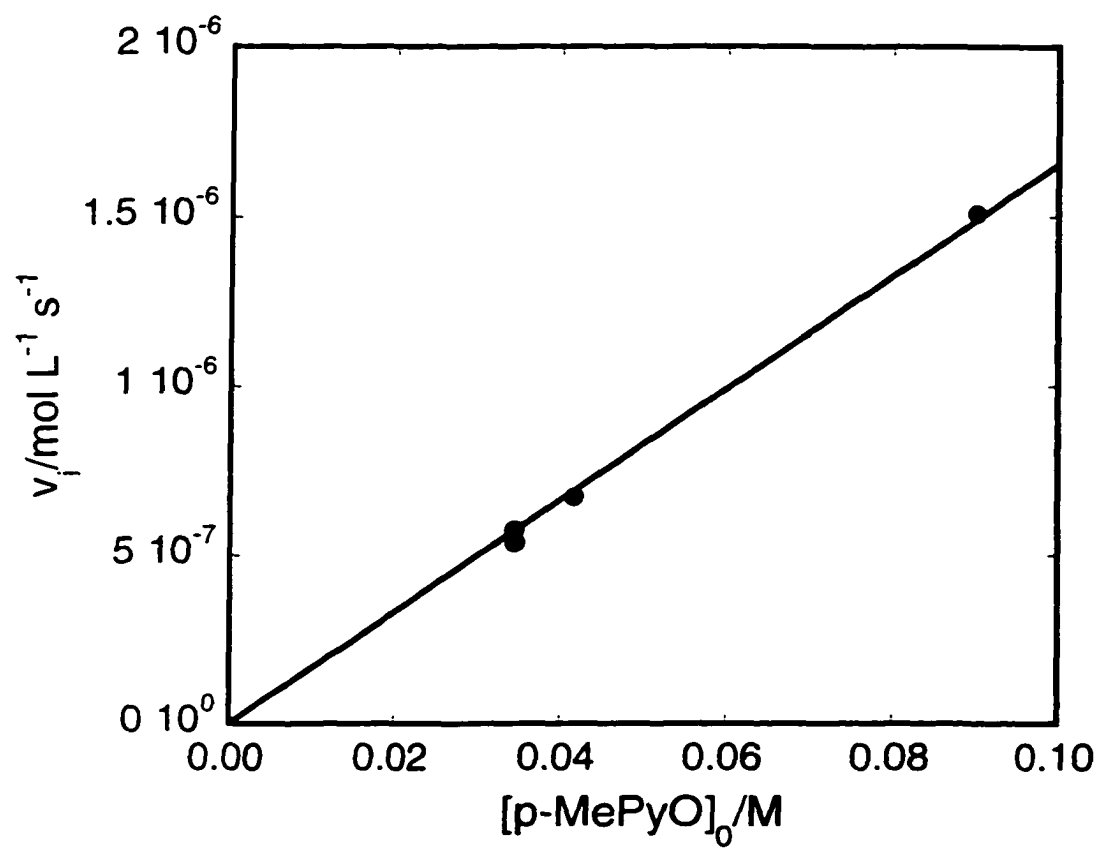


Figure S-2. Values of the initial rates for the oxidation of PPh_3 by *para*-methylpyridine N-oxide catalyzed by **D1** in the presence of 0.1 M acetic acid are a linear function of $[\text{PyO}]_0$.

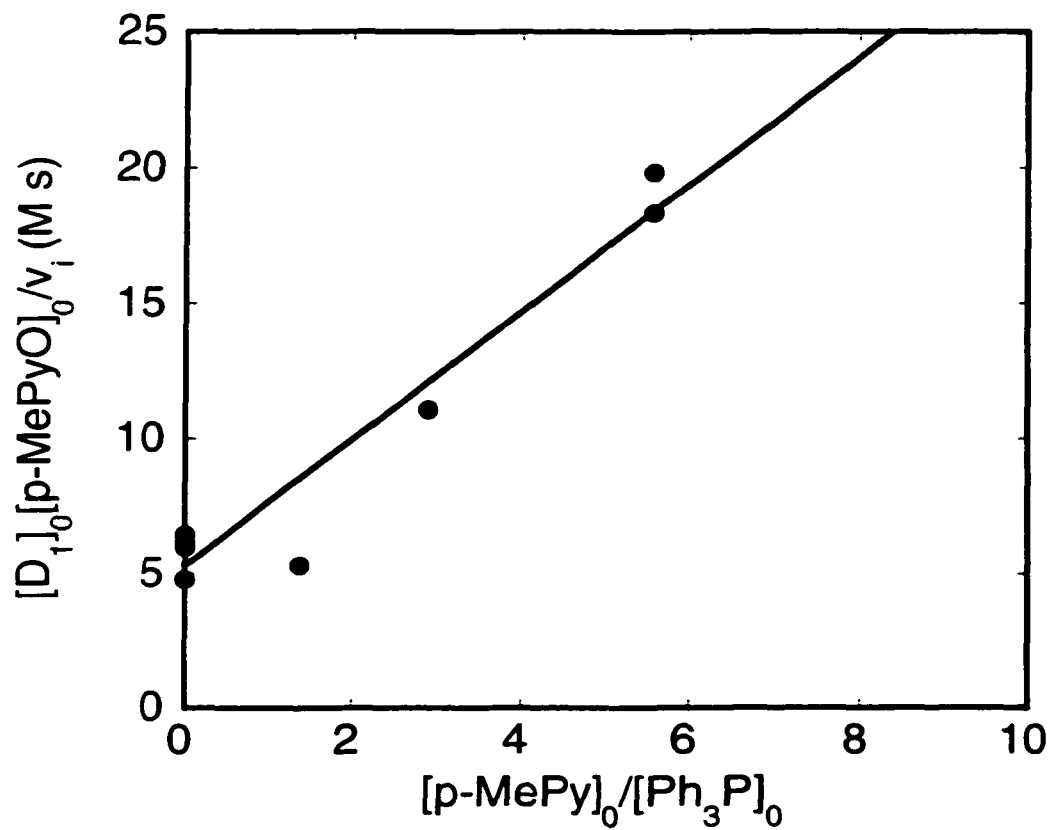


Figure S-3. Attempted linear correlation of the rate constants for $[D_1]_0[p\text{-MePyO}]_0$ against $[p\text{-MePy}]_0/[Ph_3P]_0$ for the oxidation of triphenylphosphine by *para*-methylpyridine N-oxide catalyzed by **D1** in the presence of *para*-methylpyridine.

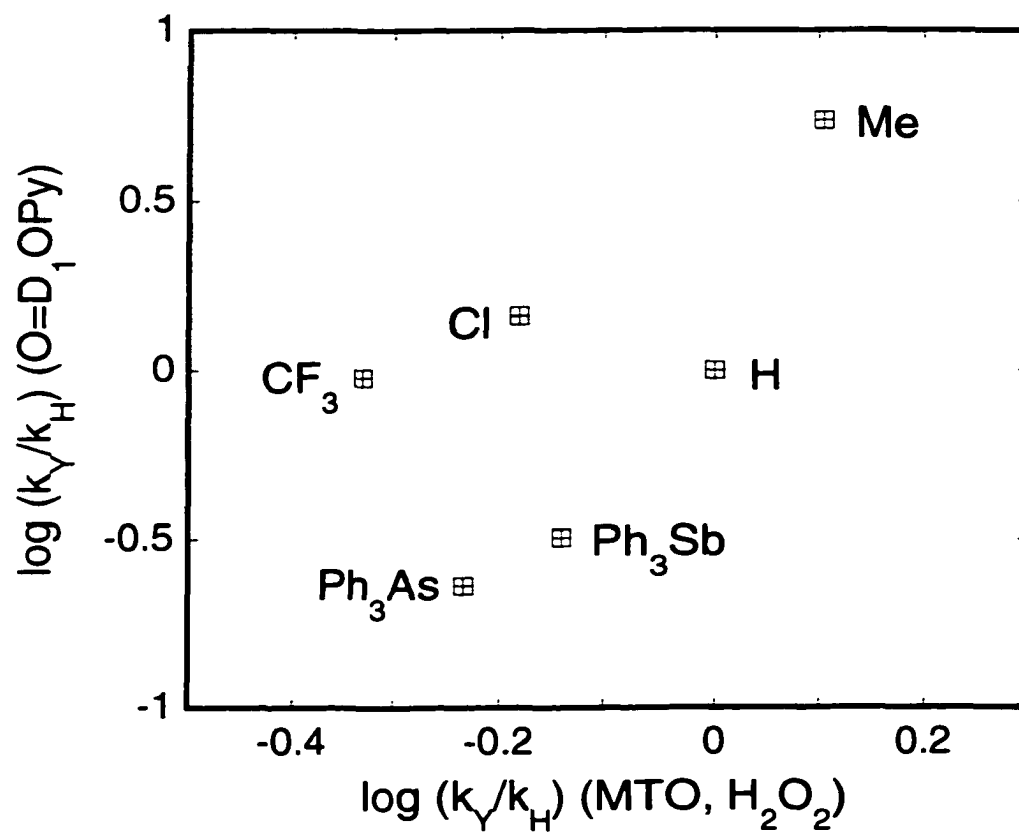


Figure S-4. Reactivity comparison for the oxidation of *para*-substituted triarylphosphines, (*p*-YC₆H₄)₃P, Y = MeO, Me, H, Cl, CF₃, triphenylarsine and triphenylantimony by *para*-methylpyridine N-oxide catalyzed by **D1**, and the oxidation by CH₃Re(=O)₂(O₂). No correlation was found.

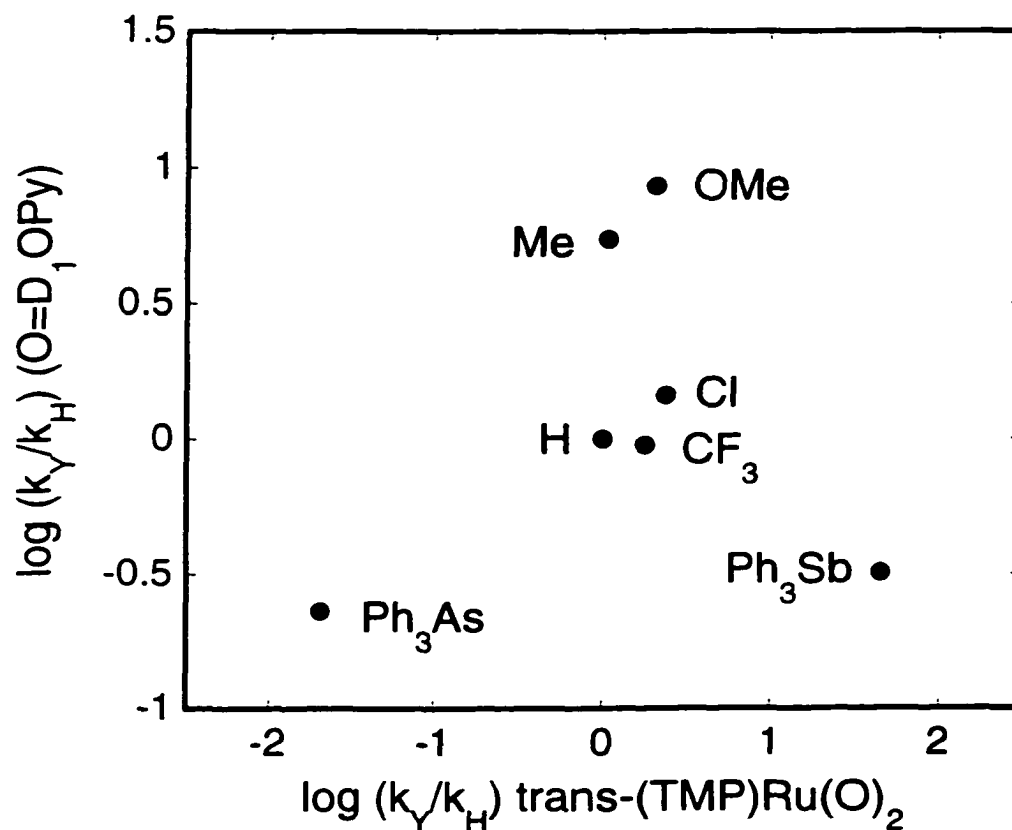


Figure S-5. Reactivity comparison for the oxidation of *para*-substituted triarylphosphines, (*p*-YC₆H₄)₃P, Y = MeO, Me, H, Cl, CF₃, triphenylarsine and triphenylantimony by *para*-methylpyridine N-oxide catalyzed by **D1**, and the oxidation by *trans*-(TMP)Ru(O)₂. No correlation was found.

CHAPTER III. MOLECULAR OXYGEN REACTIONS CATALYZED BY AN OXORHENIUM(V) COMPOUND

A manuscript accepted by *Journal of Molecular Catalysis*[†]

Ruili Huang and James H Espenson*

Abstract

The new binuclear oxothiolatorhenium(V) compound, $\text{Re}_2\text{O}_2(\text{mtp})_3$, **D1**, $\text{mtpH}_2 = 2$ -(mercaptomethyl)thiophenol, was found to activate molecular oxygen, which has no precedent in oxorhenium catalysis. The kinetics and mechanism of the oxidation of triaryl phosphines and methyl phenyl phosphines by O_2 were investigated. The reaction pathway inferred from the kinetic data involves two Re(VII) intermediates, a peroxo and a μ -oxo species. The rate constants were determined for both steps in this reaction. The μ -oxo Re(VII) intermediate further reacts with a second phosphine forming more phosphine oxide as **D1** is recovered. This step is very rapid, and does not affect the kinetics. Other substrates, taken alone, such as sulfides and dienes, which coordinate to **D1** weakly, or do not coordinate, were not oxidized by molecular oxygen. However, in the presence of a small amount of phosphine to open up the sulfur bridge in **D1**, then sulfides and dienes were also oxidized to sulfoxides and epoxides accordingly. The relative reactivities of the substrates fall in the order: phosphines > sulfides > dienes.

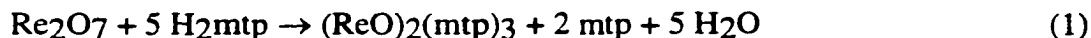
Introduction

As active as many rhenium compounds are as catalysts for selective oxidation reactions, none has been able to activate molecular oxygen. Many of them catalyze reactions of hydrogen peroxide, as recently reviewed,¹⁻³ and oxygen-atom transfer between a donor and acceptor.⁴⁻⁷ The compounds referred to are MeReO_3 , $\text{MeReO}(\text{mtp})\text{PPh}_3$, $\text{ReOCl}_3(\text{PPh}_3)$, and $\text{Re}(\text{NPh})\text{Cl}_3(\text{PPh}_3)_2$. These compounds are themselves stable towards

[†] Reproduced in part with permission from *Journal of Molecular Catalysis*, in press. Unpublished work copyright 2000 Elsevier Science.

O₂; in general, their catalytic reactions proceed as well under oxygen (air) as under argon.

We prepared a new Re(V) compound **D1**,⁸ and found that it is air-sensitive. On that basis it was reasonable to suggest that it might form an intermediate with oxygen that could carry out other chemistry. If the original compound could be recovered, then a catalytic cycle could be established. The new compound has the formula Re₂O₂(mtp)₃, where mtpH₂ = 2-(mercaptomethyl)thiophenol, (**Chart 1**). It was prepared according to this reaction



where mtp is the cyclic disulfide. Unlike many of its relatives, **D1** has no Me–Re group, which may be extraneous in any event. Here we report studies of autoxidation reactions catalyzed by **D1**. They are principally phosphine oxidations, but certain other substrates are considered in less detail.

Experimental

Except for **D1**, all materials were obtained commercially and used as received. The reaction progress was monitored by ¹H NMR spectroscopy; products and intermediates were studied with ¹H and ³¹P NMR spectroscopy using a Bruker DRX-400 spectrometer. The ¹H NMR chemical shifts were measured relative to the residual resonance of the solvents, C₆D₅H at 7.15 ppm and C₆D₅CD₂H at 2.09 ppm. The ¹H signals were integrated relative to *tert*-butanol, an internal standard. ³¹P chemical shifts were referenced to 85% phosphoric acid. The temperature was maintained at 25 °C, except as noted.

For kinetics, the oxygen concentrations were 9.1 mM (oxygen-saturated) and 1.9 mM (air-saturated). The method of initial rates was used for the kinetics. First, NMR intensities were converted to concentrations by means of the internal standard. Then the concentration-time data were fitted to a polynomial function;⁹ for phosphine oxide, for example, $C_t = m_1t + m_2t^2 + m_3t^3 \dots$. The coefficient of the leading term, m_1 , is the initial rate value in units mol L⁻¹ s⁻¹.

Results and Interpretation

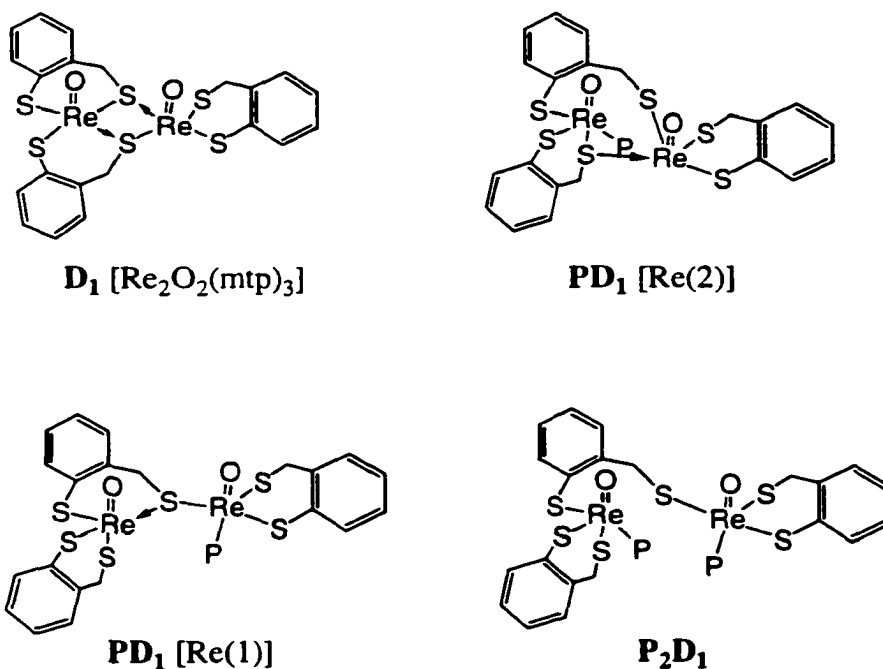
General observations. Control experiments on uncatalyzed reactions of selected phosphines by molecular oxygen were carried out. In all of these cases, <5%

oxidation had occurred in 24 h. For $P(p\text{-Tol})_3$, no oxidation occurred in 8 h. NMR studies at $-23\text{ }^{\circ}\text{C}$ were carried out in toluene- d_8 . Of course, without oxygen the phosphines are stable.

In the reactions of PAr_3 and oxygen with **D1** as a catalyst, the reactions proceed to 100% conversion. The major product is $\text{Ar}_3\text{P}=\text{O}$ (>90%), accompanied by a small amount of phosphine sulfide, $\text{Ar}_3\text{P}=\text{S}$, evidently from side reactions between PR_3 and the thiolate ligands of **D1**.

In the absence of oxygen there is an initial interaction between PAr_3 and **D1**, leading in <0.5 s to a quantitative yield of a 1:1 adduct, which we abbreviate as **PD1**, also shown in **Chart 1**. Under such solutions, and throughout all the catalysis experiments, **PD1** is the only form of the catalyst that could be detected in the NMR spectrum. **PD1** is evidently the *resting state* of the catalyst. Subsequent steps in catalysis occur over many hours, such that **PD1** is always restored by this equilibrium.

Chart 1



The smaller phosphines, PMePh₂ and PMe₂Ph, engage in more complicated interactions. The distribution of species was determined at 50 mM total phosphine and 1 mM total **D1**. These species were seen: two forms of **PD1**, in which coordination occurred at either Re atom, and the bis(phosphine) compound **P2D1**, in which both Re atoms are coordinated. Refer to the structural formulas in **Chart 1**. These conclusions are based on the ¹H and ³¹P NMR spectra, given in **Table 1**. In the kinetics experiments to be presented subsequently, where the phosphine was always used in large excess (>50-fold), most (PMePh₂) or all (PMe₂Ph) of the catalyst remains in the form **P2D1**.

Oxidation of P(*p*-Tol)3. The typical concentrations ranges for kinetics experiments were 1–30 mM P(Tol)3, 0.1–9 mM O₂, and 5–500 μM **D1**. Under air, when [O₂] < 2 mM and [P(Tol)3] > 4 mM, the reactions were completed by diffusion of atmospheric oxygen into the solution. With fixed P(Tol)3, 13.5 mM, and O₂, 1.9 mM, **PD1** was varied in the range 0.09–0.16 mM; the initial rates, *v_i* (10^{–6} mol L^{–1} s^{–1}) varied in the range 3.30–6.20, establishing a first-order dependence on catalyst concentration.

In other experiments, with 13.5 mM P(Tol)3 and 0.16 mM **PD1**, [O₂] was varied 0.1–10 mM. The variation of *v_i* with [O₂]₀ takes the form of a rectangular hyperbola, **Figure 1**. In another series, with 1.9 mM O₂ and 0.16 mM **PD1**, [P(Tol)3] was varied 1–25 mM. Again, **Figure 2**, *v_i* attains a plateau at high concentration. These dependences correspond to Michaelis-Menten kinetics. On the basis of these results, with constants to be defined subsequently, the empirical rate equation is

$$v_i = \frac{k_1 k_2 [\mathbf{PD1}]_0 [\text{O}_2]_0 [\text{P}]_0}{k_{-1} + k_1 [\text{O}_2]_0 + k_2 [\text{P}]_0} \quad (2)$$

According to this equation, rate saturation will occur at sufficiently high concentrations of P(Tol)3 or O₂. With either concentration much higher than the other, the limiting forms of *v_i* will be obtained; they are *k₁*[**PD1**][O₂] and *k₂*[**PD1**][P(Tol)3]. This point was checked as well, leading to approximate values of these constants that were then refined. To cover all the concentration ranges, we used a least-squares program, SCIENTIST, to fit all the initial rate

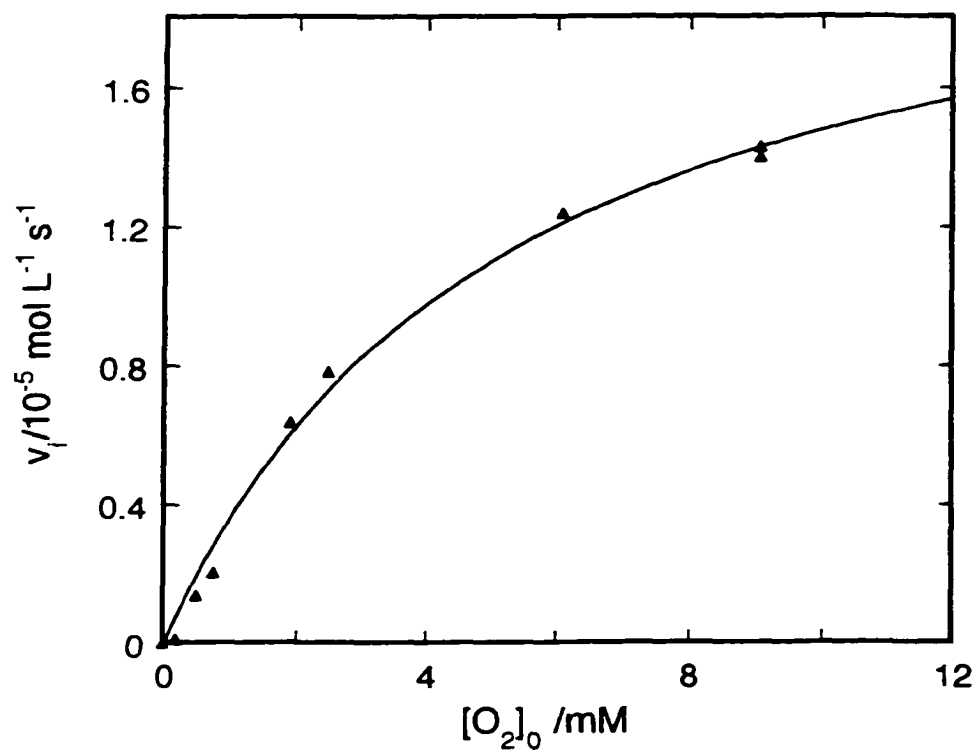


Figure 1. Kinetic data for the oxidation of $P(p\text{-Tol})_3$ by oxygen with **D1** as a catalyst. Conditions: constant phosphine (13.5 mM) and catalyst (0.16 mM), with variable oxygen concentrations in deuterobenzene at 25 °C.

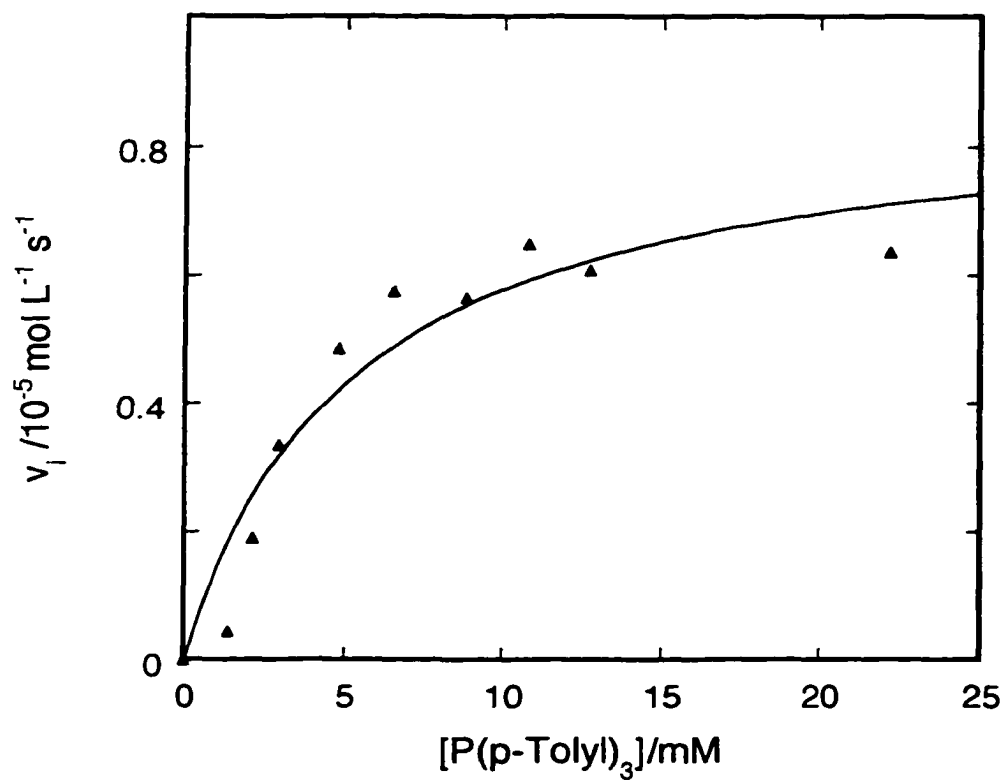


Figure 2. Kinetic data for the oxidation of P(*p*-Tol)₃ by oxygen with **D1** as a catalyst. Conditions: constant O₂ (1.9 mM) and **D1** (0.16 mM), with variable phosphine concentrations in deuterobenzene at 25 °C.

values to eq 2. The result is: $k_1 = 21.2 \pm 1.7 \text{ L mol}^{-1} \text{ s}^{-1}$, $k_2 = 13.6 \pm 1.8 \text{ L mol}^{-1} \text{ s}^{-1}$. The value of k_{-1} was too small to be determined. To show the extent to which this model fits the data, one can present the experimental values of v_i against the ones calculated from the best-fit values of the rate constants from eq 2. One expects a linear relation of unit slope. **Figure 3** shows that the agreement between data and model is quite reasonable.

Oxidation of other phosphines. Other tri(aryl)phosphines were studied in the same way, except that fewer concentration variations were made. These reactions were studied under 1 atm O_2 , such that a limiting form of the rate was attained. (Since this limit was shown to be realized for $\text{P}(p\text{-Tol})_3$, the compound with the second-highest value of k_2 , it would hold for all). This approach gave k_2 directly (see **Table 2**), according to this form

$$v_i = k_2[\text{PD1}][\text{PAr}_3] \quad (3)$$

Similar determinations were carried out for PMePh_2 and PMe_2Ph . The results are also given in **Table 2**. The sterically encumbered phosphine $\text{P}(o\text{-Tol})_3$ reacts much more slowly than $\text{P}(p\text{-Tol})_3$ with O_2 owing to its bulk. **D1** was ineffective in this case. Starting with 25 mM $\text{P}(o\text{-Tol})_3$, 5% **D1**, under air, 10% of the $(o\text{-Tol})_3\text{P=O}$ was formed after 16 hours. However, $\text{P}(p\text{-Tol})_3$ promotes the oxidation of $\text{P}(o\text{-Tol})_3$, probably by helping to break the Re-S bond and allowing O_2 to coordinate, since $\text{P}(o\text{-Tol})_3$ itself does not coordinate to **D1**. Under the same conditions, but with 4% of $\text{P}(p\text{-Tol})_3$ added in the beginning, 25% $\text{P}(o\text{-Tol})_3\text{=O}$ along with 4% (i.e., all) $\text{P}(p\text{-Tol})_3\text{=O}$ were detected after 17 h. Oxidation of the ortho isomer stops once all the essential para isomer has been consumed.

Low-temperature NMR spectroscopy. During the ambient-temperature kinetics with ^1H NMR spectroscopy, no form of the catalyst could be detected except for **PD1**. From the rate constants, it can be shown that the postulated intermediate would have a lifetime of a few seconds, too short for this technique, since about 1 min is needed to obtain the first ^1H spectrum.

To detect the intermediate, ^1H NMR studies were carried out at 250 K in toluene- d_8

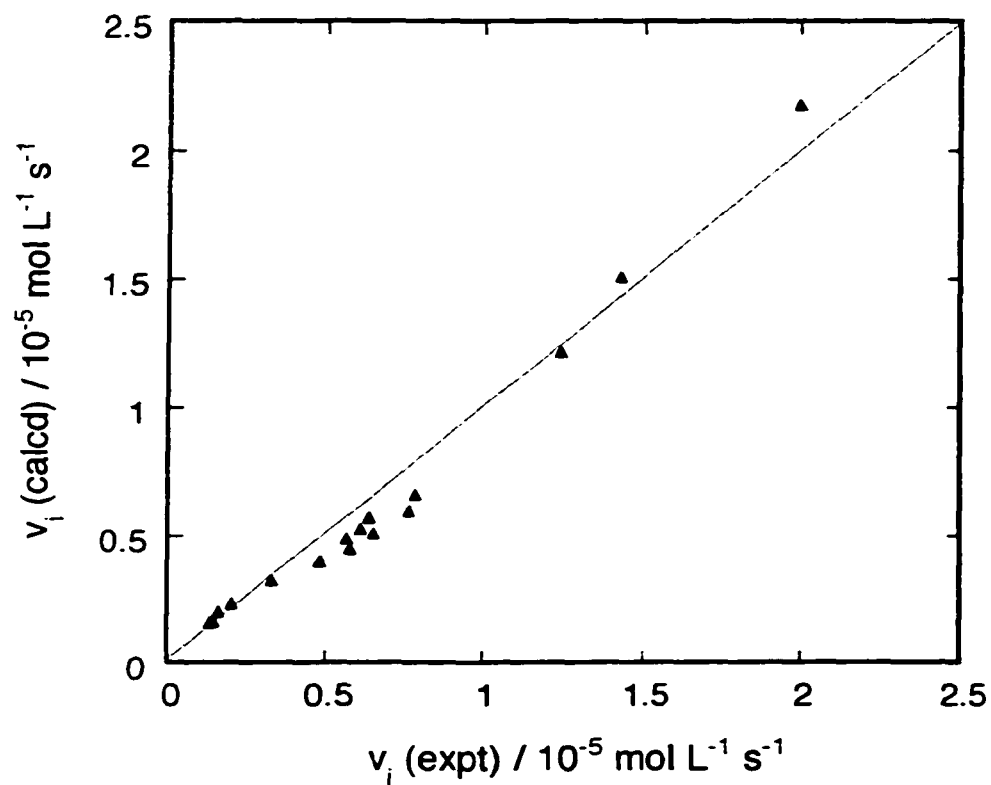


Figure 3. The data for the multi-variable rate equation that represents the oxidation of $P(p\text{-Tol})_3$ by oxygen with **D1** as a catalyst, after least-squares fitting to eq 2, are displayed as the correlation of observed against calculated values, and a line of unit slope.

solution. The concentrations were: 2.0 mM **PD1**, 5.0 mM O₂, and 25.5 mM P(*p*-Tol)₃. A new rhenium species was found ; it reached maximum intensity in about 30 min and disappeared after 5-6 h. The proton chemical shifts are consistent with **PD1(OO)** in **Scheme 1**.¹⁰

Oxidation of other substrates by O₂, catalyzed by D1. Phosphines are the substrates most likely to succeed in oxidation reactions, since the P=O bond is much stronger than other element-oxygen bonds. Experiments were also carried out with a few substrates **X** leading to products having weaker X=O bonds. This includes sulfides: (*p*-Tol)SMe and MeSEt; dienes: 2-methyl-1,3-pentadiene, trans-1,3-pentadiene and 1,3-cyclohexadiene; and one alkene: cyclohexene. Like P(*o*-Tol)₃, none of these was oxidized by O₂ with **D1** added until a low concentration of P(*p*-Tol)₃, equivalent to **D1**, was also added.

Even then, the results were marginal: 0.5–3.4% yield of sulfoxides obtained, and 1–14% of the monoepoxides of each diene. The latter was formed by preferential reaction at the less-substituted double bond, opposite to the results for MTO–H₂O₂.¹¹ No cyclohexene oxide was found. Over the reaction time, (*p*-Tol)₃PO was formed quantitatively. Clearly, the problem was that this essential phosphine was concurrently oxidized, leaving the other reaction incomplete.

Other oxygen transfer reactions. In the absence of O₂, **D1** catalyzes the oxidation of phosphines with Me₂SO. These reactions were carried out in C₆D₆ using Me₂SO at 5-10 fold excess over phosphine, and a higher concentration of **D1** (5% of phosphine). Phosphine oxide and dimethyl sulfide were formed. The reaction stoichiometry is

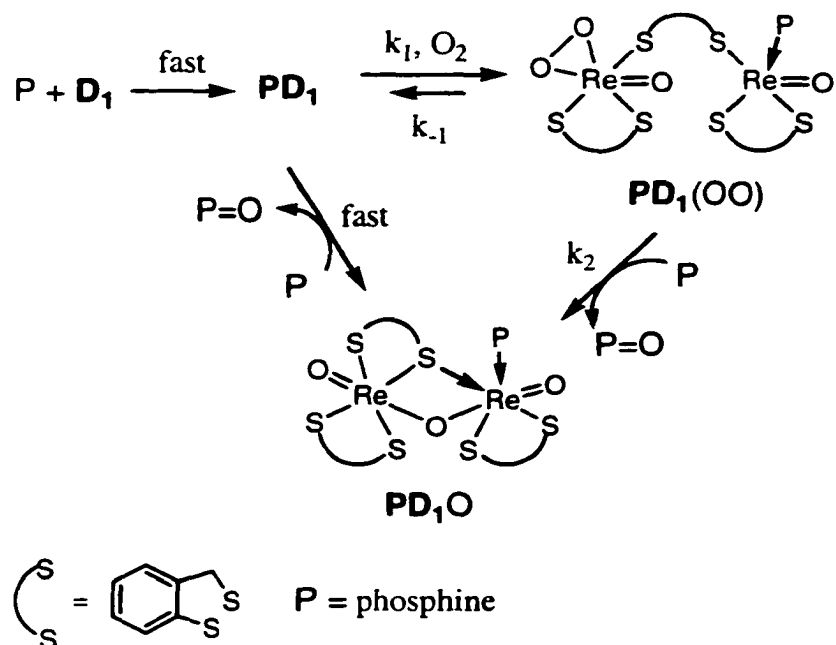


In 60-90 min, high conversions to the products were realized: PMePh₂, 90%; P(*p*-Tol)₃, 70%, and PPh₃, 65%.

Discussion

Mechanism of phosphine oxidation. A set of chemical reactions by which the catalytic cycle can be accomplished is proposed in **Scheme 1**. The first reaction, conversion of **D1** to **PD1**, was verified directly by spectroscopy. This rapid (<0.5 s) reaction was

detected by the stopped-flow method with spectrophotometric detection. In addition, the NMR data show a new resonance for **PD₁**.



Scheme 1

The second reaction has been formulated as occurring between **PD₁** and molecular oxygen, leading to a key reactive intermediate. (The rate law suggests that the second step occurs between **PD₁** and either O₂ or PR₃, but the choice of phosphine seems less plausible. It would lead to a bis(phosphine) compound, observed only for the smaller phosphines, which is in any event then likely to find its required reaction with oxygen blocked.) Given, then, that such an oxygen adduct is formed, what is its likely role in the reaction cycle?

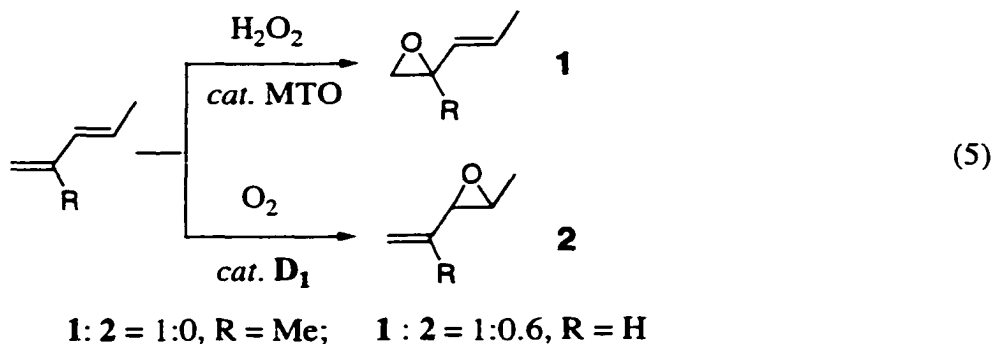
We speculate that the resultant species contains a chelated peroxide ligand, and that it is a mixed-valent, Re^{VII}-Re^V species. See **PD₁OO** in **Scheme 1**. These assignment represent our hypotheses, based on certain precedents in the literature. The ¹H NMR spectrum of the reaction intermediate does show chemical shifts that are not broadened or greatly shifted; the intermediate is therefore not likely to be a free radical.

In the next stage of reaction the intermediate **PD₁OO** reacts with phosphine, yielding the (first mole) of the phosphine oxide product. This reaction has wide precedent for chelated

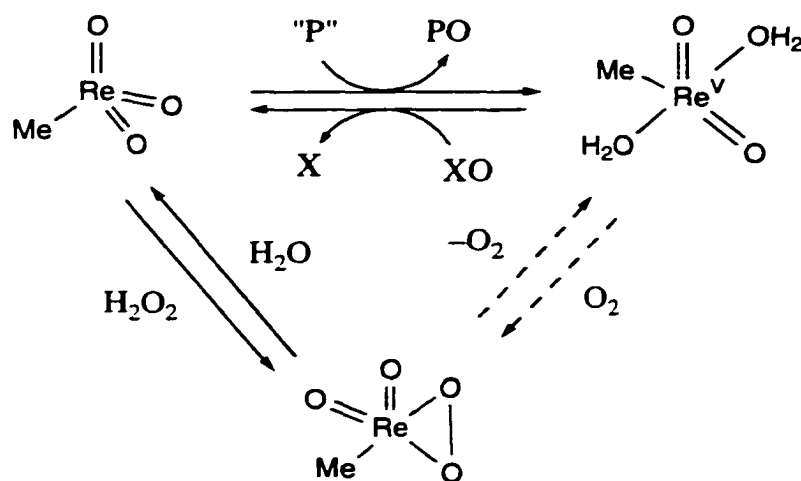
peroxorhenium compounds.^{1,12} This still leaves a single extra oxygen in catalyst, as shown in the suggested structural formula of **PD₁O**. We have chosen to represent its formula as containing $\text{Re}_2(\mu\text{-O})$, because of the final reaction in the scheme. In that step, which from the kinetics occurs much more rapidly than the two that precede it, a second phosphine is oxidized. Literature precedents suggest that the alternative, with **PD₁O** containing a terminal $\text{Re}=\text{O}$ bond, would be too slow to match the kinetic data.¹³⁻¹⁵

Oxidation of other substrates. Both organic sulfides and conjugated dienes were effectively oxidized by O_2 with **D₁** as catalyst. Both required **PD₁** not **D₁**, however; that is a catalytic quantity of $\text{P}(p\text{-Tol})_3$ is needed as an activator. The reactions stopped well short of completion, but only because the requisite phosphine was itself lost to slow concurrent oxidation. A reaction scheme similar to that presented for phosphines can accommodate these data. This affords at least circumstantial verification that **PD₁O** does not contain three terminal $\text{Re}=\text{O}$ groups. The depicted formulation of **PD₁O**, although not proved, seems more likely to meet the reactivity requirement, because the same intermediate must engage in the oxidation of these substrates as well.

The phosphine is needed to initiate *and sustain* the catalytic cycle. It must "open" the **D₁** structure to allow for entry of oxygen. Sulfides and dienes cannot do that, without which the cycle fails because O_2 cannot bind. The epoxides formed from these dienes are different from the one from those resulting from MTO-peroxide, eq 5, probably for steric reasons in the **PD₁O**–diene reaction.



Reactivity trends. The values of k_2 for the compounds $P(C_6H_5-p-Y)_3$ lie in this order: $Y = MeO > Me > CF_3 > Cl > H$. In the sense of an inductive effect, this ordering is highly irregular. It must be recognized, however, that not only does Y change, but also the nature of the catalytic intermediate. That is, the identity and surely the reactivity of **PD₁OO** varies with the choice of phosphine. The kinetic data therefore contain dual effects of Y . When the coordinated phosphine has an electron donating substituent, it also donated electron density to the other rhenium, making the oxygen more electron rich and thus less reactive. An electron-donating substituent, on the other hand, provides a phosphine more reactive towards the peroxo group. The conflict between the two can explain the trends noted.



"P" = PR_3 , H_3PO_2 ; XO = Me_2SO , PyO , ClO_4^- , etc.

Scheme 2

Conclusion

We are aware of no other oxorhenium compound that catalyzes oxidations with molecular oxygen. To a minor extent, $MeReO_2$ can do so, but its instability and sluggish reactions make it ineffective.¹⁶ The principle advanced earlier, however, appears to remain valid, as illustrated in the set of reactions presented in **Scheme 2**. $MeRe^VO_2$ is shown as a diaqua complex,^{13,17} but phosphine ligation has also been found.¹⁸ The important difference here is that oxygen uptake occurs quite well, whereas it is a marginal reaction of $MeReO_2$.

References

- (1) Espenson, J. H. *Chem. Commun.* **1999**, 479.
- (2) Gable, K. P.; Brown, E. C. *Organometallics*, **2000**, *19*, 944.
- (3) Herrmann, W. A.; K hn, F. E. *Acc. Chem. Res.* **1997**, *30*, 169.
- (4) Arterburn, J. B.; Nelson, S. L. *J. Org. Chem.* **1996**, *61*, 2260.
- (5) Abu-Omar M. M. Kahn, S. I. *Inorg. Chem.* **1998**, *37*, 4979.
- (6) Arterburn, J. B. *Tetrahedron Lett.* **1996**, *44*, 7941.
- (7) Arterburn, J. B.; Perry, M. C.; Nelson, S. L.; Dible, B. R.; Holguin, M. S. *J. Am. Chem. Soc.* **1997**, *119*, 9309.
- (8) Huang, R.; Espenson, J. H. submitted for publication.
- (9) Hall, K. J.; Quickenden, T. I.; Watts, D. W. *J. Chem. Educ.* **1976**, *53*, 493.
- (10) ¹H NMR (CH₂ shifts only): δ/ppm: 4.98 (d, 1H), 4.71 (d, 1H), 4.45 (d, 1H), 4.22 (d, 1H), 3.98 (d, 1H), 3.78 (d, 1H).
- (11) Tan, H.; Espenson, J. H. *Inorg. Chem.* **1998**, *37*, 467.
- (12) Abu-Omar, M. M.; Espenson, J. H. *J. Am. Chem. Soc.* **1995**, *117*, 272.
- (13) Abu-Omar, M. M.; Appleman, E. H.; Espenson, J. H. *Inorg. Chem.* **1996**, *35*, 7751.
- (14) Conry, R. R.; Mayer, J. M. *Inorg. Chem.* **1990**, *29*, 4862.
- (15) Gable, K. P.; Phan, T. N. *J. Am. Chem. Soc.* **1993**, 115.
- (16) Eager, M. D.; Espenson, J. H. *Inorg. Chem.* **1999**, *38*, 2533.
- (17) Yiu, D. T. Y.; Espenson, J. H. *Inorg. Chem.* **2000**, *39*, in press.
- (18) Herrmann, W. A.; Roesky, P. W.; Wang, M.; Scherer, W. *Organometallics* **1994**, *13*, 4531.

Table 1. ^{31}P chemical shifts and relative intensities (%) for 1:1 (**PD₁**), 2:1 (**P₂D₁**) adducts of methylphenylphosphines and **D₁**, as well as their corresponding free phosphines (**P**) in C_6D_6 ($[\text{P}]_{\text{T}} = 50 \text{ mM}$, $[\text{D}_1]_{\text{T}} = 6.0 \text{ mM}$).

δ/ppm	P (100%)	P ^{Re(1)} D₁ (%)	P ^{Re(2)} D₁ (%)	P₂D₁ (%)
MePh ₂ P	-26.29	-19.21 (7.3)	-24.15 (0.8)	7.25 (3.6), 6.00 (3.6)
Me ₂ PhP	-45.54	-34.92 (0)	-31.14 (0)	-3.96 (14.7), -4.66 (14.7)

Table 2. Kinetic data for the **D₁**-catalyzed oxidation of para-substituted triarylphosphines (*p*-YC₆H₄)₃P and methylphenylphosphines Me_nPh_{3-n}P, *n* = 1-3 by molecular oxygen in benzene at 25 °C.

Phosphine	$k_2 (\text{L mol}^{-1} \text{s}^{-1})$
P(C ₆ H ₄ - <i>p</i> -OMe) ₃	20.0
P(C ₆ H ₄ - <i>p</i> -Me) ₃	13.6
P(C ₆ H ₄ - <i>p</i> -CF ₃) ₃	7.46
P(C ₆ H ₄ - <i>p</i> -Cl) ₃	3.44
P(C ₆ H ₅) ₃	1.85
PMe ₂ Ph	3.29
PMePh ₂	2.18

CHAPTER IV. KINETICS AND MECHANISM OF THE METHYLTRIOXORHENIUM-CATALYZED SULFOXIDATION OF THIOKETONES AND SULFINES

A paper published in *Journal of Organic Chemistry*[†]

Ruili Huang and James H. Espenson*

Abstract

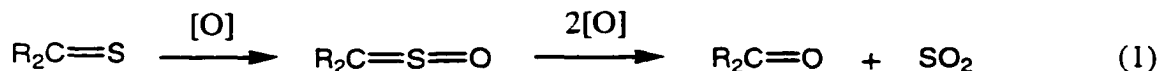
Kinetic studies have been carried out on the oxidation of thiobenzophenones and thiocamphor by hydrogen peroxide and on the second step in the sequence, oxidation of the resulting sulfines ($\text{Ar}_2\text{C}=\text{S}=\text{O}$). The first reaction follows the pattern now common to methyltrioxorhenium/ H_2O_2 reactions, in that the rate constant for the reaction between the peroxorhenium intermediate and the thioketone follows a Hammett correlation such that electron-releasing substrates react more rapidly. The reaction constant is $\rho = -1.12$. However, the plot of $\log(k_X/k_H)$ for the sulfines against 2σ , determined over the range $-1.6 < 2\sigma < +1.5$, is markedly U-shaped. This suggests a mechanism for the sulfines in which the direction of the electron flow in the transition state changes with the electron demand of the substituents on the sulfines. The product of oxidation of the sulfine is a transient sultine (from epoxidation of the $\text{C}=\text{S}$ bond). It cannot be detected, however, because it so rapidly yields sulfur monoxide. The SO was oxidized to SO_2 under these conditions rather than undergoing disproportionation to SO_2 and S. Also, SO was trapped with a 1,3-diene as a thiophene-1-oxide.

Introduction

Sulfines (thioketone S-oxides) are attractive heterocumulenes that participate in the thioepoxidation of alkenes,¹ nucleophilic addition,² and cycloaddition reactions.³⁻⁶ They are usually prepared by oxidizing the thioketones with peracids,⁷⁻¹³ ozone,^{10,14} or singlet oxygen.¹⁵ The sulfines can be further oxidized, leading ultimately to the ketone. The

[†] Reproduced with permission from Huang R.; Espenson, J. H. *J. Org. Chem.* **1999**, *64*, 6374-6379. Copyright 1999 American Chemical Society.

sequence of conversions, disregarding other intermediates at this point, is outlined in eq 1.



We have found that hydrogen peroxide can carry out both stages of this transformation when methyltrioxorhenium (CH_3ReO_3 , abbreviated as MTO) is used as the catalyst. We have undertaken a study of these reactions to describe their mechanisms. A point of particular mechanistic interest in this system is whether peroxide is activated for nucleophilic or electrophilic attack. We have studied the kinetics and mechanism of both steps in eq 1, with a particular reference to the substituent effects on the rate constants of ring-substituted thiobenzophenones.

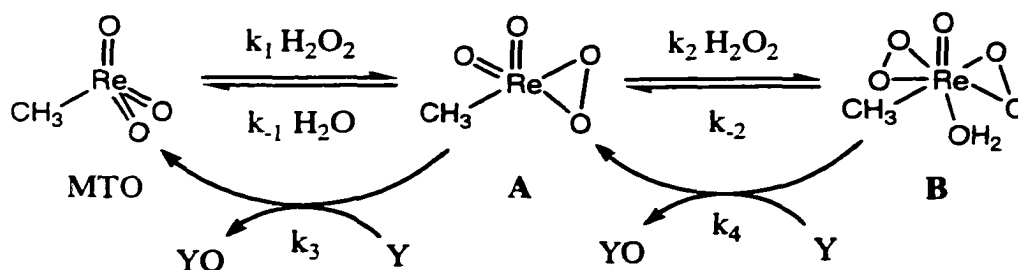
Experimental Section

Materials. The starting thiobenzophenones were prepared according to the literature method,^{15,16} except for commercially available thiocamphor, which was used as received. The thiobenzophenones are deep blue materials. The absorption maxima for the compounds $(\text{XC}_6\text{H}_4)_2\text{C}=\text{S}$, given as $\lambda_{\text{max}}/\text{nm}$ ($\epsilon/\text{L mol}^{-1} \text{ cm}^{-1}$), are $\text{X} = p\text{-NMe}_2$ 458 (2.7×10^4), $p\text{-OMe}$ 355 (2.46×10^4) and 570 (407), $p\text{-Me}$ 587 (262), H 590 (170), $p\text{-Cl}$ 600 (215), $m\text{-NO}_2$ 598 (203). Thiocamphor has λ_{max} 250 nm (ϵ $8.7 \times 10^3 \text{ L mol}^{-1} \text{ cm}^{-1}$).

Instrumentation. The reaction progress for thioketones was monitored at these wavelengths spectrophotometrically with a Shimadzu UV-3101PC instrument. The second stage, oxidation of sulfines, did not give suitable absorbance changes. Those reactions were followed by ^1H NMR with a Bruker DRX-400 spectrometer. The ^1H NMR chemical shifts were measured relative to the residual resonance of the solvent, CD_2HCN , δ 1.92 ppm. The solvent in both cases was water-acetonitrile (or, in ^1H experiments, D_2O) 1:4 by volume, and it contained 0.10 M trifluoromethanesulfonic acid to stabilize the catalyst.¹⁷ Throughout, the temperature was maintained at 25 °C.

Equilibrium Measurements. The equilibrium constants for the two stepwise MTO- H_2O_2 interactions defined in Scheme 1 were evaluated in this medium by ^1H NMR methods. The intensities of the CH_3 groups of the three species MTO, **A**, and **B** were integrated relative to a standard. The determined constants are $K_1 = 91 \text{ L mol}^{-1}$ and $K_2 = 347$

L mol⁻¹ at 25 °C, with the activity of water being ignored. These values are much as one might interpolate from other media.¹⁸ As in other circumstances, the values reflect the phenomenon of cooperativity, in that $K_2 > K_1$. We interpret that to mean that the rhenium-oxo multiple bonds are strengthened relative to those in the predecessor compound as the number of Re=O bonds is reduced at each stage.



Scheme 1

Kinetic Data. Both initial rate and full time course analyses were employed to determine the kinetics. To determine initial rates, the absorbance-time data from spectrophotometric kinetics or the integrated intensities-time data from ¹H NMR kinetics were converted to concentration-time values. The initial rate for each experiment was obtained by fitting each curve to a polynomial function: $[Y]_t = [Y]_0 - m_1t - m_2t^2 - m_3t^3 \dots$. The value of parameter m_1 was taken as the initial reaction rate, v_i . Under some circumstances the reaction was first-order with respect to the thioketone concentration. In such cases the absorbance-time data were fitted to the equation

$$\text{Abs}_t = \text{Abs}_\infty + (\text{Abs}_0 - \text{Abs}_\infty)\exp(-k_\psi t) \quad (2)$$

Trapping of SO with Dienes. 4,4'-Difluorothiobenzophenone S-oxide (13 mM) and MTO (12 mM) were mixed in acetonitrile containing 0.1 M HOTf to stabilize the MTO.¹⁷ Hydrogen peroxide (250 mM) was then added to the solution, followed immediately by 2,3-dimethyl-1,3-butadiene (100 mM). The reaction was monitored by ¹H NMR. After 1.5 h, 2,5-dihydro-3,4-dimethylthiophene-1-oxide (5.0 mM) was formed. This compound is the known product of the reaction between sulfur monoxide and the diene.¹⁹ The detected spectrum matched that of the known compound: ¹H (CD₃CN) δ 3.85 (d, 2H), 3.61 (d, 2H),

1.77 (s, 6H). The remainder of the diene (46 mM) had been oxidized to diol products. MTO-catalyzed oxidations of dienes with hydrogen peroxide have been well-characterized.²⁰

The same procedure using 4,4'-dimethoxythiobenzophenone and thiobenzophenone S-oxides with the same trapping reagent, 2,3-dimethyl-1,3-butadiene, was used. In these cases the same SO trapped product was obtained.

Results

Identification and Isolation of the Sulfines. The initially formed sulfines were identified by their UV-vis, ¹H NMR, and mass spectra in comparison with those of the known compounds.^{7,8,11,14,15,21-28} These spectra and those of the starting thiones and final product ketones are given in the Supporting Information. The only exceptions to that are two of the sulfines, which have evidently not been previously reported. These are the previously unknown compounds (*p*-FC₆H₄)₂CSO and (*m*-CF₃C₆H₄)₂CSO. The synthesis and isolation of those compounds has been reported separately.²⁹

Kinetics of Thioketone Oxidation. Control experiments for reactions between thioketones and hydrogen peroxide, without MTO, proceeded more than 10³ times more slowly than those measured with the catalyst present. Thus the uncatalyzed reaction can be neglected entirely. It was also shown that oxidation by atmospheric oxygen or photoactivation in laboratory light were not important. No effort was made to exclude either.

The typical ranges of concentrations used for kinetics experiments on thioketones in these studies were 0.01-0.1 mM thioketone, 0.1-1 mM hydrogen peroxide, and 1-100 μM MTO. The analysis of the kinetic data requires an examination of the general scheme by which MTO activates hydrogen peroxide. The general mechanism has now been established.³⁰⁻³² The reactions, shown in **Scheme 1**,³⁰ feature (a) conversion of MTO to two successive peroxorhenium complexes, (b) attack of substrate Y at an oxygen of the peroxo group, and (c) transfer of that oxygen to Y. This general picture requires a few refinements in special cases, as recently reviewed,³³ but it otherwise suffices quite well.

The kinetic data for the thioketones could be analyzed by accounting for only the left-hand loop in **Scheme 1**. That is so because these experiments were carried at low [H₂O₂], where any contribution from **B** can be ignored. Under these circumstances the rate of the reaction takes the form

$$v = \frac{k_1 k_3 [\text{H}_2\text{O}_2][\text{Y}][\text{Re}]_{\text{T}}}{k_{-1} + k_3[\text{Y}] + k_1[\text{H}_2\text{O}_2]} \cong \frac{k_1 k_3 [\text{H}_2\text{O}_2][\text{Y}][\text{Re}]_{\text{T}}}{k_{-1} + k_3[\text{Y}]} \quad (3)$$

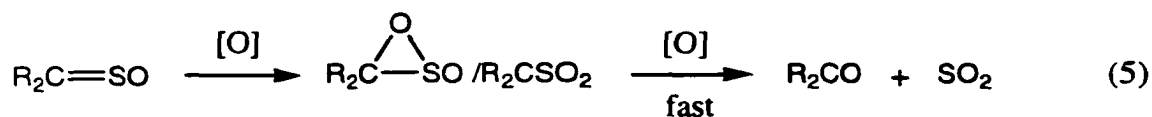
in which $[\text{Re}]_{\text{T}}$ stands for the total rhenium concentration. Under the conditions used for the thioketones, the $k[\text{H}_2\text{O}_2]$ denominator term was entirely negligible. The expression for the reaction rate in eq 3 states that the variation of the initial rate with the concentration of the thioketone will take the form of a rectangular hyperbola, with the rate attaining a thioketone-independent plateau at high concentrations. The same is true for values of k_{ψ} as a function of $[\text{R}_2\text{CS}]$. These experiments were carried out with $(p\text{-MeOC}_6\text{H}_4)_2\text{C}=\text{S}$ and with thiocamphor. Data for both compounds are displayed in **Figure 1**. From both experiments, the value $k_1 = 15.5 \pm 0.6 \text{ L mol}^{-1} \text{ s}^{-1}$ was obtained. Given $K_1 = 91 \text{ L mol}^{-1}$ from ^1H NMR experiments cited previously, we obtain the value $k_{-1} = 0.17 \text{ s}^{-1}$. Such determinations were needed to substantiate the model and establish values of k_1 and k_{-1} in this medium, but the kinetic data at the plateau provided no new data and no information about the reaction of the thioketone itself.

In most of the determinations, therefore, the thioketone concentration was kept deliberately low, such that eq 3 could be simplified even further by dropping the k_3 term in the denominator. The initial rate could then be accurately represented by

$$v_i = K_1 k_3 [\text{R}_2\text{C}=\text{S}]_0 [\text{H}_2\text{O}_2]_0 [\text{Re}]_{\text{T}} \quad (4)$$

The test of this kinetic equation is presented in **Figure 2**, which displays plots of $v_i/[\text{Y}]_0[\text{H}_2\text{O}_2]_0$ against $[\text{Re}]_{\text{T}}$ for three substrates. The values of k_3 for these compounds and for others are summarized in **Table 1**.

Kinetics of Sulfine Oxidation. The next step of oxidation converts the sulfine to a sultine and/or a sulfene:



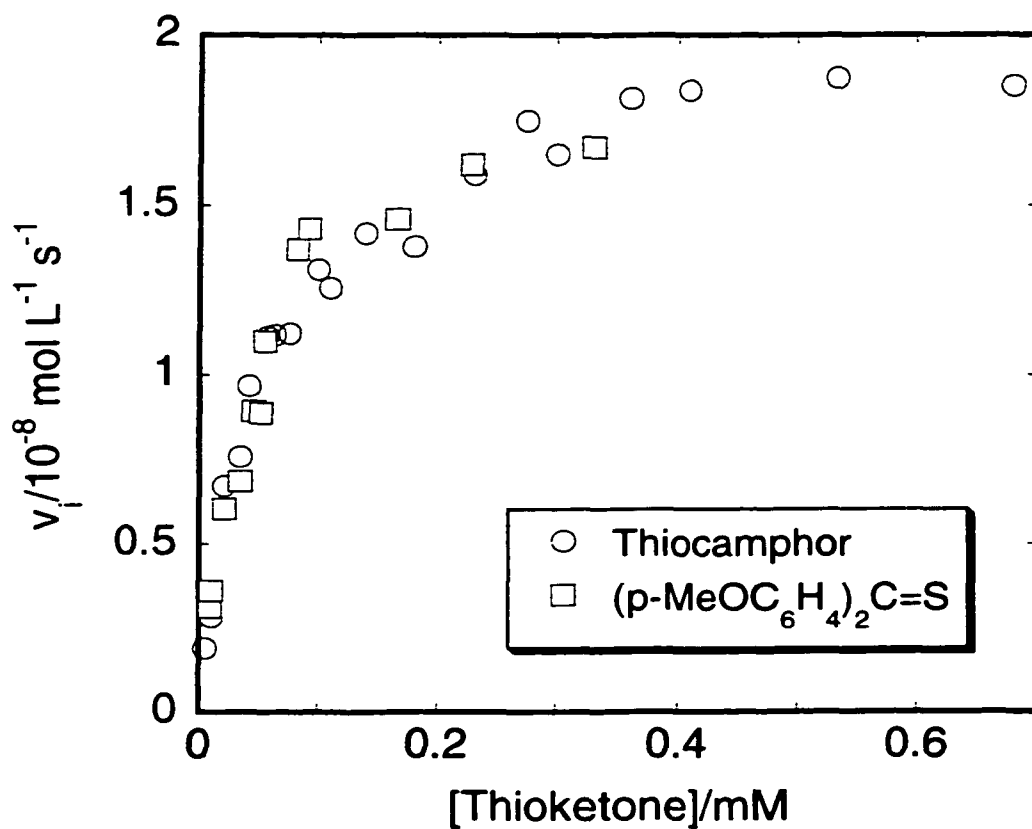


Figure 1. Kinetic data for the oxidation of thioketones to sulfines by hydrogen peroxide with MTO as a catalyst. The initial rates at constant catalyst and hydrogen peroxide concentrations describe a rectangular hyperbola against the concentration of the thioketone. Data were acquired in aqueous acetonitrile (1:4) at 25 °C. Values are shown for $(p\text{-MeOC}_6\text{H}_4)_2\text{CS}$ (squares) and for thiocamphor (circles).

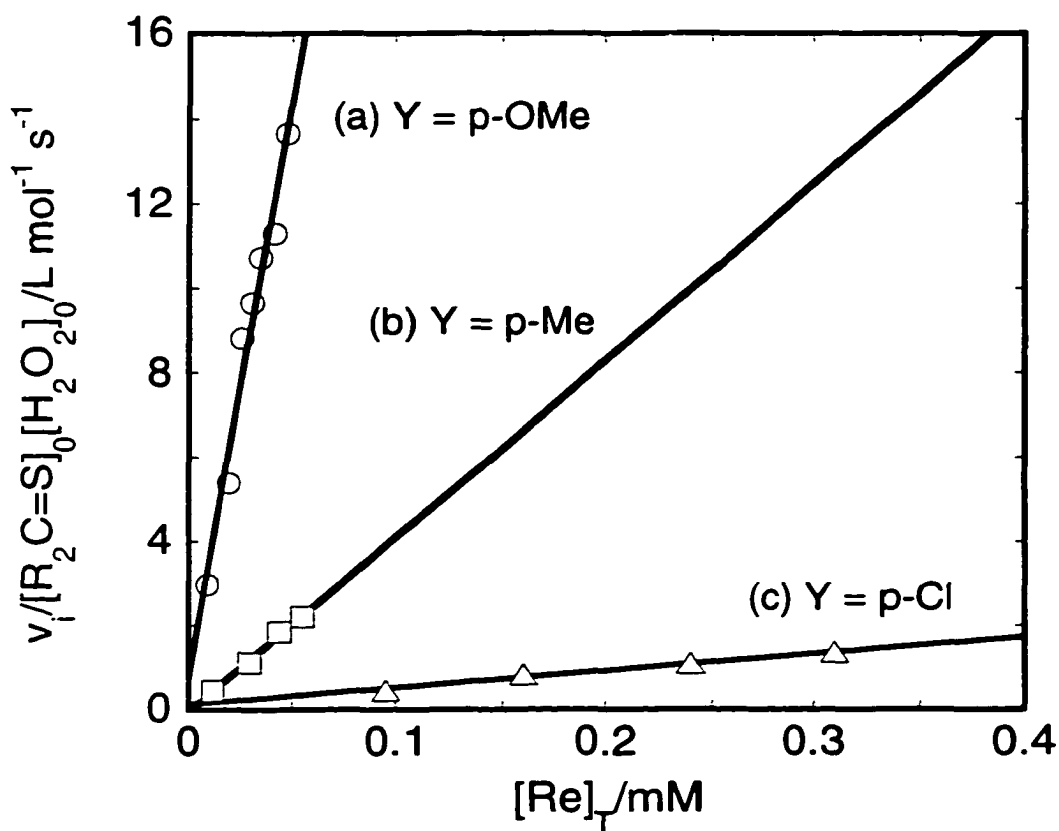


Figure 2. Kinetics of oxidation of thiobenzophenones by hydrogen peroxide. The y-axis displays the initial rate divided by $[\text{Ar}_2\text{CS}]_0[\text{H}_2\text{O}_2]_0$. This quantity is directly proportional to $[\text{Re}]_T$, in accord with eq 4. Data, acquired in aqueous acetonitrile (1:4) at 25 °C, are shown for $(p\text{-XC}_6\text{H}_4)_2\text{CS}$, with $\text{X} = \text{CH}_3\text{O}$ (a), CH_3 (b), Cl (c).

These reactions occur rather more slowly. To conduct the kinetics measurements, the thioketones were first treated with 1.0 equiv of hydrogen peroxide, in the presence of MTO. The conversion to the sulfine was shown by ^1H NMR in each case to be quantitative, within the precision of the measurement. Additional hydrogen peroxide was then added to provide $[\text{H}_2\text{O}_2]/[\text{Ar}_2\text{CSO}] \geq 20$. The disappearance of the sulfine was monitored by ^1H NMR, because the absorbance changes were not suitable. The overall concentration ranges in these experiments were 2-20 mM sulfine, 0.2-0.5 M H_2O_2 , and 0.1-10 mM MTO.

The conditions under which a thioketone is oxidized give reactions with a typical lifetime of ~ 10 min; under similar conditions the resulting sulfine requires 670 h. The addition of the electronegative oxygen atom to the sulfur greatly reduces the rate of a subsequent oxidation.

Higher peroxide concentrations were used for the sulfines to avoid a prolonged reaction time. This change means that the simplified kinetic treatment given above will not suffice, because **B** now attains a high concentration and contributes to the overall catalysis. With all the reactions in **Scheme 1**, the rate law takes the form

$$-\frac{d[\text{Y}]}{dt} = \frac{k_1 k_3 [\text{Re}]_{\text{T}} [\text{H}_2\text{O}_2] [\text{Y}] + \frac{k_1 k_2 k_4 [\text{Re}]_{\text{T}} [\text{Y}] [\text{H}_2\text{O}_2]^2}{k_4 [\text{Y}] + k_{-2}}}{k_{-1} + k_3 [\text{Y}] + k_1 [\text{H}_2\text{O}_2] + \frac{k_1 k_2 [\text{H}_2\text{O}_2]^2}{k_4 [\text{Y}] + k_{-2}}} \quad (6)$$

At these high peroxide concentrations, however, a different simplification is valid. This provides a form that is an accurate representation under the circumstances:

$$v = k_4 [\text{R}_2\text{CSO}] [\text{Re}]_{\text{T}} \quad (7)$$

To check this equation, tests were carried out to affirm the first-order dependence on sulfine concentration, the first-order dependence on the total MTO concentration (see **Figure 3**), and the absence of a kinetic term in the hydrogen peroxide concentration, which was varied

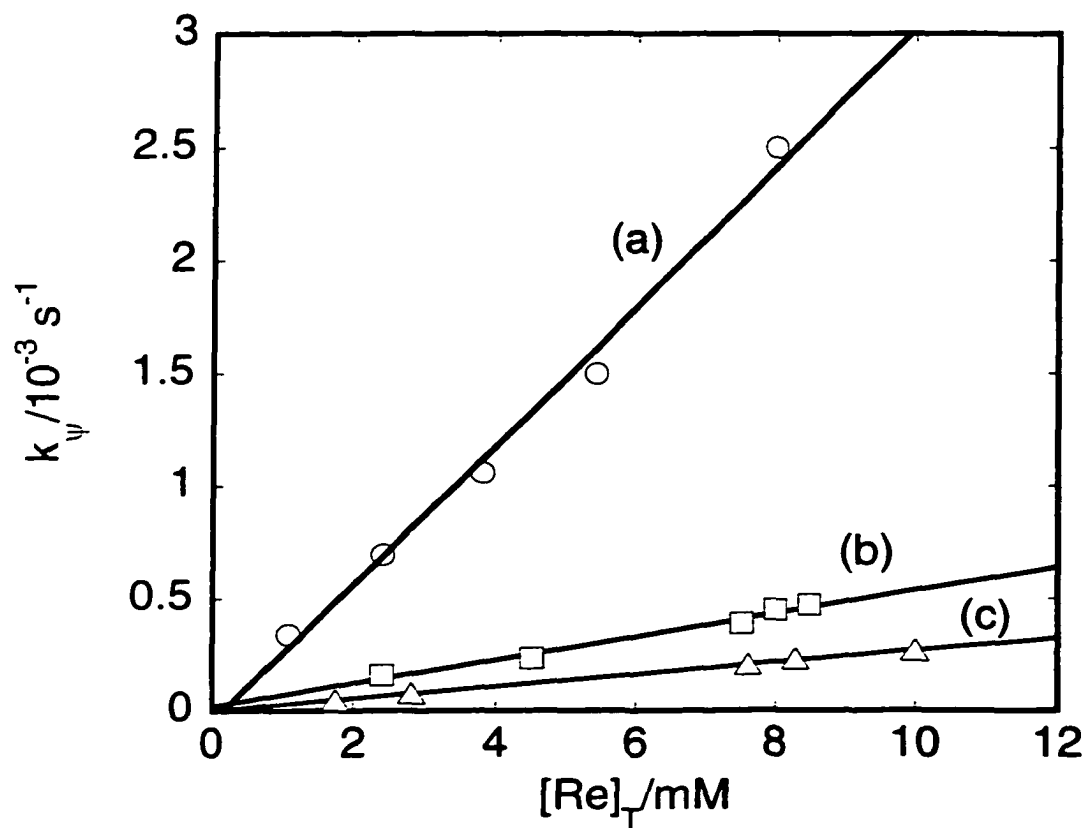
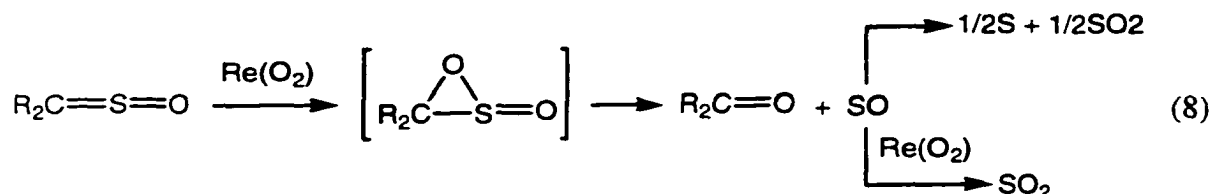


Figure 3. Values of the pseudo-first-order rate constants in aqueous acetonitrile (1:4) at 22.5 °C for the oxidation of thiobenzophenone oxides are a linear function of $[\text{Re}]_{\text{T}}$, in agreement with eq 7. Values are shown for $(p\text{-XC}_6\text{H}_4)_2\text{CSO}$, with $\text{X} = \text{CH}_3\text{O}$ (a), CH_3 (b), Cl (c).

without effect in the range 0.2-0.5 M. The values of k_4 determined for the sulfines by this procedure are summarized in **Table 1**.

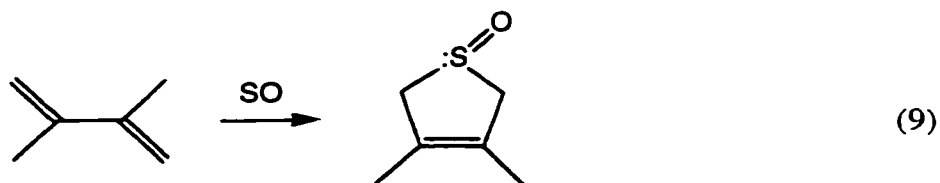
The oxidation of sulfines to ketones may proceed through a sultine or sulfene intermediate, as written in eq 5, or in some other manner. It had been suggested previously, in the oxidation of sulfines with monoperphthalic acid⁸ and perbenzoic acid,⁷ that the second oxygen was added to the C=S double bond. Theoretical calculations showed that the sultine intermediate so obtained was more stable than its isomer, the sulfene. It was further suggested that the sultine would rapidly eliminate the ketone, forming sulfur monoxide.^{7,8,34,35} That sulfur monoxide could disproportionate, and it was the previous basis for suggesting the sultine. The oxidation of SO by peroxorhenium complexes seems more probable in this medium; no elemental sulfur was found in our experiments.



Close attention was therefore paid to the NMR spectra taken during the course of this reaction. Signals from the thioketone, sulfine, and ketone were easily detected. No signal corresponding to a sultine (or sulfene) was detected. Because no intermediate or any other new species was observed, it can be concluded that the subsequent step(s) must be much more rapid than the first.

Trapping of Sulfur Monoxide. Sultine formation was not proved by trapping the sulfur monoxide released; evidence for it was the formation of elemental sulfur, suggested to come from SO disproportionation.^{7,8} Elemental sulfur was not seen in the present study because even if it was formed under these conditions, it would be oxidized very quickly to sulfur dioxide. To establish this mechanism, experiments were done to trap SO from the oxidation of sulfines. Dienes were known to be able to react with SO fast enough that SO could be trapped as thiophene 1-oxides.¹⁹ Thus 2,3-dimethyl-1,3-butadiene was put into the reaction mixture to trap the SO produced from sulfine oxidation (eq 9). 4,4'-Difluoro, 4,4'-dimethoxythiobenzophenone and thiobenzophenone were used, and even

though part of the dienes were lost to oxidation, the SO trapped product 2,5-dihydro-3,4-dimethylthiophene 1-oxide was still detected by ^1H NMR up to 10% yield based on diene. Because so much diene was oxidized, a better basis is to examine the fate of sulfur monoxide; 100% of it was trapped, about 40% being detected as the product of eq 9 and the balance as its oxidation product.



Discussion

The most important issue to be dealt with is the comparison of the mechanism for thioketones versus sulfines. A seeming complication is the experiments yielded values of k_3 for the one but k_4 for the other. In fact, this need be of no concern. For numerous substrates both rate constants have been determined. Relatively little variation has been found. The summary of rate constants in **Table 2** makes this point very clearly. There is, indeed, one exception, but that refers to the case of allyl alcohols, where hydrogen bonding with **B** plays a special role.³⁶ With this justification, in what follows the values will be discussed interchangeably.

In earlier studies, the electronic structure of the transition state has been probed by the selection of different substrates. For example, phosphines and sulfides have been studied. With compounds Ar_3P and ArSMe , certain adjustments can be made that will alter the electron density at the accepting atom without causing an important structural change. In these particular cases, the introduction of substituents in meta or para positions provides a useful indicator. A substituent that is electron-withdrawing relative to H decreases the rate constant and vice versa. When correlated by Hammett's equation, the values are $\rho = -0.63$ (PAr_3) and -0.98 (ArSMe).

So it is with thioketones. The experimental rate constants for $\text{Ar}_2\text{C}=\text{S}$ were analyzed for the effect of substituent X by a plot of $\log(k_3^{\text{X}}/k_3^{\text{H}})$ versus $2\sigma_{\text{X}}$. These points define a

linear relation, **Figure 4**, and afford the reaction constant $\rho = -1.12 \pm 0.06$ ($r = 0.962$). If the somewhat deviant value for $X = \text{CH}_3\text{O}$ is omitted, then $\rho = -1.06 \pm 0.07$ ($r = 0.994$). The value is comparable to values obtained in other oxidations of thiobenzophenones: $\rho = -0.88$ for perbenzoic acid⁷ and $\rho = -0.75$ for N-sulfonyloxaziridines.²¹

The data for the thioketones reinforce the already-established depiction of the transition state. The negative reaction constant signifies that positive charge has accumulated in the transition state. The high-valent rhenium center, an electropositive Lewis acidic center, polarizes the peroxide ion coordinated to it. Thus the peroxo oxygens are less electron-rich than those in hydrogen peroxide itself. As a result, nucleophilic centers attack at the peroxo oxygen directly, a point that has been affirmed by ¹⁸O labeling.³⁷

Against this background, the kinetic data for the oxidation of the sulfines form a marked contrast. The Hammett plot, also displayed in **Figure 4**, shows distinct curvature. Indeed, further compounds were prepared at both extremes of σ to establish that the upward curvature was experimentally and statistically valid over a wide variation.

Curvature in a Hammett plot signals a certain complexity in the mechanism. By the laws of adding exponentials, concave curvature implicates two pathways in parallel, whereas convex curvature is consistent with alternative rate-controlling steps along a single pathway.^{38,39} The first of these options is indicated by these results.

Just as with the thioketones, those sulfines that have electron-donating substituents increase in rate, with $\log k$ varying linearly with σ . The left-hand portion of the Hammett plot for the sulfines is as steep as the line for the thioketones and perhaps steeper. This is reasonable in that the sulfine, with an oxygen atom reducing electron density on the sulfur, makes the $\text{C}=\text{S}=\text{O}$ group of the sulfine more electropositive than the $\text{C}=\text{S}$ group of the thioketone. The sulfine rates are lower, but their sensitivity to substituents is somewhat greater.

The Hammett plot reverses in slope for substituents with large σ values. This has not been seen before for the oxidations of aromatic thiones or sulfines with other oxidizing reagents.^{21,33,38} Substituents that are electron-attracting cause a lesser rate diminution and then a rate increase. This effect can be explained in terms of a model in which the direction of electron flow in the transition state has been reversed. This can be explained by the

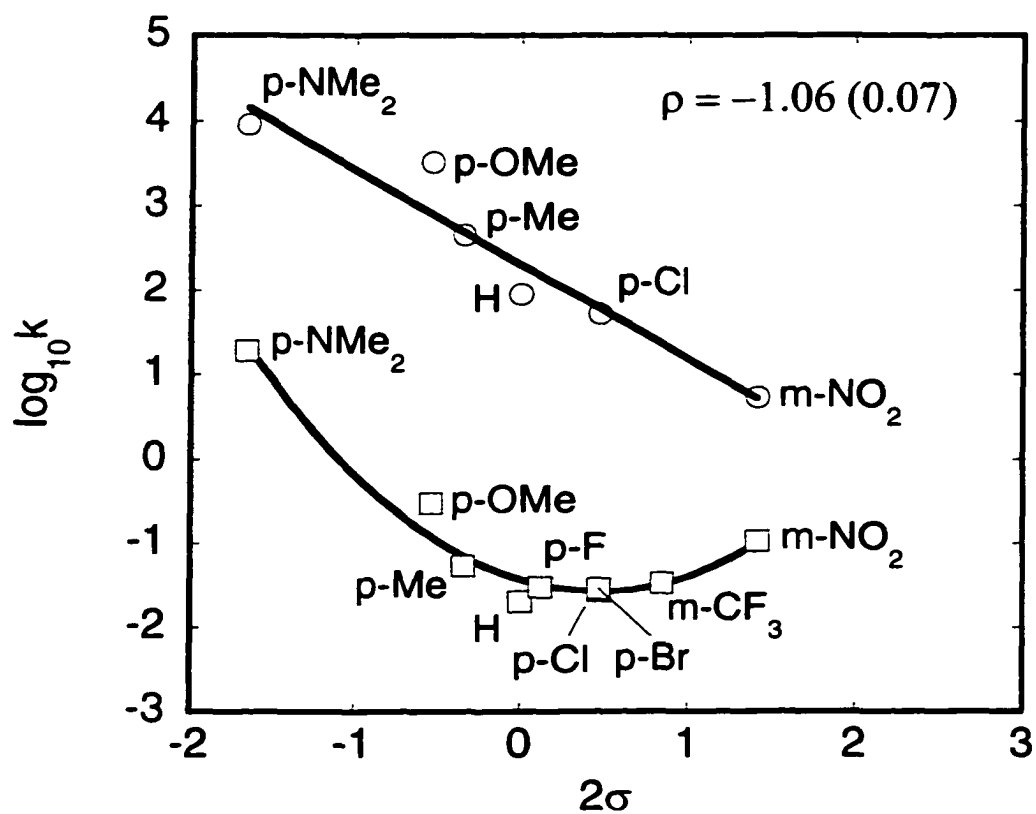
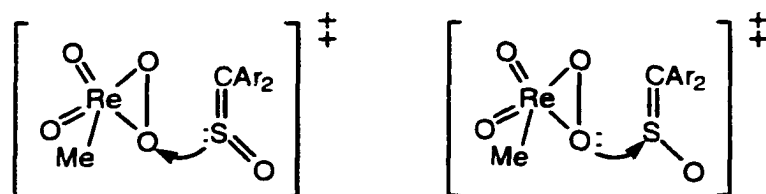


Figure 4. Hammett correlations of $\log k$ against 2σ for the MTO-catalyzed oxidations of: thiobenzophenones (upper) and thiobenzophenone S-oxides (sulfines, lower).

change of the mode of peroxide activation from electrophilic at negative σ values to nucleophilic at positive σ values. The "normal" case-found for thioketones and for most other reagents and for those sulfines with electron-donating substituents-features the nucleophilic reagent attacking the peroxo oxygen. One says that peroxide has been activated electrophilically. On the other hand, peroxides are inherently nucleophilic. Substrates with substituents that are sufficiently electron-attracting can be so attacked.

The suggested transition states are shown in these diagrams:



Whether the changeover will actually be found in any reaction series cannot be specified in advance. The matter clearly depends not only on the peroxorhenium species, common to any series, but also on the nature of the reaction partner. The sulfine, unlike the sulfide and many others, at least invites both alternatives. To our knowledge, this is the first instance of a mechanistic feature in the MTO activation of peroxide. The phenomenon has been recorded previously, however. Perhaps the closest analogy to these results is provided by the oxidation of ArSCH_3 by a peroxotitanium complex.⁴ In MTO-peroxide chemistry, the only previous example of the nucleophilic activation of peroxide appears to be in Baeyer-Villiger reactions.⁴¹ Examples elsewhere include the OsO_4 -catalyzed oxidation of *trans*-cinnamic acids by chloramines-T and $-\text{B}^{42, 43}$ and by pyridinium chlorochromate;⁴⁴ oxidation of benzyl alcohols by quinolinium dichromate;⁴⁵ oxidation of styrenes by dioxoruthenium(VI) porphyrins⁴⁶ and quaternary ammonium permanganates.⁴⁷

Thioketones are oxidized so much more rapidly than sulfines that the product of the first stage can be produced with but little subsequent oxidation. To do so, thioketone and peroxide were reacted in 1:1 quantities with a catalytic amount of MTO. Some of the reactions were monitored by ^1H NMR. The spectra showed the reaction was efficient, reaching completion in (typically) 5 min.

Some interferences were checked by adding each of the substances: cyclohexene, PhNMe₂, Me₂SO, and Me₂CO. This material was added prior to MTO/H₂O₂. The yield of the sulfine was determined by ¹H NMR. With these reagents no loss of sulfine was noted.

The addition of NaHCO₃ stopped the reaction entirely. This is a general phenomenon for MTO-peroxide chemistry, which comes about by the base-catalyzed decomposition of **A** and **B**. (Actually, this occurs by the reaction of HOO⁻ with MTO).¹⁷ This mode of decomposition is so efficient that nonacidified solutions of MTO and H₂O₂ will not long survive intact.

References

- (1) Adam, W.; Deeg, O; Weinkotz, S. *J. Org. Chem.* **1997**, *62*, 7084.
- (2) Alayrac, C; Cerreta, F.; Chapron, I.; Corbin, F.; Metzner, P. *Tetrahedron Lett.* **1996**, *37*, 4507.
- (3) Molston, G; Linden, A.; Heimgartner, H. *Helv. Chim. Acta.* **1996**, *79*, 31.
- (4) Braverman, S.; Grinstein, D.; Gottlieb, H. *J. Chem. Soc., Perkin. Trans. I*, **1998**, No. 1, 103.
- (5) Manoharan, M; Venuvanalingam, P. *J. Phys. Org. Chem.* **1997**, *10*, 768.
- (6) Saito, T; Takekawa, K.; Nishimura, J-I.; Kawamara, M. *J. Chem. Soc. Perkin. Trans. I* , **1997**, No. 20, 2957.
- (7) Battaglia, A.; Dondoni, A.; Giorgianni, P.; Maccagnani, G.; Mazzanti, G. *J. Chem. Soc. (B)* **1971**, 1547.
- (8) Zwanenburg, B.; Thijs, L.; Strating, J. *Recl. Trav. Chim. Pays-Bas* **1967**, *86*, 577.
- (9) Hasserodt, J.; Pritzkow, H.; Sundermeyer, W. *Chem. Ber.* **1993**, *126*, 7, 1701.
- (10) Zwanenburg, B.; Janssen, W. A. *J. Synthesis* **1973**, 617.
- (11) Carlsen, L.; Snyder, J. P.; Holm, A.; Pederson, E. *Tetrahedron* **1981**, *37*, 1257.
- (12) Adiwidjaja, G.; Sawluk, A.; Volz, W.; Voss, J. *Phosphorus, Sulfur, Silicon Relat. Elem.* **1993**, *74*, 1-4, 451.
- (13) Cerreta, F. *Bull. Soc. Chim. Fr.* **1995**, *67*, 132.
- (14) Tabuchi, T.; Nojima, M.; Kusabayashi, S. *J. Chem. Soc. Perkin. Trans. I* **1991**, *12*, 3043.
- (15) Ramnath, N.; Ramesh, V.; Ramamurthy, V. *J. Org. Chem.* **1983**, *48*, 214.

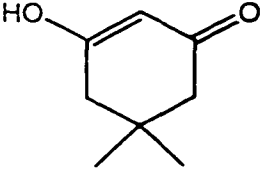
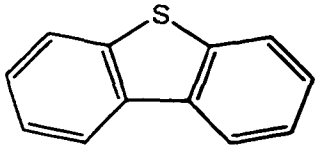
- (16) Scheeren, J.; Ooms, P.; Nivard, R. *Synthesis* **1973**, 149.
- (17) Abu-Omar, M.; Hansen, P. J.; Espenson, J. H. *J. Am. Chem. Soc.* **1996**, *118*, 4966.
- (18) Espenson, J. H.; Abu-Omar, M. M. *Adv. Chem. Ser.* **1997**, *253*, 99.
- (19) Tardif, S. L.; Rys, A.; Abrams, C. B.; Abu-Yousef, I. A.; Leste-Laserre, P. B.; Schults, E. K. V.; Harpp, D. N. *Tetrahedron* **1997**, *53*, 12225.
- (20) Tan, H.; Espenson, J. H. *Inorg. Chem.* **1998**, *37*, 467.
- (21) Maccagnani, G.; Innocenti, A.; Zani, P.; Battaglia, A. *J. Chem. Soc. Perkin. Trans. II* **1987**, 1113.
- (22) Dahn, H.; Pechy, P.; Toan, V. V.; Bonini, B. F.; Lunazzi, L. *J. Chem. Soc., Perkin Trans. 2* **1993**, *10*, 1881.
- (23) Zwanenburg, B. *Tetrahedron* **1971**, *27*, 1731.
- (24) Tangerman, A.; Zwanenburg, B. *J. Chem. Soc., Perkin Trans. 2* **1973**, 458.
- (25) Tangerman, A.; Zwanenburg, B. *J. Chem. Soc., Perkin Trans. 2* **1974**, 1141.
- (26) Veenstra, G. E.; Zwanenburg, B. *Recl. Trav. Chim. Pays-Bas* **1976**, *95*, 37.
- (27) Huisgen, R.; Mloston, G.; Polborn, K.; Palacios-Gambra, F. *Liebigs Ann. Org. Bioorg. Chem.* **1997**, *1*, 187.
- (28) Kuipers, J. A. M.; Lammerink, B. H. M.; Still, K. W. J.; Zwanenburg, B. *Synthesis* **1981**, *4*, 295.
- (29) Huang, R.; Espenson, J. H.; *J. Org. Chem.* **1999**, *64*, 6935.
- (30) Abu-Omar, M. M.; Appleman, E. H.; Espenson, J. H. *Inorg. Chem.* **1996**, *35*, 7751.
- (31) Gable, K. P. *Adv. Organomet. Chem.* **1997**, *41*, 127.
- (32) Herrmann, W. A.; Kühn, F. E. *Acc. Chem. Res.* **1997**, *30*, 169.
- (33) Espenson, J. H. *J. Chem. Soc., Chem. Commun.* **1999**, 479.
- (34) Lyaschchuk, S. I.; Strypnik, Y. G.; Bezvodnyi, V. P. *Russ. J. Org. Chem.* **1997**, *33*, 9958.
- (35) McIntosh, C. L.; De Mayo, P. *J. Chem. Soc., Chem. Commun.* **1969**, 32.
- (36) Tetzlaff, H. R.; Espenson, J. H. *Inorg. Chem.* **1999**, *38*, 881.
- (37) Vassell, K. A.; Espenson, J. H. *Inorg. Chem.* **1994**, *33*, 5491.
- (38) Leffler, J. E. *J. Org. Chem.* **1951**, *16*, 1785.

- (39) Exner, O. In *Advances in Linear Free Energy Relationships*; Chapman, N. B.; Shorter, J.; Eds.; Plenum: New York, 1972; pp 12-17.
- (40) Bonchio, M.; Calloni, S.; Di Furia, F.; Licini, G.; Modena, G.; Moro, S.; Nugent, W. A. *J. Am. Chem. Soc.* **1997**, *119*, 6935.
- (41) Herrmann, W. A.; Fischer, R. W.; Correia, J. D. G. *J. Mol. Catal.* **1994**, *94*, 213.
- (42) Sabapathymohan, R. T.; Gopalakrishnan, M.; Sekar, M. *Oxid. Commun.* **1995**, *18*, 65.
- (43) Sabapathymohan, R. T.; Gopalakrishnan, M.; Sekar, M. *Tetrahedron* **1994**, *50*, 10945.
- (44) Sabapathymohan, R. T.; Gopalakrishnan, M.; Sekar, M. *Tetrahedron* **1994**, *50*, 10933.
- (45) Aruna, K.; Manikyamba, P.; Sundaram, E. V. *Indian J. Chem.* **1994**, *33A*, 854.
- (46) Ho, C.; Leung, W. H.; Che, C. M. *J. Chem. Soc., Dalton Trans.* **1991**, 2933.
- (47) Lee, D. G.; Brown, K. C.; Karaman, H. *Can. J. Chem.* **1986**, *64*, 1054.
- (48) Abu-Omar, M. M.; Espenson, J. H. *J. Am. Chem. Soc.* **1995**, *117*, 272.
- (49) Al-Ajlouni, A.; Espenson, J. H. *J. Am. Chem. Soc.* **1995**, *117*, 9243.
- (50) Hansen, P. J.; Espenson, J. H. *Inorg. Chem.* **1995**, *34*, 5839.
- (51) Espenson, J. H.; Pestovsky, O.; Huston, P.; Staudt, S. *J. Am. Chem. Soc.* **1994**, *116*, 2869.
- (52) Abu-Omar, M. M.; Espenson, J. H. *Organometallics* **1996**, *15*, 3543.
- (53) Brown, K. N.; Espenson, J. H. *Inorg. Chem.* **1996**, *35*, 7211.

Table. 1 Kinetic data for the MTO-catalyzed oxidation of thiobenzophenones ($\text{XC}_6\text{H}_4)_2\text{C}=\text{S}$ and sulfines ($\text{XC}_6\text{H}_4)_2\text{C}=\text{S}=\text{O}$ by hydrogen peroxide

X	thioketones k_3	sulfines k_4
	($\text{L mol}^{-1} \text{s}^{-1}$) (25 °C)	($\text{L mol}^{-1} \text{s}^{-1}$) (22.5 °C)
<i>p</i> -NMe ₂	$(9.2 \pm 0.4) \times 10^3$	$(1.93 \pm 0.12) \times 10^1$
<i>p</i> -OMe	$(3.3 \pm 0.1) \times 10^3$	$(3.00 \pm 0.08) \times 10^{-1}$
<i>p</i> -Me	$(4.5 \pm 0.1) \times 10^2$	$(5.46 \pm 0.13) \times 10^{-2}$
H	$(9.0 \pm 0.1) \times 10^1$	$(2.02 \pm 0.07) \times 10^{-2}$
<i>p</i> -F		$(3.03 \pm 0.16) \times 10^{-2}$
<i>p</i> -Cl	$(5.2 \pm 0.1) \times 10^1$	$(2.71 \pm 0.09) \times 10^{-2}$
<i>p</i> -Br		$(2.90 \pm 0.06) \times 10^{-2}$
<i>m</i> -CF ₃		$(3.37 \pm 0.12) \times 10^{-2}$
<i>m</i> -NO ₂	$(5.4 \pm 0.3) \times 10^0$	$(1.06 \pm 0.01) \times 10^{-1}$
thiocamphor	$(3.0 \pm 0.1) \times 10^3$	

Table 2. Comparisons of the rate constants k_3 for **A** and k_4 for **B** in their reactions with different substrates.

substrate	k_3 (L mol ⁻¹ s ⁻¹) ^a	k_4/k_3 ^a	ref
PhSMe	2.65×10^3	0.36	37
Ph ₂ S	1.18×10^2	0.27	37
PPh ₃	7.3×10^5	3.0	48
P(C ₆ F ₅) ₃	1.30×10^3	2.7	48
<i>trans</i> -PhCH=CHOMe	14.2	0.90	49
<i>trans</i> -PhCH=CHMe	0.51	0.43	49
Cl ⁻	5.6×10^{-2}	2.3	50
Br ⁻	3.5×10^2	0.49	51
	0.19	0.58	52
	10.2	2.1	53

^a From the original references compiled in ref 33.

Supporting Information

¹H-NMR data in CD₃CN (DRX-400) for thiocamphor and for thiobenzophenones, sulfines and ketones

R	$\delta(\text{ppm})$		
	Thiones	Sulfines	Ketones
Thiocamphor	2.75 (d of m, 1H), 2.35 (d, 1H), 2.12 (t, 1H), 1.93 (m, 1H), 1.75 (t of m, 1H), 1.33 (m, 1H), 1.17 (m, 1H), 1.01 (s, 3H), 0.98 (s, 3H), 0.71 (s, 3H)	2.94 (d of m, 1H), 2.45 (d, 1H), 2.02 (t, 1H), 1.86 (m, 2H), 1.39 (m, 1H), 1.24 (m, 1H), 1.06 (s, 3H), 0.90 (s, 3H), 0.77 (s, 3H)	2.35 (d of m, 1H), 2.09 (t, 1H), 1.95 (m, 1H), 1.84 (d, 1H), 1.68 (m, 1H), 1.42 (m, 1H), 1.35 (m, 1H), 0.96 (s, 3H), 0.92 (s, 3H), 0.83 (s, 3H)
<i>para</i> -NMe ₂	7.64 (d, 4H), 6.67 (d, 4H), 3.03 (s, 12H)	7.82 (d, 2H), 7.20 (d, 2H), 6.76 (m, 4H), 2.97 (s, 12H)	6.73 (d, 4H), 7.64 (d, 4H), 3.01 (s, 12H)
<i>para</i> -OMe	7.66 (d, 4H), 6.92 (d, 4H), 3.83 (s, 6H)	7.80 (d, 2H), 7.29 (d, 2H), 7.00 (m, 4H), 3.82 (s, 3H), 3.80 (s, 3H)	7.70 (d, 4H), 7.00 (d, 4H), 3.83 (s, 6H)
<i>para</i> -Me	7.54 (d, 4H), 7.20 (d, 4H), 2.33 (s, 6H)	7.65 (d, 2H), 7.25 (m, 6H), 2.34 (s, 3H), 2.33 (s, 3H)	7.61 (d, 4H), 7.30 (d, 4H), 2.38 (s, 6H)
H	7.68 (d of m, 4H), 7.52 (t, 2H), 7.43 (t, 4H)	7.72 (m, 4H), 7.55 (m, 2 H), 7.36 (m, 4H)	7.77 (d, 4H), 7.65 (t, 2H), 7.53 (t, 4H)
<i>para</i> -F	7.73 (m, 4H), 7.16 (m, 4H)	7.88 (m, 2H), 7.42 (m, 2H), 7.24 (m, 4H)	7.81 (m, 4H), 7.24 (m, 4H)

(continued)

<i>para</i> -Cl	7.63 (d, 4H), 7.42 (d, 4H)	7.73 (d, 2H), 7.49 (m, 4H), 7.35 (d, 2H)	7.70 (d, 4H), 7.51 (d, 4H)
<i>para</i> -Br	7.55 (d & d, 8H)	7.72 (2H), 7.61 (2H), 7.57 (2H), 7.27 (d, 2H)	7.64 (d & d, 8H)
<i>meta</i> -CF ₃	7.88 (m, 4H), 7.83 (d, 2H), 7.59 (t, 2H)	8.14 (s, 1H), 8.07 (d, 1H), 7.84 (d, 1H), 7.77 (d, 1H), 7.51 – 7.62 (m, 4H)	7.98 (m, 2H), 7.92 (m, 4H), 7.68 (t, 2H)
<i>meta</i> -NO ₂	8.43 (m, 4H), 8.00 (d, 2H), 7.67 (t, 2H)	8.75 (t, 1H), 8.42 (m, 1H), 8.21 (m, 2H), 7.68 (m, 3H), 7.59 (m, 1H)	8.53 (m, 2H), 8.48 (d of m, 2H), 8.14 (d of t, 2H), 7.79 (t, 2H)

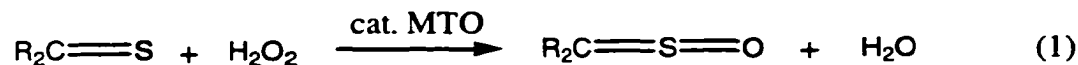
CHAPTER V. A CONVENIENT PREPARATION OF SULFINES (R₂C=S=O) FROM THIOKETONES

A paper published in Journal of Organic Chemistry[†]

Ruili Huang and James H. Espenson*

Introduction

Hydrogen peroxide is able to oxidize thiobenzophenones and thiocamphor to their sulfines, when catalyzed by methyltrioxorhenium, CH₃ReO₃ or MTO, according to this general reaction:



This method has provided a new route to sulfines that is superior to known methods. Peracids are traditionally used, such as perbenzoic acid,¹ monoperoxyphthalic acid,^{2,3} and *m*-CPBA.⁴⁻⁶ Even with a limited peracid concentration to prevent overoxidation, yields were not entirely satisfactory. On the basis of the peracids consumed, conversions were in the range 9-99%, but expressed as the conversion of thione, it was much less satisfactory, even at 0 °C. Ozonation is another common method,^{7,8} often carried out at -70 °C under nitrogen. With a 1:1 ratio of thione/O₃ at room temperature, the yield was still quite low, about 3-6% of sulfine, with most of the thione remaining unoxidized or overoxidized to the ketone.⁹ The use of ¹O₂¹⁰ proved unsatisfactory, as did other oxidizing reagents.¹¹ The conditions used in these reactions and the yields of sulfines thus obtained are summarized in **Table 1**.

Aside from oxidative methods, one should note the alkylidenation of sulfur dioxide with α-silyl carbanions at -78 °C¹² and the base-induced elimination of alkanesulfinyl derivatives.^{13,14}

[†] Reproduced with permission from Huang, R.; Espenson, J. H. *J. Org. Chem.* **1999**, *64*, 6935-6936. Copyright 1999 American Chemical Society.

Results and Discussion

In this work, reaction 1 was carried out for several thiobenzophenones, with *para*-Substituents consisting of: NMe₂, OMe, Me, H, F, Cl, Br, *m*-CF₃, and *m*-NO₂. Thiocamphor was used as well. To obtain the sulfines in high yields on a 1 mmol scale, only the requisite quantity of hydrogen peroxide was used. This method succeeds because the subsequent oxidation of the sulfines occurs $<10^3$ times as rapidly as the rate of reaction 1. With a 1:1 ratio of R₂CS/H₂O₂, no further oxidation or side products were obtained, as judged by ¹H NMR. The reaction was carried out at room temperature in organic solvents (acetonitrile, chloroform, etc.) or in aqueous mixtures.

Some of these reactions have now been carried out on a larger scale, starting with 0.7-1.0 g of the thione dissolved in 1:4 aqueous acetonitrile. The solution also contained 0.1 M trifluoromethanesulfonic acid to stabilize MTO. This catalyst was added at 1-10% (usually 1-2%) relative to the thione, followed by hydrogen peroxide (1.0 equiv). The color of solution changed from the dark blue of the thiobenzophenone to light yellow in less than 2 min, signaling the completion of the reaction. The conversion was checked at this point by ¹H NMR; the reactions were found to be completed within 5 min. Acetonitrile was removed from the product solution by rotary evaporation. Hexane and water were added, followed by excess sodium bicarbonate to neutralize the triflic acid and decompose MTO to perrhenate ions.¹⁵ The sulfine appeared in the hexane layer; the aqueous layer contained sodium triflate, excess sodium bicarbonate, and the perrhenate salt. The yellow hexane layer was washed with water several times and then rotary evaporated to remove the solvent. Higher purity material could be obtained by column or thin-layer chromatography on silica gel, eluting with ethyl acetate-hexane. Recrystallization from hexane-isooctane or hexane alone gave the sulfine as light yellow crystals.

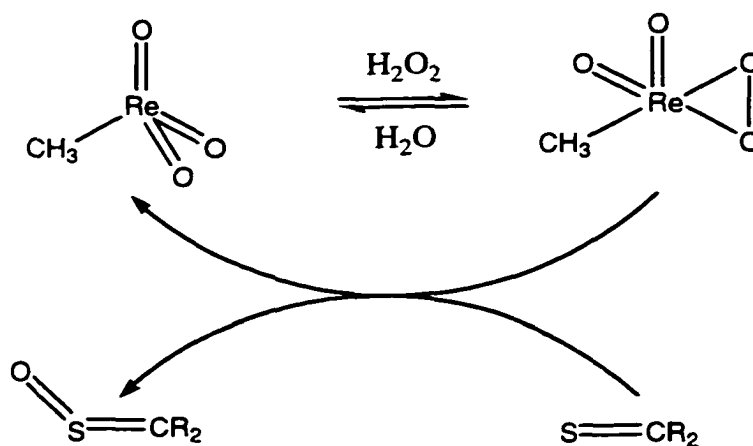
The products from 4,4'-dimethoxythiobenzophenone and thiocamphor were isolated in 95-99% isolated yield. The crude sulfines were further purified by column chromatography on silica gel. Elution was with 15% ethyl acetate-hexane. 4,4'-Dimethoxythiobenzophenone sulfoxide was recrystallized from hexane, yielding greenish-yellow needles.¹⁶ Thiocamphor sulfine was obtained as a light yellow solid; spectroscopic data for it are given in **Table 2**.

Most sulfines were obtained as yellow or yellowish crystalline materials. They are mildly photosensitive to room light and to oxygen, but are much more stable than the parent thioketones. Even if exposed to air and light, sulfines can be kept unchanged for days and are stable enough to be isolated and characterized. Some of the sulfines are stable for months when stored in the dark under argon. The melting points, colors, and isolated yields of the other materials have also been noted.¹⁷

The sulfines with the para substituents NMe₂, OMe, Me, H, Cl, Br, and *m*-NO₂ were previously known. They were identified by comparing their ¹H and ¹³C NMR spectra, mass spectra, and IR spectra with data previously reported.^{8,10,11,12-24}

Two new sulfines were prepared, with *p*-F and *m*-CF₃ substituents. They were obtained by the same procedure in >90% yields and purified by thin-layer chromatography on silica gel, eluting with 5% ethyl acetate-hexane. Yellow crystals were grown from hexane-isooctane. The spectroscopic data and elemental analyses for the new compounds are given in **Table 2**.

The success of the method rests, first, on the MTO-catalyzed reaction converting the thioketone to a sulfine. This type of transformation has been verified for a considerable number of substrates, as has recently been reviewed.^{25,26} The essence of this chemistry is captured in **Scheme 1**.



Scheme 1. Initial Stage of Oxidation

The second stage of oxidation, in which the sulfine, in more than one step, is converted to the ketone, occurs rather more slowly. Under conditions at which a thioketone is oxidized in ca. 10 min, the sulfine required 100-600 h. This timing difference is quite reasonable in that the addition of an oxygen atom to the sulfur will certainly reduce sharply the rate of a subsequent oxidation step by the same reagent. It is just this difference that enables the present procedure to give a high yield of the sulfine with so little loss to the ketone. In the case of thiocamphor, the oxidation stops at the sulfine, even with excess peroxide.

The C=S bond in thioketones is known to be strongly polarized,² unlike a C=O bond, a negative charge resides on the carbon atom. The sulfine is formed by the nucleophilic attack of the sulfur atom on the electron-deficient oxygen atom of the peroxorhenium complexes that are the active intermediates in the reaction.

References

- (1) Battaglia, A.; Dondoni, A.; Giorgianni, P.; Maccagnani, G.; Mazzanti, G. *J. Chem. Soc. B* **1971**, 1547.
- (2) Zwanenburg, B.; Thijs, L.; Strating, J. *Rec. Trav. Chim. Pays-Bas* **1967**, 86, 577.
- (3) Saito, T.; Takekawa, K.; Nishimura, J.-I.; Kawamara, M. *J. Chem. Soc., Perkin Trans. 1* **1997**, 2957.
- (4) Carlsen, L.; Snyder, J. P.; Holm, A.; Pederson, E. *Tetrahedron* **1981**, 37, 1257.
- (5) Adiwidjaja, G.; Sawluk, A.; Volz, W.; Voss, J. *Phosphorus, Sulfur, Silicon* **1973**, 74, 451.
- (6) Cerreta, F. *Bull. Soc. Chim. Fr.* **1995**, 67, 132.
- (7) Zwanenburg, B.; Janssen, W. A. J. *Synthesis* **1973**, 617.
- (8) Tabuchi, T.; Nojima, M.; Kusabayashi, S. *J. Chem. Soc., Perkin Trans. 1* **1991**, 12, 3043.
- (9) Ramnath, N.; Ramesh, V.; Ramamurthy, V. *J. Chem. Soc., Chem. Commun.* **1981**, 112.
- (10) Ramnath, N.; Ramesh, V.; Ramamurthy, V. *J. Org. Chem.* **1983**, 48, 214.
- (11) Maccagnani, G.; Innocenti, A.; Zani, P.; Battaglia, A. *J. Chem. Soc., Perkin Trans. 2* **1987**, 1113.

- (12) Van der Leij, M.; Porskamp, P. A. T. W.; Lammerink, B. H. M.; Zwanenburg, B. *Tetrahedron Lett.* **1978**, 811.
- (13) Kice, J. L.; Rudzinski, J. J. *J. Am. Chem. Soc.* **1987**, *109*, 2414.
- (14) Kice, J. L.; Kupczyk-Subotkowska, L. *J. Org. Chem.* **1991**, 56.
- (15) Abu-Omar, M.; Hansen, P. J.; Espenson, J. H. *J. Am. Chem. Soc.* **1996**, *118*, 4966.
- (16) ¹H NMR (CD₃CN): δ /ppm: 7.80 (d, 2H), 7.29 (d, 2H), 7.00 (m, 4H), 3.82 (s, 3H), 3.80 (s, 3H). MS *m/z*: 274 (M⁺, 67), 258 (M⁺-O, 11), 226 (M⁺-SO, 8.5), 211 (M⁺-SO-CH₃, 10), 196 (M⁺-SO-OCH₃, 2.4), 183 (M⁺-OCH₃-CSO, 7), 151 (M⁺-CSO-2MeO, 6), 135 (M⁺-S-MeOC₆H₄, 100), 107 (M⁺-CSO-MeOC₆H₄, 33).
- (17) For (p-XC₆H₄)₂CSO, the melting points, colors, and yields are as follows: NMe₂, 181-183 °C, gold, 88%; MeO, 84-85 °C, greenish-yellow, 95%; Me, 89-91 °C, yellow, 98%; H, 33-35 °C, greenish yellow, 92%; F, 75-76 °C, yellow, 95%; Cl, 87.5-88 °C, yellow, 95%; Br, 106-108 °C, yellow, 90%. For these meta isomers, CF₃, 53-55 °C, light yellow, 92%; NO₂, 162-164 °C, light yellow 90%. The sulfine from thiocamphor is a light yellow oily solid, mp 118-120 °C, obtained in 97% yield.
- (18) Dahn, H.; Pechy, P.; Toan, V. V.; Bonini, B. F.; Lunazzi, L. *J. Chem. Soc., Perkin Trans. 2* **1993**, *10*, 1881.
- (19) Zwanenburg, B. *Tetrahedron* **1971**, *27*, 1731.
- (20) Tangerman, A.; Zwanenburg, B. *J. Chem. Soc., Perkin Trans. 2* **1973**, 458.
- (21) Tangerman, A.; Zwanenburg, B. *J. Chem. Soc., Perkin Trans. 2* **1974**, 1141.
- (22) Veenstra, G. E.; Zwanenburg, B. *Rev. Trav. Chim. Pays-Bas* **1976**, *95*, 37.
- (23) Huisgen, R.; Mloston, G.; Polborn, K.; Palacios-Gambra, F. *Liebigs Ann. Org. Bioorg. Chem.* **1997**, *1*, 187.
- (24) Kuipers, J. A. M.; Lammerink, B. H. M.; Still, K. W. J.; Zwanenburg, B. *Synthesis* **1981**, *4*, 295.
- (25) Espenson, J. H.; Abu-Omar, M. M. *Adv. Chem. Ser.* **1997**, 253.
- (26) Espenson, J. H. *J. Chem. Soc., Chem. Commun.* **1999**, 429.

Table 1. Yields of sulfines prepared by different methods of thione oxidation

oxidizing reagent	conditions	sulfine yield (%)
MTO/H ₂ O ₂	rt, <5 min.	>90
perbenzoic acid ¹	rt ^a	80–90 ^b
monoperoxyphthalic acid ^{2,3}	0 °C, 30–45 min. ^c	38–89
<i>m</i> -CPBA ^{4,6}	0 °C, 30–40 min. ^d	50–90
ozone ⁷⁻⁹	-70–78 °C, N ₂ ^e	0–71
¹ O ₂ ¹⁰	<i>hν</i> , 0.5–48 hr.	2–25
<i>N</i> -sulphonyloxaziridines ¹¹	0 °C, N ₂ , 0.5–1.5 h ^f	70–90

^a A kinetics investigation. ^b Conversion of the thione to sulfine monitored by UV-vis, not the isolated yield. ^c 1:2 ratio of peracid to thione. ^d *m*-CPBA was the limiting reagent. ^e 1:1 ratio of ozone and thione. ^f Only two sulfines, (1R)-(+)-thiocamphor S-oxide and (1S)-(-)-thiofenchone S-oxide, were prepared by this method.

Table 2 Spectroscopic and analytical data for previously-unreported sulfines^a

method	(<i>p</i> -FC ₆ H ₄) ₂ CSO	(<i>m</i> -CF ₃ C ₆ H ₄) ₂ CSO
¹ H-NMR (CDCl ₃)	7.66 (m, 2H), 7.13 (m, 2H), 6.90 (m, 4H)	8.09 (s, 1H), 8.02 (d, 1H), 7.83 (d, 1H), 7.76 (d, 1H), 7.67-7.56 (m, 4H)
¹³ C-NMR(CDCl ₃)	185.26 (CSO), 165.21 (d, J ¹ (F, C) = 296), 162.70 (d, J ¹ (F, C) = 307), 131.53, 131.44, 130.84 (d, J ⁴ (F, C) = 15), 126.91 (d, J ⁴ (F, C) = 14), 116.10 (d, J ² (F, C) = 88), 115.64 (d, J ² (F, C) = 88)	185.51 (CSO), 134.36, 132.66, 132.16, 131.83, 131.68, 131.60, 130.01, 129.55, 128.08 (q, J ³ (F, C) = 14), 127.87 (q, J ³ (F, C) = 14), 125.98 (q, J ³ (F, C) = 15), 125.73 (q, J ³ (F, C) = 15), 124.82 (CF ₃ , q, J ¹ (F, C) = 35), 122.11 (CF ₃ , q, J ¹ (F, C) = 35)
MS	250 (M ⁺ , 75), 234 (M ⁺ - O, 18), 202 (M ⁺ - SO, 100), 183 (M ⁺ - SO - F, 16)	350 (M ⁺ , 66), 334 (M ⁺ - O, 17), 331 (M ⁺ - F, 28), 301 (M ⁺ - SO, 30), 281 (M ⁺ - CF ₃ , 100), 233 (M ⁺ - CF ₃ - SO, 43)
λ _{max} (ε) (nm) (ethyl acetate) ^b	327 (12 100); 260 (9260)	320 (19 400)
elemental analysis,	C 62.24 (62.38); H 3.15 (3.22); S 12.46 (12.81)	C 51.92 (51.43); H 2.32 (2.30); S 9.18 (9.15)
found (calcd)		
habit	yellow crystals, mp 75-76 °C	pale yellow, mp 53-55 °C

^a Thiocamphor sulfine, previously reported,¹¹ has this ¹H spectrum [2.94 (d of m, 1H), 2.45 (d, 1H), 2.02 (t, 1H), 1.86 (m, 2H), 1.39 (m, 1H), 1.24 (m, 1H), 1.06 (s, 3H), 0.90 (s, 3H), 0.77 (s, 3H)] and this MS: 184 (M⁺, 59), 167 (M⁺ - OH, 4), 135 (M⁺ - SOH, 3), 125 (5), 107 (45), 105 (43), 93 (72), 91 (100). ^b UV spectra determined at four concentrations; Beer's Law was exactly obeyed.

CHAPTER VI. TWO ROUTES TO BIS(μ - DIPHENYLPHOSPHINO)METHANE DIPLATINUM HALIDES BRIDGED BY SULFUR MONOXIDE

A paper published in *Organometallics*[†]

Ruili Huang, Ilia A. Guzei and James H. Espenson*

Abstract

The new compounds $\text{Pt}_2(\mu\text{-diphenylphosphinomethane})_2(\mu\text{-SO})\text{X}_2$ with $\text{X} = \text{Cl}$ and I , have been prepared and characterized. One route was to use $\text{Pt}_2(\mu\text{-dppm})_2\text{X}_2$ to trap the sulfur monoxide liberated from decomposition of a sultine intermediate formed from the oxidation of a thioketone sulfoxide with hydrogen peroxide, catalyzed by CH_3ReO_3 (MTO). The second and preferable route consists of the oxidation of $\text{Pt}_2(\mu\text{-dppm})_2(\mu\text{-S})\text{X}_2$ with hydrogen peroxide, catalyzed by MTO. The X-ray structural analysis of $\text{Pt}_2(\mu\text{-dppm})_2(\mu\text{-SO})\text{Cl}_2$ showed that it has an "A-frame" structure in which the bridge sulfur atom has the geometry of a distorted trigonal bipyramid.

Introduction

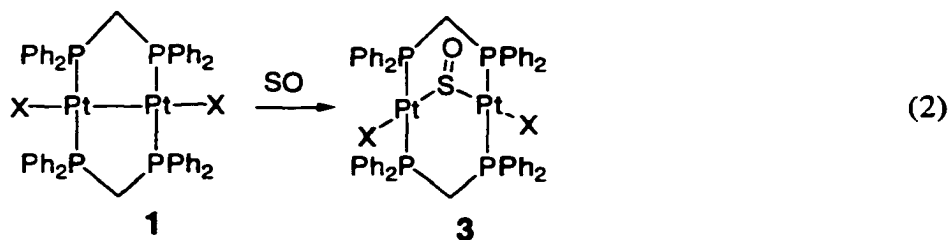
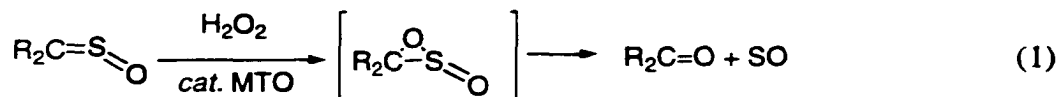
The use of simple chemical methods to generate and study reactive molecules has attracted some attention, but relatively little attention has been paid to sulfur monoxide.^{1,2} Until now, the main method for generating SO has been the pyrolysis of episulfoxides^{1,3-5} and other sulfoxides of varying structures.^{6,7} The reactive SO molecule has been trapped as a dihydrothiophene-1-oxide with dienes and trienes.^{8,9} Certain transition metal complexes have also been used to trap SO.¹⁰ Atoms and small molecules are known to insert into the Pt–Pt bond of the platinum(I) complex $\text{Pt}_2(\mu\text{-dppm})_2\text{X}_2$, **1** ($\text{X} = \text{Cl}, \text{Br}, \text{I}$) to produce so-

[†] Reproduced with permission from Huang, R.; Espenson, J. H. *Organomet.* **1999**, *18*, 5420-5422. Copyright 1999 American Chemical Society.

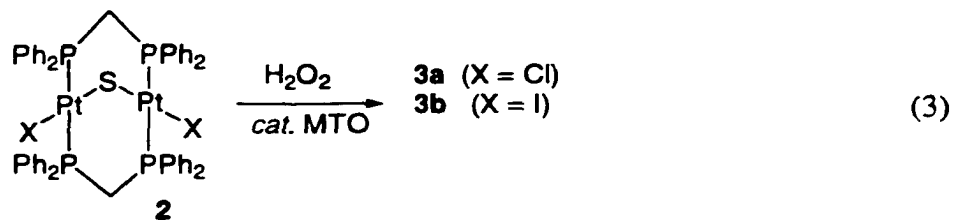
called A-frame molecules $\text{Pt}_2(\mu\text{-dppm})_2\text{X}_2(\mu\text{-Y})$, **2**, $\text{Y} = \text{S}$, SO_2 , CH_2 (from CH_2N_2), CO , etc.¹¹⁻¹⁵

Results and Discussion

We recently uncovered a reaction (eq 1) that gradually generates SO in solution.¹⁶ Sulfur monoxide was then either oxidized, or in separate experiments, trapped with a diene. We reasoned that SO logically could also be trapped by the $\text{Pt}(\text{I})$ complex **1**, eq 2, to form $\text{Pt}_2(\mu\text{-dppm})_2(\mu\text{-SO})$, **3**.



This reaction was successful, providing what we believe is the first $\mu\text{-SO}$ complex of platinum. Related complexes have been made with Pd ^{17,18} and Ni ,¹⁹ not through direct SO insertion but by oxidation of a $\mu\text{-S}$ complex. With that in mind, we carried out a parallel (and superior) synthesis of **3** based on an oxidation reaction, eq 3:



The lemon-yellow compounds **1** and the yellow **2** ($\mu\text{-S}$) were prepared by established procedures.^{20,21} From reaction 3²² a pure yellow product, **3a**, was isolated in 92% yield. Recrystallization from chloroform-hexane afforded yellow crystals. The product was identified and characterized by elemental analysis, NMR,²³ and single-crystal X-ray

diffraction.²⁴ The iodide derivative **3b** was similarly obtained in 86% yield as a yellow solid and characterized by NMR.²⁵ Without the MTO catalyst, the reaction under similar conditions is $> 10^3$ times slower.

When a second equivalent of peroxide was used, the μ -S compounds were further oxidized to the previously known μ -SO₂ complexes,^{14,20} **4a** (X = Cl) and **4b** (X = I). These yellow compounds were isolated and purified by column chromatography on silica gel with 5% methyl alcohol in chloroform as eluent. The spectroscopic data matched the known materials.²⁶

The A-frame structure of **3a** is depicted by the perspective view shown in **Figure 1**. The platinum atoms exhibit a distorted square-planar geometry, in which the bond angles for Cl-Pt-S and P-Pt-P are 171-177°, slightly deviant from linearity. The Pt-Pt distance in **3a**, 326.9 pm, indicates the absence of direct Pt-Pt bonding. The Pt-S distances, 226.2 pm, are equal. Structures of these binuclear A-frame bis(diphenylphosphino)methane (dppm) complexes have been reported: Pd₂Cl₂(μ -SO)(μ -dppm)₂ (**5**),^{17,18} Pd₂Cl₂(μ -SO₂)(μ -dppm)₂ (**6**),²⁷ Pd₂Cl₂(μ -S)(μ -dppm)₂ (**7**),²⁷ Ni₂Cl₂(μ -SO)(μ -dppm)₂ (**8**),¹⁹ Ir₂(CO)₂(μ -N-tol)(μ -dppm)₂,²⁶ and Rh₂(CO)₂(μ -S)(μ -dppm)₂.²⁸ Their Pt analogues, however, have not been structurally characterized.

Complexes **3a** and **5-8** exhibit very similar structural features, **Table 1**. In **3a**, two different tilt geometries of the SO oxygen atom were observed. The occupancy factors for oxygen atom disorder were refined to 0.66 for O(1) and 0.34 for O(2), a feature also observed for **5** and **8**. The S-O bond distance is 142.8 pm, comparable to those found for **5** (140 pm)^{17,18} and **8** (144, 146 pm). Complex **3a** contains pyramidal S, located equidistant from both metal centers. The O-S-O and Pd-S-O angles about the S atom are close to 90°, while the Pd-S-O angles are near 120°. These values are in excellent agreement with the bond angle in **5**, but the same angles in **6-8** (except for O-S-O) were much closer to 111°. The two six-membered rings Pt-S-Pt-P-C-P exhibit boat conformations with atoms C(13) and C(38) on the same side of the P-Pt-P-Pt-P plane. Two Pt and four P atoms are planar within 9 pm. The coordination environment about Pt(1) and Pt(2) is that of a slightly distorted square planar with the coordination angles in the range 87.81(8)-92.99(7)° and 87.60(8)-92.84(7)°,

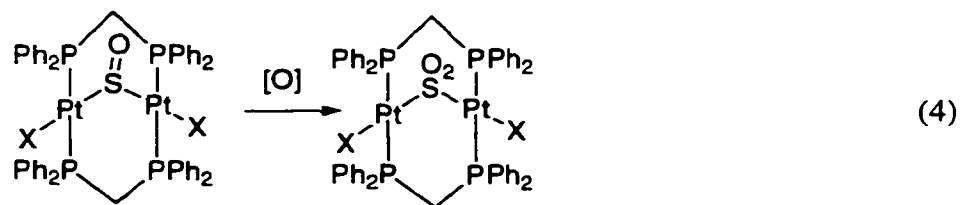
respectively. The ligating atoms lie alternatively 9 pm around Pt(1) and 14 pm around Pt(2) above and below the least-square planes of PdP₂SCl. This diagonal twist toward tetrahedral geometry has also been observed in **5-8**. The platinum-chlorine and platinum-phosphorus parameters are similar to those for the palladium and nickel complexes.

Preparation of SO-bridged dimetallic complexes by oxidation of the corresponding S-bridged complexes has limited precedent. In addition to the palladium complex **5**, one also finds Mo₂(Ntol)₂(S₂(P(OEt)₂)₂(μ-O₂CMe)(μ-SR)(μ-SO) **9**²⁹ and Mn₂Cp₂(CO)₄(μ-SO) **10**.^{30,31} Compounds **3a**, **5**, the nickel complex **8** (from Ni(cod)₂, dppm, and thionyl chloride), and **9** all have pyramidal M₂SO units, whereas compound **10** has a planar M₂SO unit. The locations of the oxygen atom were disordered in **3a**, **5**, and **8** but not in **9** and **10**. In **10** the planar Mn₂SO unit renders it incapable of that disorder; the lack of disorder in compound **9** was due to the two orientations being grossly inequivalent.

Previous methods used for the preparation of the SO-bridged complexes **5**,^{17,18} **8**,¹⁹ **9**,²⁹ and **10**^{30,31} usually needed very low temperature (-20 to -95 °C), an inert atmosphere (under N₂, **8** and **9**), the avoidance of light (**9**), and/or the use of a concentrated oxidizing reagent (30% H₂O₂, **5**). The nickel complex **8** was obtained in 20-25% yield, compared to 60-95% for the others. Complexes **5** and **9** decompose quickly when taken out of solution or exposed to air or light. The μ-SO complexes of platinum, **3a** and **3b**, are very stable as crystals and in solution. They are not sensitive to laboratory light or oxygen, and can be kept unchanged for months. The oxidation of the μ-S complexes by H₂O₂/MTO provides the superior means for generating them. This reaction proceeds in air in a few minutes at room temperature, affording a product that can be isolated and purified in high yield.

Complexes **1** are known to react with S and SO₂ to yield, respectively, **2**, Y = S, and **4**, Y = SO₂. Trapping by **1** of the SO released during reaction 1 also provides the μ-SO product, confirmed by comparison of the ¹H NMR spectra. In a typical experiment 4,4'-difluorothiobenzophenone S-oxide (40 mM) and MTO (12 mM) were dissolved in acetonitrile containing 0.1 M trifluoromethanesulfonic acid. Hydrogen peroxide (80 mM) was added, followed by **1a** (7.5 mM). After 1.5 h, during which time the ¹H spectrum was monitored, 1.0 mM **3a** was found in the reaction mixture. The various reactions are shown in

eqs 1, 2, and 4. The low yield of the desired product is a consequence of the SO trap, **1a**, itself being rapidly oxidized by H₂O₂/MTO, a point that was independently confirmed.



Summary

This research has provided the first examples of sulfur monoxide-bridged diplatinum phosphines. Direct insertion of sulfur monoxide was used, as was the oxidation of the μ -S compound with hydrogen peroxide in an MTO-catalyzed reaction. To our knowledge, this is the first μ -SO compound prepared by direct insertion of sulfur monoxide into a metal-metal bond. The structure was confirmed spectroscopically and crystallographically.

References

- (1) Abu-Yousef, I. A.; Harpp, D. N. *Sulfur Rep* **1997**, 20, 1.
- (2) Abu-Yousef, I. A.; Harpp, D. N. *Tetrahedron Lett.* **1995**, 36, 201.
- (3) Hartzell, G. E.; Paige, J. N. *J. Am. Chem. Soc.* **1966**, 88, 2616.
- (4) Hartzell, G. E.; Paige, J. N. *J. Org. Chem.* **1967**, 32, 459.
- (5) Saito, S. *Tetrahedron Lett.* **1968**, 4961.
- (6) Dover, F. H.; Solomon, K. E. *J. Phys. Chem.* **1980**, 84, 3024.
- (7) Chow, Y. L.; Tam, J. N. S.; Blier, J. W. *J. Chem. Soc., Chem. Commun.* **1970**, 1604.
- (8) Dodson, R. M.; Sauers, F. R. *J. Chem. Soc., Chem. Commun.* **1967**, 1189.
- (9) Dodson, R. M.; Nelson, J. P. *J. Chem. Soc., Chem. Commun.* **1969**, 1159.
- (10) Schenk, W. A. *Angew. Chem., Int. Ed. Engl.* **1987**, 26, 98.
- (11) Puddephatt, R. J. *J. Chem. Soc. Rev* **1983**, 12, 99.
- (12) Balch, A. L. *Adv. Chem Ser* **1982**, 196, 243.
- (13) Brown, M. P.; Fisher, J. R.; Franklin, S. J.; Puddephatt, R. J.; Thomson, M. A. *Adv Chem Ser* **1982**, 196, 231.
- (14) Muralidharan, S.; Espenson, J. H.; Ross, S. A. *Inorg. Chem.* **1986**, 25, 2557.

- (15) Brant, P.; Benner, L. S.; Balch, A. L. *Inorg. Chem.* **1979**, *18*, 3422.
- (16) Huang, R.; Espenson, J. H. *J. Org. Chem.* **1999**, *64*, 6374.
- (17) Lee, C.-L.; Besenyei, G.; James, B. R.; Nelson, D. A.; Lilga, M. A. *J. Chem. Soc., Chem. Commun.* **1983**, 1175.
- (18) Besenyei, G.; Lee, C.-L.; Gulinski, J.; Rettig, S. J.; James, B. R.; Nelson, D. A.; Lilga, M. A. *Inorg. Chem.* **1987**, *26*, 3622.
- (19) Gong, J. K.; Fanwick, P. E.; Kubiak, C. P. *J. Chem. Soc., Chem. Commun.* **1990**, 1190.
- (20) Brown, M. P.; Puddephatt, R. J.; Rashidi, M.; Seddon, K. R. *J. Chem. Soc., Dalton Trans.* **1977**, 951.
- (21) Brown, M. P.; Fisher, J. R.; Franklin, S. J.; Puddephatt, R. J. *J. Chem. Soc., Chem. Commun.* **1978**, 749.
- (22) Compound **2a** (250 mg, 0.20 mmol) and MTO (2.5 mg, 10 μ mol) in 15 mL chloroform were treated with 1 equiv of hydrogen peroxide. ^1H -nmr showed that reaction 3 was complete upon mixing. The product was obtained by column chromatography on silica gel with chloroform as eluent.
- (23) ^1H -NMR (CDCl_3) of **3a**: δ 7.00-7.90 (aromatic, m, 40 H); 4.12 (CH_2 , m, 2 H); 2.87 (CH_2 , m, 2H); ^{31}P : δ 16.12, 13.51 ppm. Elemental analysis for $\text{Pt}_2\text{Cl}_2\text{P}_4\text{C}_{50}\text{H}_{44}\text{SO}$: C, found 46.00 (calcd. 46.99), H 3.61 (3.47), S 1.85 (2.51), P 10.14 (9.69).
- (24) Crystallographic data for **3a**: Tetragonal unit cell, P4_1 , $a = 21.1745(8)$, $b = 21.1745(8)$, $c = 14.2897(8)$ Å, $\alpha = \beta = \gamma = 90^\circ$, $V = 6406.9(5)$ Å³, $Z = 3$, $T = 183(2)$, $D_{\text{calcd}} = 1.737 \text{ Mg/m}^3$, $R(\text{F}) = 3.89\%$ for 14518 independently observed ($I \geq 2\sigma(I)$) reflections ($3^\circ \leq 2\theta \leq 57^\circ$). All atoms other than H were refined with anisotropic displacement coefficients. All hydrogen atoms were included in the structure factor calculation at idealized positions and were allowed to ride on the neighboring atoms with relative isotropic displacement coefficients. The oxygen atom is disordered over two positions in a 66:34 ratio. There are also 3.33 solvate

molecules of chloroform in the asymmetric unit. All software and sources of the scattering factors are contained in the SHELXTL (version 5.1) program library (G. Sheldrick, Bruker Analytical X-Ray Systems, Madison, WI).

- (25) ^1H NMR/ CDCl_3 : δ 7.00–7.90 (aromatic, m, 40 H), 4.48 (CH_2 , m, 2 H), 2.61 (CH_2 , m, 2 H) ppm; ^{31}P NMR/ CDCl_3 : δ 12.66, 9.88 ppm.
- (26) Changquing, Y.; Sharp, P. R. *Inorg. Chem.* **1995**, *34*, 55.
- (27) Balch, A. L.; Benner, L. S.; Olmstead, M. M. *Inorg. Chem.* **1979**, *18*, 2996.
- (28) Kubiak, C. P.; Eisenberg, R. *J. Am. Chem. Soc.* **1977**, *99*, 6129.
- (29) Wang, R.; Mashuta, M. S.; Richardson, J. F.; Noble, M. E. *Inorg. Chem.* **1996**, *35*, 3022.
- (30) Lorenz, I.-P.; Messelhäuser, J.; Hiller, W.; Conrad, M. *J. Organomet. Chem.* **1986**, *316*, 228.
- (31) Lorenz, I.-P.; Messelhäuser, J.; Hiller, W.; Haug, K. *Angew. Chem., Int. Ed. Engl.* **1985**, *24*, 228.

Table 1 Selected structural parameters for **3a** and **5-8**.

complex	d_{M-X}/pm				
	M · · · M	M-Cl	M-S	M-P	M-S-M
Pt ₂ Cl ₂ (μ -SO)(μ -dppm) ₂ 3a	327.0(2)	241.1(1)	226.2(2)	231.5(2)	92.57(7)
Pd ₂ Cl ₂ (μ -SO)(μ -dppm) ₂ 5^a	322.5(4)	240.2(9)	227.3(5)	233.7(7)	90.4(3)
Pd ₂ Cl ₂ (μ -SO ₂)(μ -dppm) ₂ 6a^{b,c}	338.3(4)	238.1(4)	223.4(4)	234.4(4)	98.4(4)
Pd ₂ Cl ₂ (μ -SO ₂)(μ -dppm) ₂ 6b^{b,c}	322.0(4)	238.1(4)	224.1(4)	235.9(19)	91.9(4)
Pd ₂ Cl ₂ (μ -S)(μ -dppm) ₂ 7^c	325.8(2)	237.2(5)	229.8(5)	231.6(13)	90.3(2)
NiCl ₂ (μ -SO)(μ -dppm) ₂ 8^d	330.8(1)	237.2(5)	212.7(2)	222.7(12)	101.98(7)

^a References 17, 18. ^b **6a**, **6b**-two independent molecules. ^c Reference 27. ^d Reference 19.

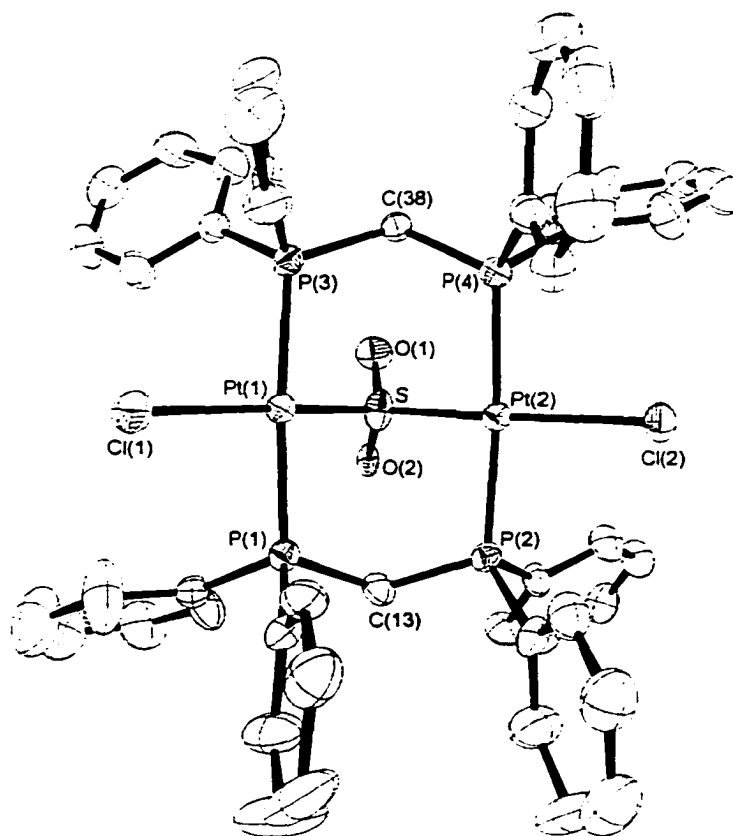


Figure 1 Perspective view of $\text{Pt}_2(\text{dppm})_2\text{Cl}_2(\mu\text{-SO})$, **3a** with thermal ellipsoids at the 30% probability level. The two fractionally-occupied oxygen positions are shown as O(1) and O(2). Selected bond lengths (pm) and bond angles ($^\circ$): Pt(1)–Pt(2) = 326.9(2); Pt(1)–Cl(1) = 240.98(19); Pt(2)–Cl(2) = 241.13(18); Pt(1)–S = 226.2(2); Pt(1)–P(1) = 231.5(2); Pt(1)–P(3) = 231.54(19); Pt(2)–S = 226.2(2); Pt(2)–P(2) = 231.5(2); Pt(2)–P(4) = 231.2(2); S–O(1) = 142.8(7); S–O(2) = 142.8(7); Cl(1)–Pt(1)–S = 172.22(7); P(1)–Pt(1)–P(3) = 176.32(7); Cl(2)–Pt(2)–S = 171.26(8); P(2)–Pt(2)–P(4) = 174.26(7); Pt(1)–S–Pt(2) = 92.57(7); Pt(1)–S–O(1) = 118.2(4); Pt(1)–S–O(2) = 120.2(5); Pt(2)–S–O(1) = 118.4(4); Pt(2)–S–O(2) = 120.4(6); O(1)–S–O(2) = 89.8(7).

Supporting Information

Synthetic and Spectroscopic Procedures

Synthesis of $\text{Pt}_2(\text{dppm})_2\text{X}_2(\mu\text{-SO})$, **3a** (X = Cl) and **3b** (X = I)

Spectroscopic data for **3a** and **3b**

Synthesis of $\text{Pt}_2(\text{dppm})_2\text{X}_2(\mu\text{-SO}_2)$, **4a** (X = Cl) and **4b** (X = I)

Spectroscopic data for **4a** and **4b**

Table S-1. Crystal data and structure refinement for **3a**

Table S-2. Atomic coordinates ($\times 10^4$) and equivalent isotropic displacement parameters ($\text{\AA}^2 \times 10^3$) for **3a**

Table S-3. Bond lengths [\AA] and angles [$^\circ$] for **3a**

Table S-4. Anisotropic displacement parameters ($\text{\AA}^2 \times 10^3$) for **3a**

Table S-5. Hydrogen coordinates ($\times 10^4$) and isotropic displacement parameters ($\text{\AA}^2 \times 10^3$) for **3a**

General Considerations

Spectroscopic procedures

The ^1H and ^{31}P NMR spectra were recorded on a Bruker DRX-400 spectrometer. CDCl_3 was used as the reference in the ^1H experiments and 85% H_3PO_4 for ^{31}P NMR. The Pt–Pt bonded complexes **1a** and **1b**, and the sulfur-bridged complexes **2a** and **2b** were synthesized according to literature procedures. [Brown, M. P.; Puddephatt, R. J.; Rashidi, M.; Seddon, K. R. *J. Chem. Soc., Dalton Trans.* **1977**, 951; Brown, M. P.; Fisher, J. R.; Franklin, S. J.; Puddephatt, R. J. *J. Chem. Soc., Chem. Commun.* **1978**, 749]. All other chemicals were purchased from commercial sources and used as received.

Synthesis of the SO-bridged diplatinum complexes **3a** and **3b**:

250 mg (0.20 mmol) of the yellow compound **1a** and 2.5 mg of MTO (0.01 mmol, 5 mol%) were dissolved in 10 mL of chloroform at room temperature and treated with one equivalent of hydrogen peroxide. All the starting materials disappeared within 5 min as checked by ^1H NMR. An excess of sodium bicarbonate and water were added to the reaction mixture. The water layer was disposed after it turned dark, and the chloroform layer was washed with water and dried with sodium sulfate. The chloroform solution was concentrated by rotary evaporation to less than 1 mL. Column chromatography on silica gel with chloroform yielded 220 mg (92%) of the μ -SO bridged yellow product **3a**. Single crystals were grown by slow diffusion of hexane into a chloroform solution of **3a**. The iodide derivative **3b** was synthesized with a similar procedure in 86% yield.

Spectroscopic data for

$\text{Pt}_2(\text{dppm})_2\text{Cl}_2\mu\text{-SO } \mathbf{3a}$:

^1H NMR (CDCl_3): δ 7.00–7.90 (aromatic, m, 40 H), 4.12 (CH_2 , m, 2 H), 2.87 (CH_2 , m, 2 H) ppm.

^{31}P NMR (CDCl_3): δ 16.12, 13.51 ppm.

$\text{Pt}_2(\text{dppm})_2\text{I}_2\mu\text{-SO } \mathbf{3b}$:

^1H NMR (CDCl_3): δ 7.00–7.90 (aromatic, m, 40H), 4.48 (CH_2 , m, 2H), 2.61 (CH_2 , m, 2H) ppm.

^{31}P NMR (CDCl_3): δ 12.66, 9.88 ppm.

Synthesis of the SO_2 -bridged diplatinum complexes **4a** and **4b**:

The SO_2 -bridged complexes **4a** and **4b** were synthesized with a similar procedure as the one used for synthesizing **3a**, other than instead of one equivalent, two equivalent of hydrogen peroxide was used. The product was isolated and purified by column chromatography on silica gel with 5% methyl alcohol in chloroform as eluent. Isolated yields = 95% (**4a**), 90% (**4b**). Yellow crystals were grown by slow diffusion of hexane into a chloroform solution of **4a** or **4b**.

Spectroscopic data for

Pt₂(dppm)₂Cl₂(μ-SO₂) **4a**:

¹H NMR (CDCl₃): δ 7.00–7.90 (aromatic, m, 40 H), 4.34 (CH₂, m, 2H), 2.55 (CH₂, m, 2 H) ppm.

³¹P NMR (CDCl₃): δ 22.58 ppm.

Pt₂(dppm)₂I₂(μ-SO₂) **4b**:

¹H NMR (CDCl₃): δ 7.00–7.90 (aromatic, m, 40 H), 4.64 (CH₂, m, 2H), 2.25 (CH₂, m, 2 H) ppm.

³¹P NMR (CDCl₃): δ 25.81 ppm.

X-ray crystallography

Crystallographic data for **3a** [C₅₀H₄₄Cl₂OP₄Pt₂S·4/3 CHCl₃]: tetragonal, P4₁, *a* = 21.1745(8) Å, *c* = 14.2897(8), *V* = 6406.9(5) Å³, *Z* = 4, *T* = 183(2) K, *D*_{calc} = 1.737 mg/m³, *R*(*F*) = 3.89% for 14518 independent reflections (4 ≤ 2θ ≤ 56). All non-hydrogen atoms in the molecule of the complex were refined with anisotropic displacement coefficients. All hydrogen atoms were treated as idealized contributions. The oxygen atom is disordered over two positions in a 66:34 ratio. The disordered solvate molecules of chloroform were refined as follows. In the solvate molecule with atom C(51) all chlorine atoms are equally disordered over two positions each and were refined isotropically. In the solvate molecule containing atom C(52) the chlorine atoms are disordered over two positions each in a 70:30 ratio and the entire molecule was refined isotropically. The molecule with atom C(54) is 1/3 occupied and was refined isotropically with an idealized geometry. The final difference Fourier map contained several high peaks (ca. 1.84–1.01 e/Å³) in the vicinity of the disordered chloroform molecules. All software and sources of the scattering factors are contained in the SHELXTL (version 5.1) program library (G. Sheldrick, Bruker Analytical X-Ray Systems, Madison, WI). The absorption correction was based on fitting a function to the empirical transmission surface as sampled by multiple equivalent measurements (Blessing, R.H. *Acta Cryst.* **1995**, *A51*, 33–38.). Further details on the structure of **3a** are available in the Supporting Information.

Table S-1. Crystal data and structure refinement for **3a**.

Empirical formula	$C_{53.33}H_{47.33}Cl_{12}OP_4Pt_2S$	
Formula weight	1675.72	
Temperature	183(2) K	
Wavelength	0.71073 Å	
Crystal system	Tetragonal	
Space group	$P4_1$	
Unitcell dimensions	$a = 21.1745(8)$ Å	$\alpha = 90^\circ$
	$b = 21.1745(8)$ Å	$\beta = 90^\circ$
	$c = 14.2897(8)$ Å	$\gamma = 90^\circ$
Volume	$6406.9(5)$ Å ³	
Z	4	
Density (calculated)	1.737 Mg/m ³	
Absorption coefficient	5.031 mm ⁻¹	
F(000)	3245	
Crystal size	0.45 ≤ 10 ≤ 10 mm ³	
Theta range for data collection	1.72 to 28.29°	
Index ranges	-27 ≤ h ≤ 16, -27 ≤ k ≤ 25, -19 ≤ l ≤ 17	
Reflections collected	35459	
Independent reflections	14518 [R(int) = 0.0414]	
Completeness to theta = 28.29°	96.3%	
Absorption correction	Empirical with SADABS	
Refinement method	Full-matrix least-squares on F ²	
Goodness-of-fit on F ²	14518/26/666	
Final R Indices [I > 2σ(I)]	1.026	
R indices (all data)	R1 = 0.0389, wR2 = 0.0828	
Absolute structure parameter	R1 = 0.0579, wR2 = 0.0873	
Largest diff. peak and hole	-0.006(6) 1.843 and -1.607 e.Å ⁻³	

Table S-2. Atomic coordinates ($\times 10^4$) and equivalent isotropic displacement parameters ($\text{\AA}^2 \times 10^3$) for **3a**. $U(\text{eq})$ is defined as one third of the trace of the orthogonalized U_{ij} tensor.

	x	y	z	$U(\text{eq})$
Pt(1)	1127(1)	5780(1)	1142(1)	23(1)
Pt(2)	2209(1)	4974(1)	2255(1)	24(1)
Cl(1)	465(1)	5785(1)	-230(2)	36(1)
Cl(2)	2802(1)	4002(1)	2286(2)	36(1)
P(1)	1950(1)	6208(1)	286(1)	26(1)
P(2)	2987(1)	5500(1)	1425(2)	26(1)
P(3)	351(1)	5325(1)	2064(1)	24(1)
P(4)	1367(1)	4465(1)	2957(1)	24(1)
S	1724(1)	5917(1)	2439(2)	35(1)
O(1)	1409(4)	6042(4)	3304(5)	37(3)
O(2)	2086(6)	6480(5)	2555(10)	25(5)
C(1)	2146(4)	5814(4)	-805(6)	35(2)
C(2)	1912(4)	5225(4)	-1020(5)	32(2)
C(3)	2090(4)	4917(5)	-1819(6)	44(2)
C(4)	2518(4)	5189(6)	-2407(7)	61(3)
C(5)	2762(5)	5770(7)	-2199(8)	75(4)
C(6)	2584(4)	6091(5)	-1407(7)	51(2)
C(7)	1816(4)	7031(4)	-35(6)	37(2)
C(8)	2101(5)	7521(4)	385(7)	50(3)
C(9)	1945(6)	8145(5)	177(8)	65(3)
C(10)	1526(5)	8268(5)	-503(10)	74(4)
C(11)	1239(6)	7774(6)	-943(12)	108(6)
C(12)	1373(6)	7148(5)	-694(10)	89(5)
C(13)	2715(4)	6238(4)	897(5)	30(2)
C(14)	3635(3)	5757(3)	2165(6)	31(2)

Table S-2 (continued)

C(15)	3820(4)	5368(4)	2888(6)	39(2)
C(16)	4312(4)	5533(4)	3477(7)	43(2)
C(17)	4606(4)	6110(4)	3345(7)	47(2)
C(18)	4432(4)	6500(4)	2655(7)	42(2)
C(19)	3949(4)	6339(4)	2038(6)	41(2)
C(20)	3343(4)	5085(4)	452(6)	37(2)
C(21)	3856(5)	5372(4)	3(7)	51(3)
C(22)	4123(5)	5095(6)	-810(8)	68(3)
C(23)	3861(5)	4526(5)	-1117(7)	57(3)
C(24)	3365(5)	4255(5)	-668(7)	50(3)
C(25)	3110(4)	4522(4)	127(6)	39(2)
C(26)	-205(4)	5901(4)	2513(6)	30(2)
C(27)	-325(4)	6443(4)	1975(6)	39(2)
C(28)	-732(4)	6888(4)	2279(7)	49(2)
C(29)	-1066(4)	6819(4)	3103(7)	48(2)
C(30)	-944(4)	6294(4)	3628(8)	47(2)
C(31)	-512(4)	5831(4)	3352(6)	38(2)
C(32)	-139(3)	4699(4)	1559(6)	28(2)
C(33)	27(4)	4403(4)	743(6)	34(2)
C(34)	-331(4)	3898(4)	412(6)	37(2)
C(35)	-864(4)	3694(4)	887(6)	43(2)
C(36)	-1023(4)	3995(4)	1715(7)	41(2)
C(37)	-665(3)	4491(4)	2062(6)	35(2)
C(38)	664(3)	4947(3)	3126(5)	24(2)
C(39)	1087(4)	3761(3)	2343(6)	30(2)
C(40)	1350(4)	3564(3)	1496(6)	35(2)
C(41)	1102(5)	3042(4)	1053(7)	46(2)
C(42)	615(5)	2719(4)	1407(7)	48(3)
C(43)	335(4)	2915(4)	2234(8)	49(2)

Tabel S-2 (continued)

C(45)	1538(4)	4192(4)	4127(5)	27(2)
C(44)	573(4)	3414(4)	2703(7)	38(2)
C(46)	1434(4)	4546(4)	4917(6)	45(2)
C(47)	1609(4)	4327(5)	5798(6)	53(3)
C(48)	1909(4)	3767(5)	5897(6)	46(2)
C(49)	2039(5)	3403(5)	5104(7)	57(3)
C(50)	1866(5)	3600(4)	4252(6)	46(2)
C(51)	2482(3)	6570(2)	4761(4)	61(3)
CI(3)	2347(4)	7280(3)	5360(6)	85(2)
CI(4)	2341(3)	5776(2)	5014(5)	84(2)
CI(5)	3062(2)	6704(3)	3925(4)	66(2)
CI(3')	2424(3)	7086(3)	5727(4)	60(2)
CI(4')	2577(3)	5871(3)	5421(5)	78(2)
CI(5')	3299(3)	6618(4)	4473(6)	115(3)
C(52)	1000(3)	7490(4)	2973(4)	122(6)
CI(6)	1657(4)	7919(5)	3407(8)	181(4)
CI(7)	456(3)	7589(3)	3901(4)	105(2)
CI(8)	652(3)	7879(3)	2010(4)	95(2)
CI(6')	1800(4)	7704(7)	3047(12)	107(5)
CI(7')	639(11)	7210(11)	4001(10)	190(9)
CI(8')	810(10)	7668(10)	1799(6)	142(8)
C(53)	-659(4)	8499(3)	-379(5)	151(8)
CI(9)	-304(5)	8886(4)	582(7)	278(5)
CI(10)	-236(2)	8749(2)	-1378(5)	161(2)
CI(11)	-486(3)	7689(2)	-218(4)	148(2)
C(54)	1063(7)	9230(7)	-3924(11)	132(18)
CI(12)	1245(10)	8684(12)	-4820(13)	268(13)
CI(13)	1429(7)	8930(9)	-2904(12)	186(7)
CI(14)	238(6)	9163(8)	-3759(13)	170(6)

Table S-3. Bond lengths [Å] and angles [°] for **3a**.

Pt(1)–S	2.262(2)
Pt(1)–P(1)	2.315(2)
Pt(1)–P(3)	2.3154(19)
Pt(1)–Cl(1)	2.4098(19)
Pt(2)–S	2.262(2)
Pt(2)–P(4)	2.312(2)
Pt(2)–P(2)	2.315(2)
Pt(2)–Cl(2)	2.4113(18)
P(1)–C(1)	1.817(9)
P(1)–C(7)	1.824(8)
P(1)–C(13)	1.842(8)
P(2)–C(20)	1.809(9)
P(2)–C(14)	1.817(8)
P(2)–C(13)	1.829(8)
P(3)–C(26)	1.814(8)
P(3)–C(32)	1.830(8)
P(3)–C(38)	1.839(7)
P(4)–C(45)	1.805(8)
P(4)–C(38)	1.820(7)
P(4)–C(39)	1.830(8)
S–O(2)	1.428(7)
S–O(1)	1.428(7)
C(1)–C(2)	1.376(11)
C(1)–C(6)	1.394(12)
C(2)–C(3)	1.367(11)
C(3)–C(4)	1.363(14)
C(4)–C(5)	1.368(15)
C(5)–C(6)	1.372(14)

Table S-3 (continued)

C(7)–C(8)	1.341(12)
C(7)–C(12)	1.352(13)
C(8)–C(9)	1.395(13)
C(9)–C(10)	1.340(15)
C(10)–C(11)	1.364(18)
C(11)–C(12)	1.402(15)
C(14)–C(15)	1.379(11)
C(14)–C(19)	1.411(11)
C(15)–C(16)	1.385(11)
C(16)–C(17)	1.383(12)
C(17)–C(18)	1.338(12)
C(18)–C(19)	1.393(11)
C(20)–C(25)	1.371(12)
C(20)–C(21)	1.399(12)
C(21)–C(22)	1.420(13)
C(22)–C(23)	1.397(15)
C(23)–C(24)	1.357(14)
C(24)–C(25)	1.380(12)
C(26)–C(31)	1.370(11)
C(26)–C(27)	1.404(11)
C(27)–C(28)	1.375(12)
C(28)–C(29)	1.360(13)
C(29)–C(30)	1.366(13)
C(30)–C(31)	1.398(12)
C(32)–C(33)	1.370(11)
C(32)–C(37)	1.398(10)
C(33)–C(34)	1.392(11)
C(34)–C(35)	1.388(12)
C(35)–C(36)	1.386(12)

Table S-3 (continued)

C(36)–C(37)	1.386(11)
C(39)–C(40)	1.397(11)
C(39)–C(44)	1.410(11)
C(40)–C(41)	1.379(11)
C(41)–C(42)	1.335(13)
C(42)–C(43)	1.386(14)
C(43)–C(44)	1.348(12)
C(45)–C(46)	1.373(11)
C(45)–C(50)	1.444(11)
C(46)–C(47)	1.392(12)
C(47)–C(48)	1.352(13)
C(48)–C(49)	1.398(14)
C(49)–C(50)	1.338(12)
C(51)–Cl(5)	1.738(3)
C(51)–Cl(4)	1.746(3)
C(51)–Cl(3)	1.754(3)
C(51)–Cl(3')	1.764(3)
C(51)–Cl(4')	1.767(3)
C(51)–Cl(5')	1.781(3)
C(52)–Cl(6')	1.758(3)
C(52)–Cl(7')	1.758(3)
C(52)–Cl(8)	1.764(3)
C(52)–Cl(8')	1.764(3)
C(52)–Cl(7)	1.769(3)
C(52)–Cl(6)	1.773(3)
C(53)–Cl(10)	1.766(3)
C(53)–Cl(9)	1.767(3)
C(53)–Cl(11)	1.769(3)
C(54)–Cl(12)	1.767(3)

Table S-3 (continued)

C(54)–Cl(13)	1.768(3)
C(54)–Cl(14)	1.769(3)
S–Pt(1)–P(1)	87.81(8)
S–Pt(1)–P(3)	89.07(8)
P(1)–Pt(1)–P(3)	176.32(7)
S–Pt(1)–Cl(1)	172.22(7)
P(1)–Pt(1)–Cl(1)	90.36(7)
P(3)–Pt(1)–Cl(1)	92.99(7)
S–Pt(2)–P(4)	90.62(8)
S–Pt(2)–P(2)	87.60(8)
P(4)–Pt(2)–P(2)	174.26(7)
S–Pt(2)–Cl(2)	171.26(8)
P(4)–Pt(2)–Cl(2)	89.74(7)
P(2)–Pt(2)–Cl(2)	92.84(7)
C(1)–P(1)–C(7)	105.0(4)
C(1)–P(1)–C(13)	102.8(4)
C(7)–P(1)–C(13)	102.9(4)
C(1)–P(1)–Pt(1)	116.4(3)
C(7)–P(1)–Pt(1)	113.0(3)
C(13)–P(1)–Pt(1)	115.2(3)
C(20)–P(2)–C(14)	106.1(4)
C(20)–P(2)–C(13)	103.2(4)
C(14)–P(2)–C(13)	102.7(3)
C(20)–P(2)–Pt(2)	117.3(3)
C(14)–P(2)–Pt(2)	112.5(3)
C(13)–P(2)–Pt(2)	113.5(3)
C(26)–P(3)–C(32)	105.0(4)
C(26)–P(3)–C(38)	103.6(3)
C(32)–P(3)–C(38)	102.4(3)

Table S-3 (continued)

C(26)–P(3)–Pt(1)	112.5(3)
C(32)–P(3)–Pt(1)	118.6(3)
C(38)–P(3)–Pt(1)	113.2(2)
C(45)–P(4)–C(38)	102.8(3)
C(45)–P(4)–C(39)	104.4(4)
C(38)–P(4)–C(39)	104.8(4)
C(45)–P(4)–Pt(2)	113.3(3)
C(38)–P(4)–Pt(2)	115.2(2)
C(39)–P(4)–Pt(2)	114.9(3)
C(3)–C(2)–C(1)	121.3(8)
C(4)–C(3)–C(2)	119.8(9)
C(3)–C(4)–C(5)	119.8(10)
C(4)–C(5)–C(6)	121.4(10)
O(2)–S–O(1)	89.8(7)
O(2)–S–Pt(2)	120.4(6)
O(1)–S–Pt(2)	118.4(4)
O(2)–S–Pt(1)	120.2(5)
O(1)–S–Pt(1)	118.2(4)
Pt(2)–S–Pt(1)	92.57(7)
C(2)–C(1)–C(6)	118.9(8)
C(2)–C(1)–P(1)	121.7(6)
C(6)–C(1)–P(1)	119.2(7)
C(5)–C(6)–C(1)	118.9(9)
C(8)–C(7)–C(12)	118.8(9)
C(8)–C(7)–P(1)	123.8(7)
C(12)–C(7)–P(1)	117.3(7)
C(7)–C(8)–C(9)	122.1(10)
C(10)–C(9)–C(8)	119.7(10)
C(9)–C(10)–C(11)	118.8(11)

Table S-3 (continued)

C(10)–C(11)–C(12)	121.1(13)
C(7)–C(12)–C(11)	119.4(11)
P(2)–C(13)–P(1)	116.2(4)
C(15)–C(14)–C(19)	119.0(7)
C(15)–C(14)–P(2)	118.1(6)
C(19)–C(14)–P(2)	122.9(6)
C(14)–C(15)–C(16)	121.1(8)
C(17)–C(16)–C(15)	118.6(8)
C(18)–C(17)–C(16)	121.5(8)
C(17)–C(18)–C(19)	121.1(9)
C(18)–C(19)–C(14)	118.7(8)
C(25)–C(20)–C(21)	120.1(8)
C(25)–C(20)–P(2)	122.1(7)
C(21)–C(20)–P(2)	117.7(7)
C(20)–C(21)–C(22)	120.3(9)
C(23)–C(22)–C(21)	117.0(10)
C(24)–C(23)–C(22)	121.6(9)
C(23)–C(24)–C(25)	121.2(10)
C(20)–C(25)–C(24)	119.6(9)
C(31)–C(26)–C(27)	118.8(8)
C(31)–C(26)–P(3)	122.9(6)
C(27)–C(26)–P(3)	118.3(6)
C(28)–C(27)–C(26)	120.3(8)
C(29)–C(28)–C(27)	121.4(8)
C(28)–C(29)–C(30)	118.1(8)
C(29)–C(30)–C(31)	122.6(9)
C(26)–C(31)–C(30)	118.7(8)
C(33)–C(32)–C(37)	119.8(8)
C(33)–C(32)–P(3)	121.5(6)

Table S-3 (continued)

C(37)–C(32)–P(3)	118.5(6)
C(32)–C(33)–C(34)	120.1(8)
C(35)–C(34)–C(33)	121.1(8)
C(36)–C(35)–C(34)	118.1(8)
C(35)–C(36)–C(37)	121.4(8)
C(36)–C(37)–C(32)	119.4(8)
P(4)–C(38)–P(3)	115.5(4)
C(40)–C(39)–C(44)	118.0(7)
C(40)–C(39)–P(4)	121.9(6)
C(44)–C(39)–P(4)	120.0(6)
C(41)–C(40)–C(39)	118.9(8)
C(42)–C(41)–C(40)	122.1(9)
C(41)–C(42)–C(43)	120.0(9)
C(44)–C(43)–C(42)	119.9(9)
C(43)–C(44)–C(39)	121.0(9)
C(46)–C(45)–C(50)	116.7(7)
C(46)–C(45)–P(4)	123.7(6)
C(50)–C(45)–P(4)	119.3(6)
C(45)–C(46)–C(47)	121.3(8)
C(48)–C(47)–C(46)	120.8(8)
C(47)–C(48)–C(49)	119.4(8)
C(50)–C(49)–C(48)	120.8(9)
C(49)–C(50)–C(45)	121.0(9)
Cl(5)–C(51)–Cl(4)	114.9(4)
Cl(5)–C(51)–Cl(3)	108.1(4)
Cl(4)–C(51)–Cl(3)	134.2(4)
Cl(5)–C(51)–Cl(3')	119.1(4)
Cl(4)–C(51)–Cl(3')	115.0(4)
Cl(3)–C(51)–Cl(3')	22.5(3)

Table S-3 (continued)

Cl(5)–C(51)–Cl(4')	115.1(4)
Cl(4)–C(51)–Cl(4')	26.1(3)
Cl(3)–C(51)–Cl(4')	118.5(5)
Cl(3')–C(51)–Cl(4')	96.3(4)
Cl(5)–C(51)–Cl(5')	31.2(3)
Cl(4)–C(51)–Cl(5')	105.6(4)
Cl(3)–C(51)–Cl(5')	102.8(5)
Cl(3')–C(51)–Cl(5')	102.4(5)
Cl(4')–C(51)–Cl(5')	93.5(5)
Cl(6')–C(52)–Cl(7')	117.1(10)
Cl(6')–C(52)–Cl(8)	109.2(7)
Cl(7')–C(52)–Cl(8)	128.9(9)
Cl(6')–C(52)–Cl(8')	102.8(9)
Cl(7')–C(52)–Cl(8')	140.1(11)
Cl(8)–C(52)–Cl(8')	20.7(7)
Cl(6')–C(52)–Cl(7)	123.5(7)
Cl(7')–C(52)–Cl(7)	29.6(8)
Cl(8)–C(52)–Cl(7)	105.0(5)
Cl(8')–C(52)–Cl(7)	122.6(8)
Cl(6')–C(52)–Cl(6)	24.5(6)
Cl(7')–C(52)–Cl(6)	102.7(9)
Cl(8)–C(52)–Cl(6)	111.2(6)
Cl(8')–C(52)–Cl(6)	113.7(9)
Cl(7)–C(52)–Cl(6)	100.8(6)
Cl(10)–C(53)–Cl(9)	105.9(6)
Cl(10)–C(53)–Cl(11)	106.9(4)
Cl(9)–C(53)–Cl(11)	105.1(5)
Cl(12)–C(54)–Cl(13)	105.5(6)
Cl(12)–C(54)–Cl(14)	105.0(5)

Table S-3 (continued)

Cl(13)–C(54)–Cl(14)	107.1(5)
---------------------	----------

Table S-4. Anisotropic displacement parameters ($\text{\AA}^2 \times 10^3$) for **3a**. The anisotropic displacement factor exponent takes the form: $-2\text{\AA}^2[h^2a^*2U^{11} + \dots + 2hka^*b^*U^{12}]$.

	U ¹¹	U ²²	U ³³	U ²³	U ¹³	U ¹²
Pt(1)	19(1)	26(1)	24(1)	2(1)	-2(1)	-1(1)
Pt(2)	20(1)	24(1)	28(1)	3(1)	-2(1)	0(1)
Cl(1)	28(1)	50(1)	30(1)	3(1)	-10(1)	-4(1)
Cl(2)	31(1)	28(1)	48(1)	6(1)	-2(1)	7(1)
P(1)	21(1)	29(1)	29(1)	5(1)	-3(1)	-1(1)
P(2)	18(1)	25(1)	34(1)	3(1)	-1(1)	-2(1)
P(3)	20(1)	30(1)	22(1)	-1(1)	1(1)	2(1)
P(4)	25(1)	24(1)	24(1)	2(1)	0(1)	-2(1)
S	37(1)	33(1)	34(1)	-8(1)	-13(1)	11(1)
O(1)	41(6)	41(5)	30(5)	-5(4)	2(4)	-1(4)
O(2)	23(9)	25(9)	26(9)	-2(6)	-17(6)	0(6)
C(1)	20(4)	49(6)	36(5)	7(4)	3(4)	5(4)
C(2)	32(5)	45(5)	20(4)	-1(4)	1(3)	1(4)
C(3)	35(5)	55(6)	42(5)	-7(5)	-6(4)	4(4)
C(4)	26(5)	114(10)	43(6)	-22(6)	6(4)	13(6)
C(5)	50(7)	125(11)	49(7)	-17(7)	25(5)	-36(7)
C(6)	35(5)	76(7)	42(5)	-2(5)	6(5)	-18(5)
C(7)	24(4)	40(5)	48(6)	18(4)	-1(4)	-6(4)
C(8)	62(7)	34(5)	54(6)	13(4)	-15(5)	-9(5)
C(9)	84(8)	28(5)	82(9)	7(5)	-7(7)	-3(5)
C(10)	62(7)	36(6)	124(12)	34(7)	-12(7)	-18(5)
C(11)	74(9)	73(9)	176(16)	63(10)	-36(10)	-4(8)
C(12)	82(9)	52(7)	133(12)	34(7)	-67(9)	-22(6)

Table S-4 (continued)

C(13)	31(4)	25(4)	34(5)	6(3)	-3(3)	-4(3)
C(14)	28(4)	28(4)	37(5)	7(4)	-8(4)	2(3)
C(15)	42(5)	27(5)	48(6)	1(4)	-7(4)	-5(4)
C(16)	39(5)	37(5)	53(6)	4(4)	-17(4)	-8(4)
C(17)	35(5)	52(6)	53(6)	-11(5)	-20(4)	5(4)
C(18)	32(5)	35(5)	60(6)	-7(4)	-8(4)	-10(4)
C(19)	36(5)	40(5)	48(6)	5(4)	-5(4)	-13(4)
C(20)	23(4)	43(5)	43(5)	5(4)	-1(4)	13(4)
C(21)	52(6)	34(5)	67(7)	-1(5)	21(5)	-3(4)
C(22)	56(7)	84(9)	63(7)	-6(6)	35(6)	10(6)
C(23)	49(6)	69(7)	53(7)	-15(5)	4(5)	17(5)
C(24)	54(6)	52(6)	44(6)	-12(5)	-4(5)	12(5)
C(25)	38(5)	41(5)	38(5)	6(4)	-5(4)	9(4)
C(26)	23(4)	30(4)	37(5)	2(3)	-2(3)	1(3)
C(27)	44(5)	33(5)	38(5)	9(4)	1(4)	8(4)
C(28)	59(6)	33(5)	53(6)	8(5)	-8(5)	15(4)
C(29)	39(6)	44(6)	60(7)	-19(5)	0(5)	15(4)
C(30)	47(6)	46(6)	47(5)	-1(5)	20(5)	6(4)
C(31)	40(5)	44(5)	29(5)	-4(4)	-1(4)	1(4)
C(32)	22(4)	34(5)	29(4)	6(4)	-10(3)	3(3)
C(33)	27(4)	43(5)	30(5)	3(4)	0(3)	-5(4)
C(34)	34(5)	41(5)	35(5)	-12(4)	-2(4)	0(4)
C(35)	39(5)	48(6)	43(6)	-1(4)	-13(4)	-5(4)
C(36)	22(4)	49(6)	53(6)	-1(5)	7(4)	-3(4)
C(37)	24(4)	45(5)	36(5)	-5(4)	0(3)	-8(4)
C(38)	24(4)	27(4)	21(4)	1(3)	6(3)	4(3)
C(39)	31(4)	27(4)	32(5)	4(4)	-6(4)	1(3)
C(40)	37(5)	34(5)	35(5)	2(4)	-2(4)	7(4)
C(41)	58(6)	35(5)	45(6)	-12(5)	-13(5)	5(5)

Table S-4 (continued)

C(42)	51(6)	29(5)	62(7)	-5(4)	-18(5)	8(4)
C(43)	26(5)	39(5)	82(8)	2(6)	-5(5)	-4(4)
C(44)	30(5)	34(5)	50(6)	3(4)	4(4)	3(4)
C(45)	26(4)	28(4)	27(4)	4(3)	-2(3)	-4(3)
C(46)	50(6)	50(6)	34(5)	4(4)	1(4)	22(4)
C(47)	47(6)	86(8)	27(5)	-17(5)	-5(4)	23(5)
C(48)	43(5)	65(7)	29(5)	20(5)	-2(4)	6(5)
C(49)	75(8)	45(6)	52(7)	16(5)	-14(5)	-2(5)
C(50)	68(7)	36(5)	34(5)	3(4)	1(5)	8(5)
C(51)	56(6)	37(5)	90(8)	-11(6)	-17(6)	11(5)
C(53)	103(13)	129(16)	220(20)	6(17)	-17(15)	-18(11)
Cl(9)	317(11)	216(8)	300(11)	-150(8)	-93(9)	42(7)
Cl(10)	127(4)	129(4)	227(6)	53(4)	-14(4)	12(3)
Cl(11)	207(5)	141(4)	96(3)	-8(3)	18(4)	-47(4)

Table S-5. Hydrogen coordinates ($\times 10^4$) and isotropic displacement parameters ($\text{\AA}^2 \times 10^3$) for **3a**.

	x	y	z	U(eq)
H(2A)	1621	5029	-606	39
H(3A)	1917	4515	-1963	53
H(4A)	2646	4975	-2960	73
H(5A)	3061	5956	-2611	90
H(6A)	2756	6495	-1272	61
H(8A)	2419	7440	839	60
H(9A)	2134	8482	516	77
H(10A)	1432	8691	-675	89
H(11A)	943	7856	-1428	129
H(12A)	1154	6809	-984	107
H(13A)	3040	6382	446	36

Table S-5. (continued)

H(13B)	2688	6561	1396	36
H(15A)	3605	4979	2984	47
H(16A)	4445	5257	3962	51
H(17A)	4938	6232	3753	56
H(18A)	4642	6894	2584	51
H(19A)	3834	6614	1542	50
H(21A)	4026	5754	244	61
H(22A)	4465	5288	-1132	81
H(23A)	4033	4324	-1653	68
H(24A)	3191	3874	-905	60
H(25A)	2775	4318	448	47
H(27A)	-111	6503	1398	46
H(28A)	-829	7251	1906	58
H(29A)	-1361	7127	3308	58
H(30A)	-1161	6241	4204	56
H(31A)	-432	5474	3737	45
H(33A)	387	4541	403	40
H(34A)	-207	3690	-148	44
H(35A)	-1114	3357	651	52
H(36A)	-1386	3860	2051	49
H(37A)	-776	4686	2637	42
H(38A)	763	5281	3588	29
H(38B)	329	4678	3398	29
H(40A)	1695	3787	1228	42
H(41A)	1283	2907	479	55
H(42A)	461	2356	1092	57
H(43A)	-24	2698	2470	59
H(44A)	391	3533	3285	46
H(46A)	1238	4947	4861	54

Table S-5. (continued)

H(47A)	1517	4574	6336	64
H(48A)	2029	3622	6501	55
H(49A)	2254	3012	5170	69
H(50A)	1959	3346	3722	55
H(51A)	2118	6618	4321	73
H(52A)	1099	7037	2842	146
H(53A)	-1122	8585	-428	181
H(54A)	1200	9670	-4077	158

GENERAL CONCLUSIONS

A new binuclear oxothiolatorhenium(V) compound, $\text{Re}_2\text{O}_2(\text{mtp})_3$ (**D**₁, mtp = 2-mercaptomethylthiophenol), was synthesized by reacting dirhenium(VII) heptoxide (Re_2O_7) with H_2mtp . This compound was characterized spectroscopically and crystallographically. **D**₁ is the first thiolato rhenium complex made by Re_2O_7 and a thiol. No other rhenium complex has been found with the same type of structure.

The thiolato bridge in **D**₁ was opened, and sometimes **D**₁ was monomerized, through ligand coordination to one or both of the Re(V) centers. **D**₁ was found to be an efficient catalyst for the oxidation of phosphines, arsines, stilbenes, sulfides and dienes by pyridine N-oxides, the oxidation of phosphines by dimethylsulfoxide. The kinetics and mechanism for the oxidation of triarylphosphines by pyridine N-oxides, as well as the relative reactivities of all substrates were studied. The reactivities were found to have the order: phosphines>stilbenes>arsines>sulfides>dienes. The reaction was proposed to go through a Re(VII) intermediate with pyridine N-oxide as one of the ligands. The N-O bond was activated through coordination to rhenium and the oxygen atom was abstracted by a phosphine forming a phosphine oxide.

The most remarkable feature of this new Re(V) species is that it activates molecular oxygen, which has no precedent in oxorhenium catalysis. Substituted triarylphosphines and methylphenylphosphines were oxidized to phosphine oxides in high yields. Kinetics and mechanism for this reaction were investigated. The reaction pathway was suggested to involve two Re(VII) intermediates, the peroxo ($\text{Re}(\text{O}_2)$) and μ -oxo (Re_2O) Re(VII) species. Other substrates, such as sulfides and dienes, which coordinate weakly, or do not coordinate to the Re(V) center, were not oxidized by molecular oxygen. However, in the presence of a small amount of phosphine to open up the sulfur bridge and allow O_2 to coordinate, sulfides and dienes were also oxidized to sulfoxides and epoxides accordingly. These reactions provide a strong evidence for the existence of the peroxorhenium(VII) intermediate. The reactivity of the O-bridged dirhenium(VII) intermediate is similar to the Re(VII) intermediate in the **D**₁-catalyzed pyridine N-oxide oxidations. The relative reactivities of all substrates were studied and found to have the order: phosphines>sulfides>dienes.

Methyltrioxorhenium (abbreviated as MTO), catalyzes the two-step oxidation of thioketones to sulfines (thioketone S-oxides) and to ketones by hydrogen peroxide. The kinetics and mechanism of both steps were studied. MTO activates hydrogen peroxide by forming a monoperoxo and a bisperoxocomplex both of which are efficient oxidants. The substituted thiobenzophenones were found to attack the peroxo rhenium oxygen nucleophilically. The Hammett correlation of the second-order rate constants against the 2σ values of the substituents is a straight line with a negative slope. On the other hand, a non-linear Hammett plot was obtained for the second oxidation step, from sulfines to ketones. The Hammett plot is remarkably V-shaped, with the unsubstituted thiobenzophenone at the bottom. The rate is accelerated with both extremely electron-donating and withdrawing substituents. This suggests a mechanism for the sulfines in which the direction of the electron flow in the transition state changes with the electron demand of the substituents on the sulfines. The product of oxidation of the sulfine is a transient sultine (from epoxidation of the C=S bond), which cannot be detected. Sulfur monoxide was released from the rapid decomposition of the sultine, and was trapped with a 1, 3-diene as a thiophene-1-oxide.

The oxidation rate for the sulfine is largely reduced (more than 10^3 times) comparing to that of the parent thioketone, due to the strongly electron-withdrawing oxygen atom on the sulfur. The reaction was stopped at the sulfine as the final product without it being over oxidized to ketone when one equivalent of hydrogen peroxide is used. This makes the controlled oxidation of thioketones by the MTO/H₂O₂ system a far more superior method for the synthesis of sulfines. A series of sulfines, including a couple of previously unknown sulfines, were synthesized in high yields by this method.

The sulfur bridge of a binuclear platinum(I) complex was oxidized step-wise to a sulfoxide, then sulfone by hydrogen peroxide catalyzed by MTO. The SO-bridged diplatinum(I) complex was crystallographically characterized being the first platinum example of complexes of this type. The same compound was obtained by trapping the sulfur monoxide released from the oxidation of a sulfine by MTO/H₂O₂ with the corresponding platinum-bonded complex. The previously known diplatinum(I) complex with a sulfone bridge was obtained in a similar way by inserting sulfur dioxide into the Pt-Pt bond.

ACKNOWLEDGMENTS

I would like to thank Professor James H. Espenson, for his kind support, valuable guidance, unceasing encouragement and for providing a freely and stimulating scientific environment throughout my graduate career.

I would also like to thank Professor William S. Jenks for helpful discussions and theoretical calculations; the other members in my Program of Study Committee, Professor L. Keith Woo, Professor Victor S. Y. Lin, and Professor Peter J. Reilly for their efforts in reading and improving this dissertation.

I am also thankful to Dr. Weidong Wang, Dr. Andreja Bakac, and other members of my research group, past and present, for many insightful scientific discussions. I am grateful to Dr. Xiaodong Liu, Mr. Jinyuan Chen, and Dr. Jinchao Yang, for their ever-lasting support and friendship.

My appreciation also goes to Dr. Ilia A. Guzei for the crystallographic work, Dr. Dave Scott and Dr. Shu Xu for assistance in NMR spectroscopy.

My special thanks go to my husband, parents and sister, for their endless love and support.

This work was performed at Ames Laboratory under Contract No. W-7405-Eng-82 with the U. S. Department of Energy. The United States government has assigned the DOE Report number IS-T 1911 to this thesis.